PHOTOVOLTAIC PANEL HOT SPOTS MODEL

BY

Ibrahim Hassan Ali Banat

A Thesis Presented to the

DEANSHIP OF GRADUATE STUDIES

KING FAHD UNIVERSITY OF PETROLEUM & MINERALS

DHAHRAN, SAUDI ARABIA

In Partial Fulfillment of the

Requirements for the Degree of

MASTER OF SCIENCE

In

Electrical Engineering

October, 2016

KING FAHD UNIVERSITY OF PETROLEUM & MINERALS

DHAHRAN- 31261, SAUDI ARABIA

DEANSHIP OF GRADUATE STUDIES

This thesis, written by **Ibrahim Hassan Banat** under the direction his thesis advisor and approved by his thesis committee, has been presented and accepted by the Dean of Graduate Studies, in partial fulfillment of the requirements for the degree of **MASTER OF SCIENCE IN ELECTRICAL ENGINEERING.**

Dr. Chokri Belhaj Ahmed

(Advisor)

Dr. Al-Shaikhi, Ali Ahmad

Department Chairman

Dr. Mohamed Deriche

(Member)

Dr. Salam A. Zummo

Dean of Graduate Studies

Dr. Ben-Mansour, Rached

(Member)

27/11/16

Date

Ibrahim Banat

2016

DEDICATION

I dedicate this thesis to my lovely parents and to the loving memory of my family.

ACKNOWLEDGMENTS

Primarily, I am highly thankful to Allah for His boons that continue to flow into my life, and because of you, I made this through against all odds.

I thank my family for constant love and assistance that have constantly received. Thanks go also to all my friends and colleagues.

I thankful my beloved father, mother and family who have been a fixed root of help and support within the challenges of graduate study. You have successfully accomplished made me the person I am getting. You will be forever in my heart and mind.

My appreciations go to the staff of the Electrical Engineering Master Program at King Fahd University of Petroleum & Minerals University.

With a mighty pleasure I would wish to recognize the support and assistances made possible by staff from the start of study years with their precious the courses and lectures; the technical assistance of the Lab team and the priceless supervision of my committee members Dr. Mohamed Deriche and Dr. Ben-Mansour Rached..

Finally, my furthermost appreciation goes to my advisor, Dr. Chokri Belhaj Ahmed for his special support, help and discerning feedbacks and perceptions throughout the duration of this thesis.

TABLE OF CONTENTS

LIST OF TABLES

LIST OF FIGURES

LIST OF SYMBOLS AND ABBREVIATIONS

CASSY Lab	:	Computer Assisted Science System
FF	:	Fill Factor
FLIR	:	Forward Looking Infrared Radiometer
IR	:	Infrared
$\mathbf{I_{mp}}$	:	Current at Maximum Power Point
$\mathbf{I_{sh}}$	:	Shunt Current
$\mathbf{I_{sc}}$	:	Short Circuit Current
$\mathbf{I_{ph}}$	:	Photon Current
$\mathbf{I_D}$	:	Diode Current
$\mathbf{I_0}$	:	Diode Saturation Current
K	:	Boltzmann's Constant
MATLAB	:	Matrix Laboratory
MPP	:	Maximum Power Point
m	:	Diode Ideality Factor
$\mathbf{N_s}$	:	Number of Series cells in the panel
OTC	:	Operating Test Condition

PV	:	Photovoltaic
P_L	:	Load Power
q	:	Charge of Electron
R_s	:	Series Resistance
R_{sh}	:	Shunt Resistance
R_L	:	Load Resistance
STC	:	Standard Test Condition
SIF	:	Shade Impact Factor
T	:	Cell Temperature
USB	:	Universal Serial Bus
V_{mp}	:	Voltage at Maximum Power Point
V_{REV}	:	Reverse Breakdown Voltage
V_{oc}	:	Open Circuit Voltage
V_t	:	Thermal Voltage

ABSTRACT

Full Name : Ibrahim Hassan Ali Banat

Thesis Title : Photovoltaic Panel Hotspots Model

Major Field : Electrical Engineering

Date of Degree : October, 2016

The hot spot phenomenon is regarded as preliminary damage occurring in solar panels. The hot spot reduces the production power of the panel and its lifetime. In extreme cases, the panel could be physically destroyed due to excessive heat. The hot spots consequence of localized warming of solar cells due to faults that oftentimes result from partial and full shading or different outside forces reasons that lead to power dissipation instead of power generation of the module. However, there remains a shortage of widely agreeable methods for processing with them in real life and practical works. Moreover, this heating area can destroy and decay panel efficiency. Bypass diodes are generally installed in solar cells to kill that phenomenon risk, but it does not eliminate the hot spot perfectly.

This thesis focuses on the electrical and the thermal behavior of the solar cells that are working under the backward biased situations. This contains a) estimate the reverse I-V curves that are subject to the shading levels applied to the cell, b) thermography of solar cells operated under reverse biased to investigate the shunt and bypass diode current distribution, and c) investigation of the critical temperatures which leads to overheating cells under shade.

Solar panel with full detailed hot spot current distribution model is developed. The model is based on the Bishop circuit. The model uses an electrical, detailed representation of

Photovoltaic Panel (PV) represented in Matlab /Simulink. Simulation results confirm that shading rates can control the hot spot effect on power output because it depends on the backward voltage and leakage current, and observed the bypass diode working process in all operating conditions. Also, the model has a capability of dealing with a variation of temperature and irradiation on the shunt and series resistances. The model was examined for different shading levels. The obtained results were compatible with the previous related work. The model reached detailed estimation of the current distribution and all power calculations inside the test panel strings. The results have been satisfactory.

The model obtained is generally applicable as a tool for all power calculations during the hot spot risk, so it can be used for any model configuration under any operating conditions of irradiation and temperatures.

This thesis presents observations on PV panel affected with a hot spot. The visual and infrared (IR) investigation, maximum power, currents and operating voltage online tests have been carried out.

The thesis consists of five main chapters, shading phenomena, solar cell modeling and parameter extraction, hot spot phenomena model and simulation, experimental works and results, and finally conclusion and future works.

ملخص الرسالة

الاسم الكامل: ابراهيم حسن علي بنات

عنوان الرسالة: تصميم نظام محاكاة النقاط الساخنة الناتجة عن تعرض الخلايا الشمسية للظل وازدياد درجة حرارتها

التخصص: الهندسة الكهربائية

تاريخ الدرجة العلمية: أكتوبر/2016

تعتبر ظاهرة النقاط الساخنة في الخلايا الشمسية المتولدة عن ازدياد درجات الحرارة عن حدها المسموح نتيجة خلل معين في اداء الخلية خطرا حقيقيا يهدد عمل وكفائة الخلايا خاصة في البيئة التى تمتاز بارتفاع درجات الحرارة خلال فصل الصيف كما في المملكة العربية السعودية. هذه الظاهرة اصبحت محل اهتمام ودراسة الباحثين في الطاقة المتجددة. حيث انها تهدد العمر الزمني لعمل الالواح الشمسية وكذلك تقلل من كفائة انتاجها للتيار الكهربائي بشكل ملحوظ.

تنشأ النقاط الساخنة لعدة اسباب منها: تعرض الخلايا الشمسية للتظليل الكلي او الجزئي اما بسبب الالواح المجاورة او المباني المرتفعة او الهوائيات المنتشرة في منطقة تركيبها، او من فضلات الطيور واوراق الاشجار المتطايرة والاتربة المتراكمة لفترات زمنية طويلة. مما يؤدي الى عدم انتظام توزيع ضوء الشمس على سطح الخلايا وهذا يؤدي بدوره الى عدم انتظام سريان التيار الكهربائي في الخلايا المظلله حيثُ انها اصبحت مظلمة وغير قادرة على انتاج التيار كباقي الخلايا الغير مظلله، مما يجعلها تعمل في حالة الانحياز العكسي وبالتالي تيارا اقل يمر فيها عن تيار باقي الخلايا التى تعمل بشكل منتظم في منطقة الانحياز الامامي.

الالواح الشمسية تتكون من مجموعة كبيرة من الخلايا المتصلة على التوالي التى تحمل نفس التيار الذي تنتجة خليه واحده . في حالة حصول ظاهرة النقاط الساخنة مع ارتفاع درجة الحرارة، فان الخلايا المظلمة توثر على تيار باقي الخلايا المتصله معها وبالتالي تتغير الخصائص الكهربائية وتصبح جميعها متغيرة مع درجة حرارة الخليه خاصة قيم المقاومات الداخلية. هذا كله يؤدي الى تبديد الطاقة الكهربائية عبر هذه المقاومات في الخلايا المصابة على شكل حرارة تزيد من حرارة اللوحة مما يؤثر على كفائه انتاجها للطاقة ومن ثم تدمير الالواح واحراقها مع مرور الوقت.

مصانع انتاج الخلايا الشمسية اوجدت بعض الحلول للحد من تاثير هذه الظاهره. وبعضها يعتبر ناجحا الى حد ما مثل تركيب ثنائيات موصلة بالتوازي مع كل مجموعه من الخلايا الشمسية لتحييد الخلايا المصابة واستمرار سريان نفس التيار الكهربائي للخلايا التى تعمل بشكل سليم. لكنها لا تلغي اثر الظاهرة بشكل كامل.

هذه الرسالة تناقش الظاهرة بالتفصيل، وتدرس ازدياد ونقصان المقاومات المتصلة على التوالي والتوازي بالتركيب الداخلي للخلية، وكيف تتغير مع درجات الحرارة، ومقدار الطاقة المفقودة من خلالها، كذلك تدرس عمل الخلية الشمسية في منطقة الانحياز العكسي وترسم المنحنيات الكهربائية لها في تلك المنطقة. كل ذلك باستخدام برنامج المحاكاة الماتلاب. وتصميم نظام يرتكز على التركيب الداخلي للخلية لتتبع تطور الظاهرة وسريان التيار الكهربائي في الخلايا المصابة وثنائيات الحماية وكذلك التيار المتبدد في مقاومات الخلية المظلمة. ومن ثم ندرس اثر الظل على الخلايا عند اشتداد درجات الحرارة وكيف يعمل الثنائي وكيف تتوزع درجات الحرارة في مناطق الخلية. لعمل ذلك والتحقق من صحة التصميم استخدمنا تقنية الاشعة تحت الحمراء باستخدام كاميرا حرارية متطورة لتصوير سلوك عمل الخلية عند حدوث الظل، وكذلك التقاط صور حرارية للخلية التي تعمل عند الانحياز العكسي للجهد، وتحديد التيار الذي يعبر كل جزء في تلك الخلية.

تتكون الرسالة من خمسة فصول رئيسية: ظاهرة التظليل الكلي والجزئي على الخلايا الشمسية، التركيب الداخلي للخلية الشمسية والمعادلات الخاصة للحصول على عناصر دائرتها الكهربائية، تصميم نظام لمحاكاة ظاهرة النقاط الساخنة، التجارب العملية والنتائج، أخيرا : الاستنتاجات والتوصيات والاعمال المستقبلية.

CHAPTER 1

INTRODUCTION

In this prefatory chapter, the present technical purposes to perform this thesis study into PV modules and the corresponding working, mismatch problems are discussed. Afterwards, full explanation of the theoretical background of the thesis argued in this research and the main objectives are observed. The chapter concluded by the structure of the thesis for the rest of the chapters.

1.1 Overview of PV Panels and Mismatch Problems

The sun's energy is recommended as the most significant renewable source, whereas it is available at the earth's surface. Rising attention on renewable power resources has given rise to the market for solar power to expand quickly, especially in the places of unstable distribution generation. Thus, factories and manufacturers are supposed to be more authentic and flexible when dealing with power generated from PV stations or panels, hence more accurately needed to deliver a maximum power production.

PV panels have recently become economical and a necessary technology in today’s world for generating clean power generation.

The most interest of solar energy is an infinite supply source of daylight and clean source production. In contrast, the main disadvantage is the cost so it's considered as one of the high-cost generators. Based on semiconductor technology, the principle operation of solar cells that when two semiconductors are put into contact with each other the electricity will flow between them. This is called the photovoltaic phenomenon, was first discovered by

Becquerel in 1839. The first solid PV cell built in 1883 by Charles Fritts, by coating the semiconductor selenium with a thin layer of gold to form a heterojunction. 1% efficiency was of Charles Fritts device [1]. First and practical development of solar cells panels' technology started in the 1950s.

In general solar cells mathematical model designed depends on current and voltage relation (I-V Curve) that results from definitions model suggested by Phang and Chan (1987). The I-V curve described the single solar cell characteristics supposed that one lumped diode only. This curve is fundamental for the mathematical relationship of the solar cell modified by Jain & Kapoor (2004) and Desoto et al. (2006).

The modifications and simplification are continued and proceed to develop the accurate I-V curve. Some models are designed by assuming the parallel resistance is very high and sometimes tends to infinity, so in this case, the model of the four parameters is formed. Many approaches have been proposed to solve that mathematical model. Three approaches for solving the model were developed by Khezzar et al. (2009). Chenni et al. (2007) progressed a simplified approach by supposing that the sunlight (I_{ph}) is equal to the short circuit current of the cell. Zhou et al. (2007) inserted the notation of a fill factor (FF) to estimate the output power at maximum points.

Even so, to get an accurate model that reflects the whole parameters of PV cells and to estimate the power efficiency, the solar panel requires -besides the main parameters of diode and sunlight source- to include the two resistances series (R_s) and parallel (R_p). The PV module introduced by King et al. (2004) is perfect for situations where the solar panels will be working on several operation points of irradiation and temperatures.

For this study, the modified I-V curve of five parameters for both series and parallel configuration module was solved using a numerical method provided by datasheet specifications provided by the manufacturer and validated with measurements by experimental works.

Manufacturers always give the following specification data on solar modules: the short circuit current; the open circuit voltage; the current and voltage at the maximum power point; and the temperature coefficients related to open circuit and short circuit points. These data of operation are needed to find a solution to the five parameter model.

The suggested PV model is flexible so it is simulated by Matlab /Simulink and different irradiation levels that are used for comparison with the experimental datasheet.

As research goes on today within private industry and at national laboratories, there is stress on raising conversion efficiencies and mass production strategies to further cut the price of developing solar systems. Therefore, technical control challenges are various and need a great deal of concentration to dealing with it. So output power delivered to the consumer is the first main optimization problem in PV technology. However, in many industrial or commercial projects, the PV panels might be operated at non-uniform illumination. The causes for non-uniform illumination conditions have multiple cases, may be the tree leaves, the shadow of clouds, bird dung, or the shadow of neighbor's PV modules with others, etc. This leads to non-uniformity and then nonlinearities in I-V curve characteristics [2].

While the shadows are continuous and not murdered, other undesired effects will seem:

- The output energy generated from the module is much less than manufactured. At some applications, the annual power losses can amount to 10%. Hence, it could be for “missing of load” increases [3].

- If the shaded cell has hot spot phenomenon that resulting damage the panel. The shaded PV cells will operate in the reverse bias mode and may be reached breakdown voltage value and become a load within the string thus dissipated power. Bypass diodes are equipped in parallel with cells for saving them from hot spot risk by providing an alternative path for passing the current. However, commercial, only one diode is replaced with a string that includes a group of cells [4].

Both researchers and industrial factories working in the solar energy sector have done a lot of efforts for implementing the suitable PV structures, dealing with many materials for manufacturing PV systems and testing the performance. However, challenges in designing and fabricating solar cells still remain and focus on the performance of PV panels, one of the challenges is the behavior of shunts. A lot of work has been studied for shunt effects and is known to be common mismatch problems in PV cell that reducing output power, current, voltage and fill factor.

1.2 Main Thesis Objectives

The main objective of this research work is to reach a mathematical model that reflects the hot spot phenomenon, based on the experimental investigation.

- To model I-V and P-V curves for non-healthy module due to excessive environmental factors such as dust, shade, heat, and temperature.
- To reach physical model configuration of PV parameters series and shunt resistance under effect causes by dust and shading.
- To track shunt behavior and their effect on the PV performance with numerical simulation method.
- To validate the reached model by experimental investigations by an IR camera.

In this work, commercially solar panels are used and prepared for study. Legal documents are then utilized to determine the temperature distribution within the module and watch the degradation of power. All electrical testing is planned to measure the PV panel characteristics. The hot spot temperatures and currents distribution of defective cells are then estimated and measured. The performance of power generated by the panel is tested once more to compare with manufactured data. Computer Assisted Science System (CASSY) was employed to plot both characteristic curves of the panels under test.

1.3 Thesis Contribution

Solar panel with full detailed hot spot current distribution model is developed under any level of shading effect.

The model is able to discover and follow the current distribution under hot spot phenomenon in three paths of the panel: 1) module current, 2) bypass diode current, and 3) string and leakage current. Besides, the model is able to deal with all power calculations during the shading effect.

The hot spot model is generally applicable as a tool for hot spot risk and power calculations, so it can be used for any panel configuration with its electrical specifications and under any operating conditions of irradiation and temperatures.

1.4 Thesis Structure and Organization

This part sums up the following five chapters supporting an overview of the subject of the research.

The thesis is made of five main chapters, shading phenomenon effect on PV performance, PV modeling and parameter extraction, hot spot phenomenon modeling and simulation, experimental works and results and lastly conclusion and future works.

Chapter 2: The suggested Matlab / Simulink program analytically modeling and fitting the behavior of solar cells under different shading levels and operating conditions. This chapter also analyzes the conduct of the PV panel with and without bypass diode connection.

Chapter 3: Describes the mathematical modeling equations of the solar cell and five parameter extractions. Matlab programs can show the electrical characteristics of a practical solar cell and how it acts under different environmental conditions. The simulation is capable of evaluating the five parameter model and study the variation of shunt and series resistances on the output power of the panel.

Chapter 4: In this chapter a full explanation of how the I-V and P-V curves illustrate the performance when all parameters of the solar cell are included. Study the I-Vs, worst case cell deterioration and stress due to reverse bias and leakage current due to a hot spot phenomenon. Simulate a model to evaluate hot spot and the currents distribution inside defective cells. Three methods are developed to evaluate hot spotting risk under various scenarios.

Chapter 5: The results of the experimental works of the solar panels used in the research work are shown in this chapter. The cell mismatch in the panel is discussed depends on the hot spot creation and initiation in the work field and validate the model of hot spot that simulated in Simulink, then investigate the currents distribution in the overheating arrears and bypass diode by thermography technique using advanced thermal camera to see the heat locations and thermal stress due to hot spot risk.

Chapter 6: Conclusions and future works of the thesis are summarized in this chapter.

CHAPTER 2

Shading Phenomenon Effects on PV Panel Performance

2.1 Literature Survey

A lot of resources and publications have been received and reviewed to support and enhance an appropriate understanding of the subjects related to failures, shading, and monitoring PV modules. Literature survey is reviewed and divided into mismatch problems and shading effects.

First of all the solar cells behaves like a current source, that is, the photo-current is zero or very small if the sunlight irradiation cannot reach the solar cell due to covering result of shadowing, dust, snow, high buildings and leaves [4, 5].

Reference [6] discussed the power dissipated in PV modules with respect to mismatch issues under non-uniform operation conditions. Panels are found to have a negligible mismatch loss compared to multiple directions on panels facing unless they located or grouped in the same string. The mismatch loss was unclear, simply it was desired by reducing the power rating - a factor of 1-2 %- . The output power of the string under influence of cover cell was found to be proportioned to the amount of sunlight allowed during the shading effect.

Cells under shading condition dissipate a large amount of power, loss in shunt resistance and transform into heat. This excessive thermal may destroy the normal cells. To protect the covered cell, protective devices called bypass diodes are inserted in parallel with the strings that form the panel [7].

Reference [8] discussed the main function of inserting bypass diodes across the string. It protects the module against the hot spot phenomenon and less the percentage burn of affected cells. Reference [9] described a reduction in power caused by a shadow and prove that the degradation can be over 30 times the cell physical size, according to the number of protected devices within the string. A Shade Impact Factor (SIF) notation was implemented to show the relationship between power dissipation and coverage area.

Paper [10] described an electronic system could observe solar panel efficiency with low power dissipation and cost-effectiveness. A computer via USB wireless device was designed and connected to develop the communication module. Partial shading and mismatch conditions were obliged to test. Power degradation due to non-uniform illuminations was recorded.

In paper [11], a mathematical equation is written by authors under partial shading. Diodes configuration was shown by the formulas and investigated how much power dissipated in the string. It was not favorable to connect more than 6 diodes in PV panel due to the cost, also it would not enhance of power savings.

2.2 Mismatch Reasons

In real life, several reasons that lead to producing many differences in electrical characteristics of the panel.

Investigations into the mismatch of PV panels have been performed on the outdoor test and reported in [12, 13]. The report said that the performance of cells lies in the same array will decrease by changing rates of illumination because of localized defects such as the oxidation of solar cell contacts.

As mentioned in [13-14] the main reason for causing an efficiency drop in PV cells is shading effect. This is where the shading covered a portion of the panel string, producing a non-uniform illumination distribution as indicated in figure 1-a.

Figure 1: Shading effect on solar panels

Short circuit problems can also happen with soiling of the PV string or sub-modules where the dirt and dust that has accumulated on the solar surface. Completely or partially dust will prevent the sun photo-current for hitting the cells as illustrated in figure 1-b. Partial and full shading are interested in concentrating on this work since the panels set up on the top and roofs are more sensitive to the shading due to nearby objects such as high buildings, antennas, and clouds.

The PV systems can be used to examine the impact of shading of defective cells or strings and estimate the desire of serial configuration regarding the bypass diodes connected to the string across the panel.

Physically in a PV panel's series configuration, the same amount of current must flow across each cell. When the shading happened, cells force to operate at current higher than their short circuit current which means backward voltage is applied to the shaded cells,

thereby leading to dissipate power inside the module as a heat and cause “hot spots phenomenon”.

Bypass diode protects the shaded cells against negative voltage and saves the module to reach the breakdown voltage so it allows the current to flow around shaded cells.

The bypass diodes have multi functions, but the primary purpose is the protection against hot spot risk and cuts down the percentage destruction of defective cells. As common in manufacturing, one diode is needed for about 18 to 24 cells. Also, the bypass diode is able to decrease the negative voltage across the string as it operates in a reverse bias mode, thus the shaded cell that located in the affected string will be limit within the normal operation point of the bypass diode (0.8V).

2.3 PV Panels under Shading Effect

The position of the PV panel is a most important issue to get better output power. Therefore PV panels should be tilted in the right placement and suitable installation, and therefore the sunlight should strike the panel at day time while the sun is a peak in the sky.

Figure 2 shows the shade of a tree twig as it covered large parts of PV panels. Therefore, the study of the shadow of the solar cells is one of the hottest topics to determine the cell efficiency.

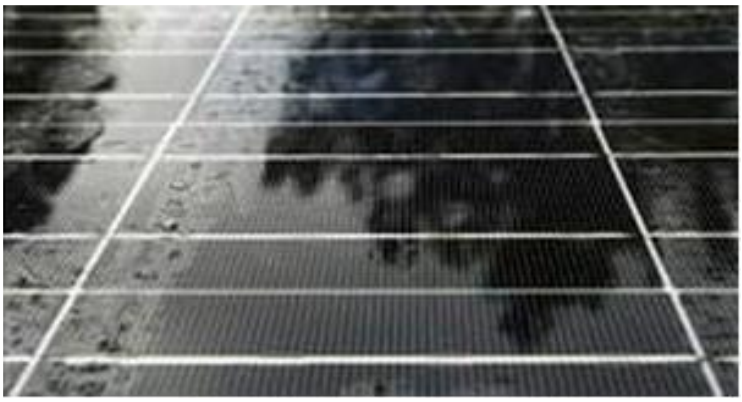

Figure 2: Shading by trees on PV panels

The output power efficiency of the panels depends on many factors. For example, array configuration, temperature, irradiation, and shadow, which cover the cell [15]. Shading considers the principal movement of the hot spot phenomenon, and as a consequence, the operation of the solar panels is severely affected by degradation in electrical characteristics of the PV module.

PV panels under shading condition suffer in their performance because:

- The total output power will diminish as the shaded cells operated in reverse biased so they dissipate power instead of getting power.
- The power dissipated in the single shaded cell would increase the temperature affecting surrounding cells and cause local heating. Thus increasing temperature may damage the cells that create high temperature inside the panel and leads to a hot spot phenomenon which results in the entire panel to be failed [14].
- Solar cell gets fully damaged when the cell is reached the breakdown voltage under a long time of shading [15].
- When a little part of the cell in the string is shaded, then the overall output power of the module approximately turns to zero.

Figure 3 (a and b) shows examples of partial and full shading covered individual cell, horizontal and vertical strings that could happen in the real world.

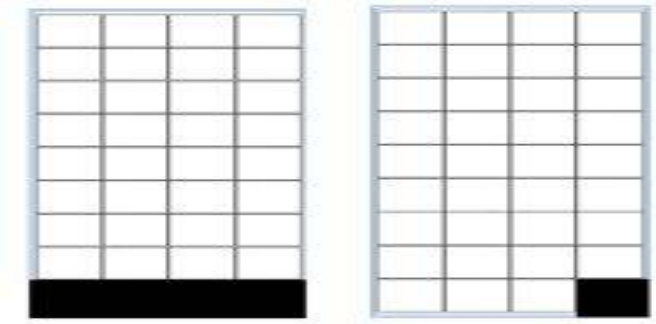

(a): Examples of full cell shading

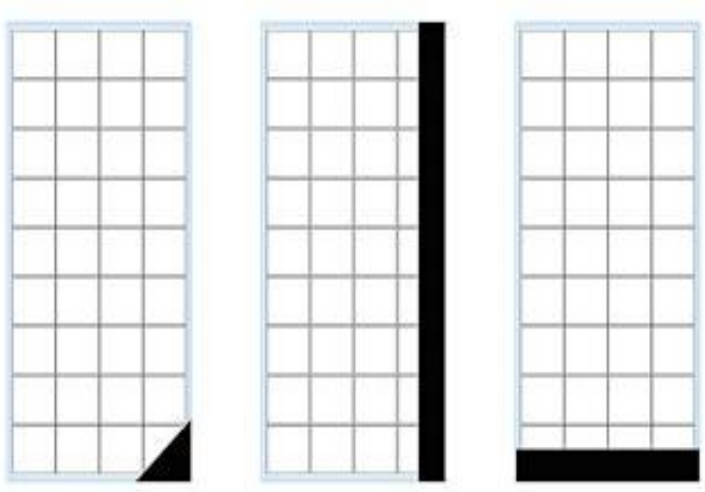

(b): Examples of partial cell shading

Figure 3: Different types of shading

2.4 PV Losses and Electrical Characteristics with Bypass Diode

The solar cell under shading has a harmful influence on the characteristics of the string. A defective cell with a lower current forcing the unshaded cells in the affected string to produce the same amount of current. Then the module current is limited by the defective cell, however the voltages reaming unchanged [15].

The shading effect on the I-V curve can be observed in figure 4 without the bypass diode. In the simplest mode, if three cells are serially connected and one cell is covered by half, 50%, the current produced by this cell has dropped by close to half of its nominal value so the current of the combined curve dropped similarly. The voltages of series cells are added and the current is dropped by a defective cell.

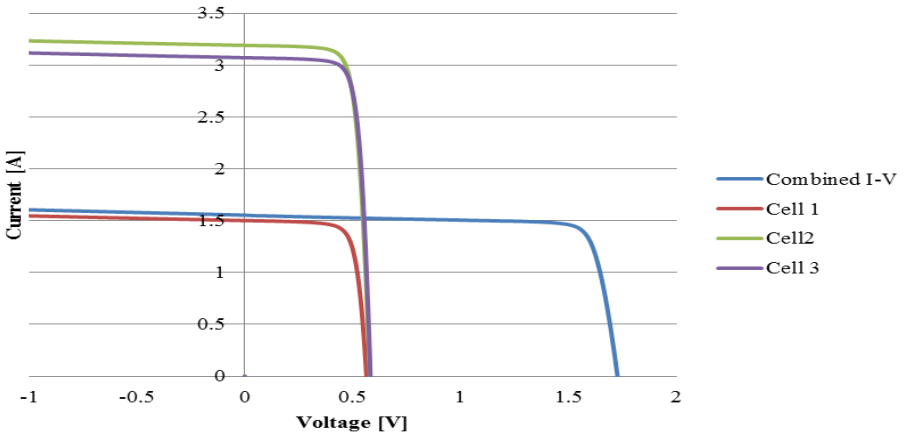

Figure 4: Partial shading impact on I-V of three cells [17]

The effect of shading patterns can be reduced by using bypass diode devices as illustrated in the previous section. The bypass diode is conducted when the negative voltage in the affected string is equal to the operating point of the diode voltage [16]. Figure 5 shows the connection of bypass diodes across three panels connected in series.

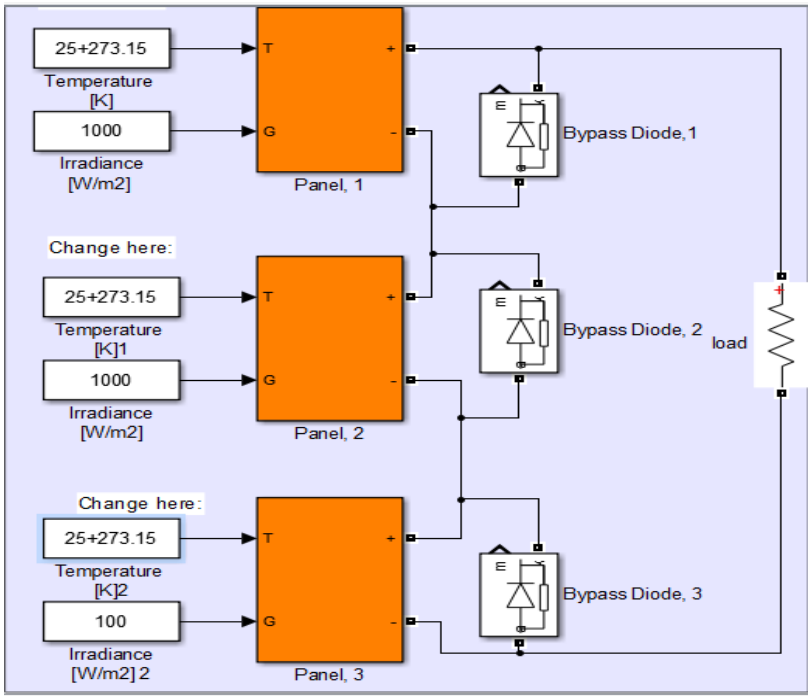

Figure 5: Three PV panels protected with bypass diodes

The conductivity of the bypass diode causes significant step in the I-V curve. The position of the step point corresponds to the behavior of the shaded cell with negative voltage [17] and the operating point of the bypass. In figure 6 the behavior of shaded one cell with 50% out of three cells with bypass diode can be understood. The final I-V curve has a stepping point referred to the activation stage in the forward bias of the bypass diode.

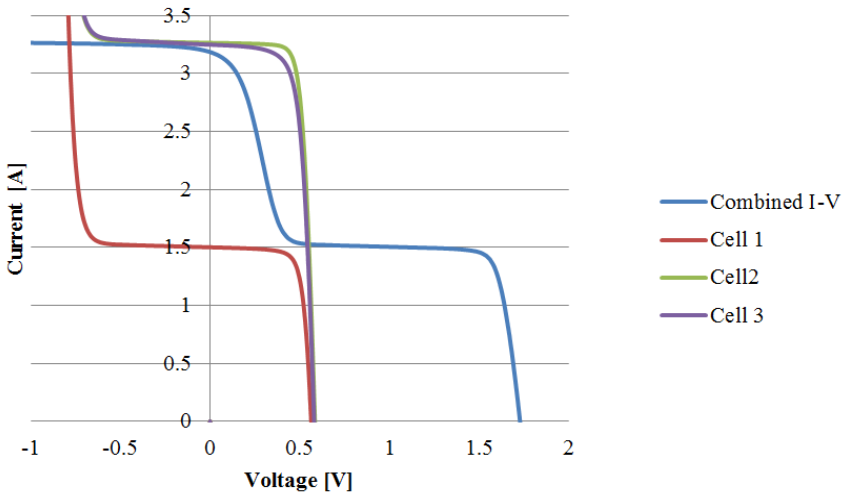

Figure 6: Partial shading impact on I-V of three cells with bypass diode [17]

As illustrated in the literature and figure 6, the diodes are usually used in panels to save them against the hot spot problem.

In figure 7, the load is tied between the ends of three strings which consist of a group of solar cells connected in series that worked under partial shading. I_1, I_2, and I_3 are photo-currents that flow in each string which proportional to the level of irradiation. Three bypass diodes are inserted in parallel corresponds to each string.

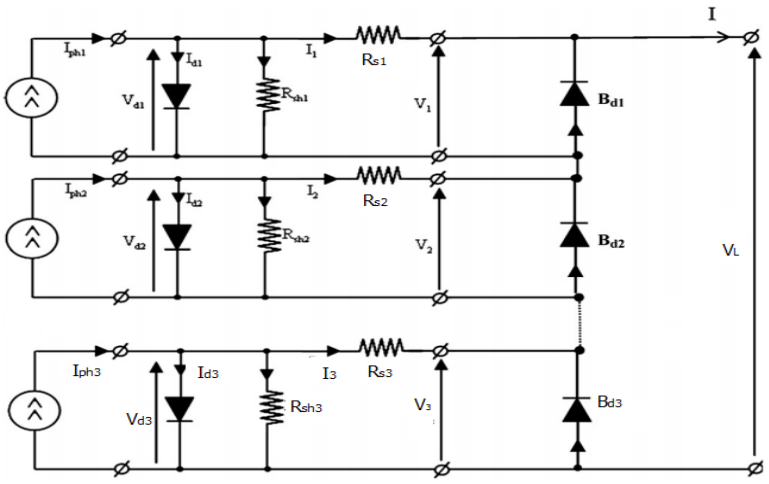

Figure 7: Equivalent circuit of three strings and bypass diodes [18]

The irradiation patterns are varied between these strings, where the first string has a full illumination of 1000 W/m^2. The second string working at half of full irradiation with 500 W/m^2, and the last one received a very low level of irradiation around 150 W/m^2. S_1>S_2>S_3 is corresponding to three levels of current strings I_1>I_2>I_3.

A total power transferred to the load is generated by a full illumination string S_1, but that amount of power is affected by the other strings, low illumination makes zero power contribution to the load however these strings are bypassed.

The following two graphical representations 8 and 9 show both electrical curves of solar panel consist of 72 cells connected in series with 3 bypass diodes under non-uniform illumination. The plots demonstrate how the protective devices behave under shading conditions. It introduces many steps in the current-voltage curve and many peaks in the power - voltage curve divided between global and local peaks depends on the string configuration of PV module and shading pattern distribution between them.

I-V and P-V curves are plotted at the standard test condition (STC) for temperature and different patterns for irradiation.

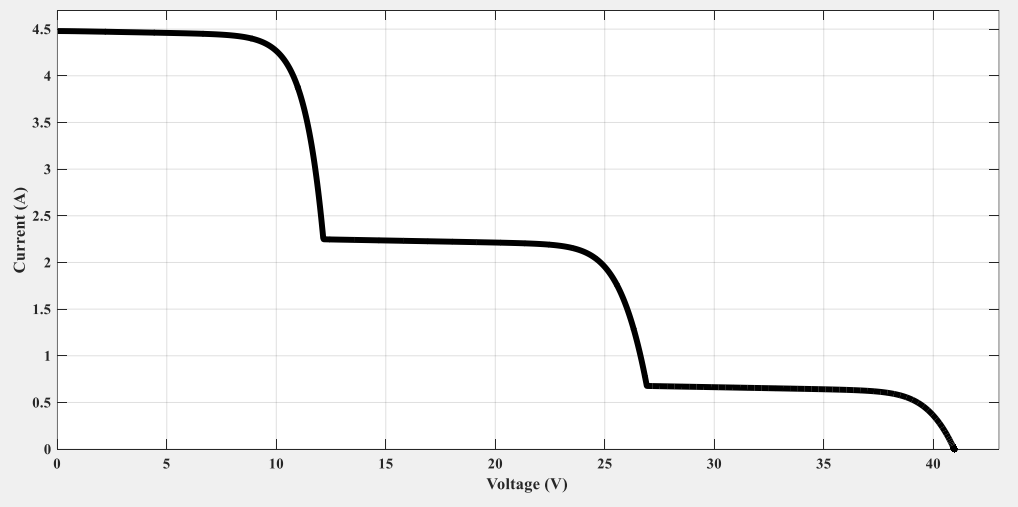

Figure 8: I-V characteristic of 72 cells under different partial shading patterns

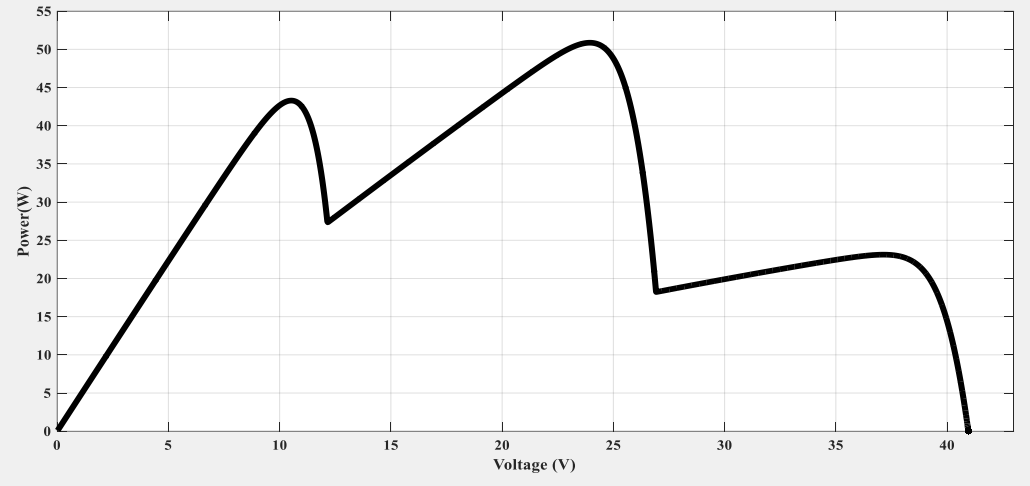

Figure 9: P-V characteristic of 72 cells under different partial shading patterns

From figure 9, it's clear that a large amount of power delivered to the load generated by highly irradiation level string, and the rest of power dissipated as a heat in shaded cells, so the use of bypass devices can enhance the reliability of the module and save the defective strings from damage and burn.

CHAPTER 3

PV Modeling and Parameters Extraction

3.1 Fundamentals of Solar Cell

PV modules are devices, which transform sunlight directly into electricity. The semiconductor material with a p-n junction is a main component of the crystalline silicon solar cell. Meaning that silicon crystal lattice is carried out by combining doping atoms in that lattice. For instance, boron atoms to produce a p-layer and phosphorus atoms to produce n-layer, thus p-n junction is produced and the free electrons in the n-layer diffuse into p-layer resulting in a depletion area to be established as described in figure 10-a.

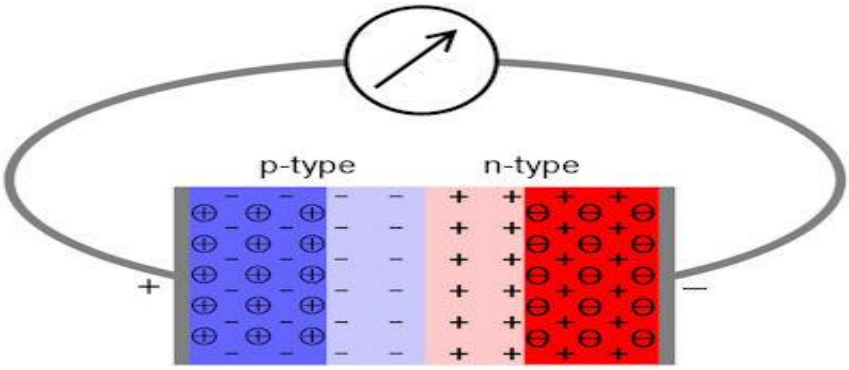

(a): Non-illuminated semiconductor p-n junction [72]

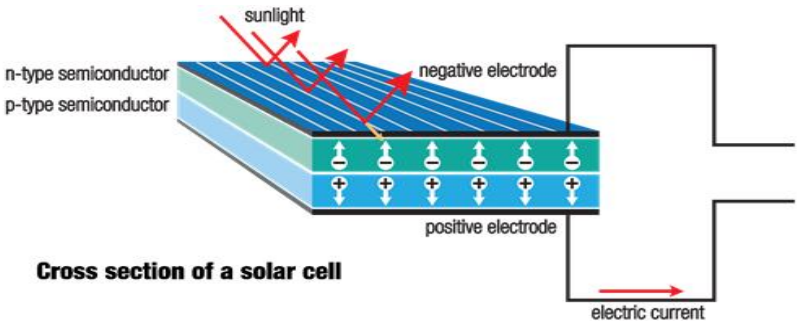

(b): Illuminated semiconductor p-n junction [20]

Figure 10: Illuminated and non-illuminated solar cell

Figure 10-b illustrates the illumination process and shows the behavior of p-n junction under sunlight, thus free electrons are drawn towards the n-layer while the holes leave in the opposite direction due to the electrical field. The voltage creates across the cell terminal due to the diffusion [20].

3.2 PV Model Equivalent Circuit

An ideal solar cell is described by a single diode connected in parallel with a photo-current source (figure 11-a). But for real solar cell, there are several circuits that include resistors connected in parallel and series. For instance, figure 11-b has a series resistance [20], figure 11-c has both parallel and series resistances [21]. Other cells contain two diodes connected in parallel as in figure 11-d [22]. The solar cell in figure 11-c is the most normally used in industrial applications. Moreover, the shunt resistance has a high value, but the series resistance has a low value to include the effect of the fill factor, thus the equivalent representation has a simple module equations and an accurate design to model a solar cell.

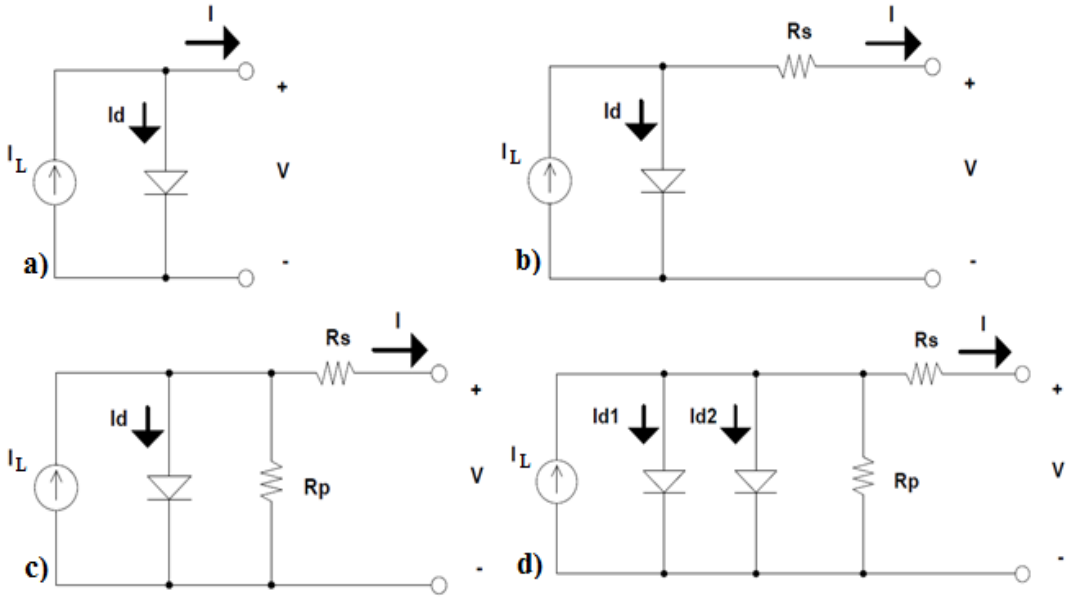

Figure 11: Equivalent circuits of solar cell presented in literature

3.2.1 PV Curves Description

The first curve that describes the electrical characteristics of the solar cell is called I-V curve. It can illustrate the electrical behavior of the real conditions of temperature and irradiance level. If the string operates under shadow conditions, the curve combined with current and voltage will describe the shaded influence. If the irradiance is uniform and there are no external obstacles, the I-V curve will be typically as depicted in figure 12 with a yellow color line. The second curve appeared in the same figure (blue color line) is indicated by the P-V curve, that describes the power transferred to the load and shows the maximum power point of the PV module.

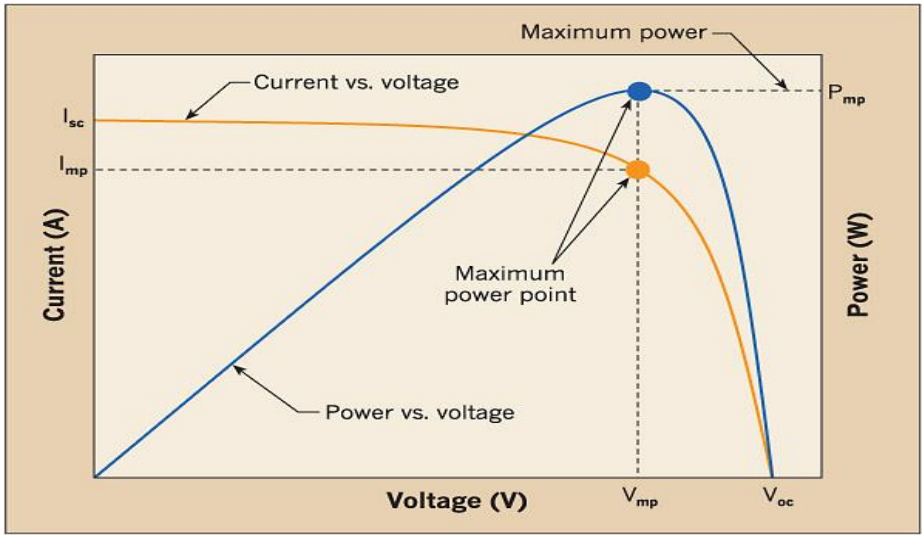

Figure 12: PV curves characteristics

<u>The key nomenclature utilized in the above curve is described as follows:</u>

- **Short Circuit Current (I_{sc})** – It is the maximum current in ampere delivered by the cell under specific conditions of ambient temperature and irradiance i.e. the output voltage is zero when the load is short-circuited. The output energy at this condition equals zero.

- **Open Circuit Voltage (V_{oc})** – Represents the cell's voltage under specific temperature and light, i.e. the output current is zero, thus V_{oc} is the voltage when the load is open-circuited. The output energy at this condition equals zero.
- **Maximum Power (P_{max})** – It is the maximum power that can be generated from the cell under specific conditions of the environment. The point of the I-V curve at which the current and voltage have the highest values is called Maximum Point (MP).
- **Current at Maximum Power (I_{mp})** –The current that causes in maximum energy.
- **Voltage at Maximum Power (V_{mp})** – The voltage that causes in maximum energy.
- **Fill Factor (FF)** – Indicates to the percentage value of maximum power to the total power produced by V_{oc} and I_{sc}.

3.3 Extraction of PV Parameters

3.3.1 Modelling Techniques in Literature

Several papers discuss the simulation and modeling of solar cells, models, and systems. The panels have been changed and enhanced for different understandings of research. For example, in [23] a module is utilized to estimate whether bypass and blocking diodes are usually connected and used, both [24] and [25] dealing with the shadowing effects on the PV panels and determine the output force.

A practical PV cell is traditionally consists of a photo-current source, one parallel diode, two types of resistance divided into series and shunt. As illustrated in figure 13, a practical model of the solar cell.

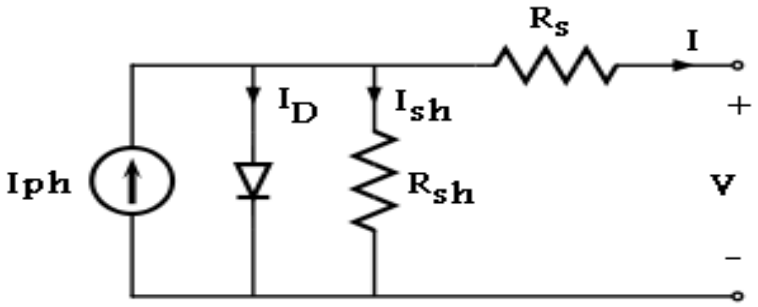

Figure 13: Practical circuit of a solar cell [25]

The equivalent circuit shown in figure13 is called the single-diode model is used in this work because it achieved more accurate during the simulation when dealing with shading and the hot spot phenomenon.

The single diode solar cell has been applied to various reasons. The reliability and efficiency of PV cells with the type of mono-crystalline silicon were modeled in [26-27] that need some modifications to estimate the behavior of solar cell parameters. The voltage depends on the photo-current in amorphous silicon type is presented in [26]. In references [28, 29] the complexity of the circuit is decreased by the ignored the value of the shunt, but that scales down the accuracy of the entire module.

3.3.2 Equivalent to Series Configuration Parameters

In this study, a series connection of a single solar cell is utilized. The simulation process of PV panels is always dealing with simulate one or more solar cells. Thereby, these cells are included in sub models or strings to give a whole panel. In a pragmatic mode, it is not possible to determine the parameters for each individual solar cell. Thus, in the event of a huge number of cells, such as hundreds or possibly thousands of PV cells, the scaling process is needed to scale the five parameters of solar cell, where the parameters are

sunlight current Iph, diode saturation current Io, diode ideality factor m, series resistance Rs and finally shunts resistance R_{sh}.

The method used here depends on the assumption that all of the cells within a panel are the same and have similar specifications and exposure to the same environmental conditions. The technique is used extensively in literature is illustrated in reference [30]. Figures 14 (a and b) show the diagram of a series configuration and its equivalent representation.

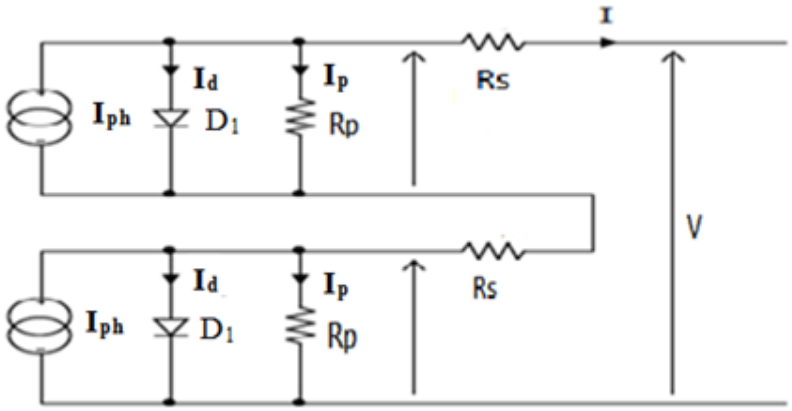

(a) Two serially cells

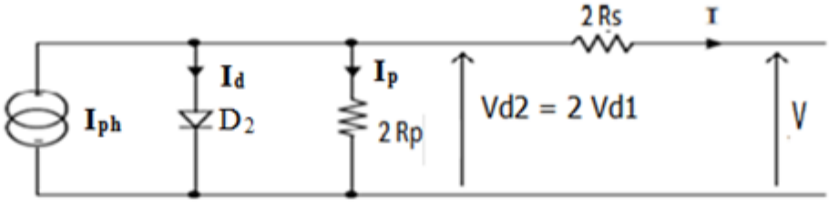

(b) Equivalent configuration

Figure 14: Circuit representation of (a) two cells and (b) equivalent parameters

The parameters referred to currents, I_{ph}, I_d, I_p and I are still not changed after scaling process and having the same values in a single representation and scaled circuit. Therefore, the output voltage of the module consists of adding the individual operation voltage cell, so the voltage across diode V_d and voltage drop in R_s of the scaled circuit must be twice the

value of the cell as illustrated in figure 14-a. Finally, the resistances R_s and R_p of the scaled circuit should be twice of the single cell resistance.

Because of the non-linear relation of the diode, the method of scaling D_2 parameters to maintain I_d is not easy. Thereby to equate this parameter, the Shockley diode relation is used in both circuits in figure 14 and equated to give the following relation:

$$I_O\left(e^{(q\,Vd1/mKT)} - 1\right) = I_O\left(e^{(qVd2/mKT)} - 1\right) \quad (3\text{-}1)$$

To preserve the diode current, the exponential terms in the pervious relation must be the same, so for the scaled equivalent representation a factor of diode 2 is brought into the denominator to decrease V_{d2} to V_{d1}.

3.3.3 Mathematical Representation of Five Parameters PV Model

In this section, 5 parameters of PV model are described to form the shape of the I-V curve. In this study extracting these parameters is needed, especially Rsh and Rs to converge the model to be outfitted with the experimental works. The approached used, is derived from [31].

The process of extraction parameters depends on the iterative approach called Newton's method that illustrated in [32]. The operating values of the solar panel are used as input data, the open and short circuit points also a maximum of both voltage and current can be found in the manufacturer's datasheet or from experimental works. The algorithm depends on a much iterative for evaluating the values of resistances and built the characteristic curves to converge around the maximum operating points at standard test conditions [31].

3.3.3.1 I-V Curve Equation of PV Model

As shown in figure 13, it is possible to apply Kirchhoff current law. So the mathematical equations of the currents through each branch in the cell is described as follows:

$$I = I_{ph} - I_D - I_{sh} \quad (3\text{-}2)$$

Where I_{ph} is the photo-current. I_{ph} varies linearly with irradiation at a specific temperature of the cell. I_d is the current passing across the diode, which gives the non-linear relationship for PV model. I_{sh} is the current thought parallel resistor branch. Each current has relevant relation so substituting these expressions, we have:

$$I = I_{ph} - I_o \left[e^{\frac{V+I.R_S}{m.V_t}} - 1 \right] - \left[\frac{V+I.R_S}{R_P} \right] \quad (3\text{-}3)$$

$$V_t = \frac{K.T}{q} \quad (3\text{-}4)$$

Where: I and V are the output current and voltage through a specific load respectively, m is diode ideality factor, V_t is thermal voltage, q is the electron charge equals to 1.602×10^{-19} C, k is the Boltzmann constant equals to $1.3806503 \times 10^{-23}$ J/K), and T is temperature in kelvin.

The solar panel is commercial consists of a number of cells connected in series. N_S indicates to the number of series cells for one panel. For instance, in this study, $N_S = 72$ for solar panel

The output current of the model has the following mathematical equations:

$$I = I_{ph} - I_o \left[e^{\frac{V+I.N_S*R_S}{m*N_S.V_t}} - 1 \right] - \left[\frac{V+I.N_S*R_S}{N_S*R_P} \right] \quad (3\text{-}5)$$

With:

$$I_{ph} = [I_{sc} + K_i (T_c - T_{ref})] \, G/G_{ref} \quad (3\text{-}6)$$

Where I_{sc} is the photo- current at STC (25 °C and 1000W/m^2), T and T_{ref} represent the ambient and nominal temperatures [Kelvin], G [W/m^2] is the illumination level, G_{ref} is the nominal illumination and the temperature coefficient K_i of I_{sc}.

The saturation current I_0 according to the temperature effect could be written as (3-7) [33], [34], [35], [36]:

$$I_o = I_{o,ref} \left(T_{ref}/T\right)^3 exp \left[\frac{q\, E_g}{m\, K}\left(\frac{1}{T_{ref}} - \frac{1}{T}\right)\right] \quad (3\text{-}7)$$

Where E_g is the band gap energy of the diode, and $I_{0,ref}$ is the reference saturation current at nominal conditions.

$$I_{o,ref} = \frac{I_{sc,ref}}{\exp\left(\frac{V_{oc,ref}}{m * V_{t,ref}}\right) - 1} \quad (3\text{-}8)$$

The saturation current I_0 of PV cell depends on both dark current density of the diode and the cells area effective [39].

3.3.3.2 Parameters of PV Model

Prior to an equivalent circuit of the PV model, it is important to explain the remaining necessary three parameters and how they vary with environmental conditions.

a) Ideality Factor (m)

The parameter m is considered the first unknown of the solar cell. In this study, m is supposed to rely on the PV's material and be independent of environmental conditions. Thereby the value of the m may be arbitrarily assumed. Many papers explain how to evaluate the accuracy value of this parameter [40]. Usually, it lies in the range of 1 and 1.5 and the selection depends on the remaining parameters to adjust the shape of the current-voltage curve. Many values for m are found in reference [38] according to the analysis of empirical data. And then any initial value of m can be assumed that capable of adjusting the curve of the solar cell. The accuracy of the I-V curve can improve by varying this parameter.

The open circuit voltage of the cell is changed with this parameter, so if it increased the V_{oc} increased. The ideal value of the ideality factor is equal to one, but the practical value for silicon solar cell lies between 1 and 2. Green (1992) [40] says that ideality factor takes a value between 1 and 2; high currents that mean being near 1, and low currents indicate rising towards 1.5. The ideality factor variation and influence on the I-V curve is illustrated in figure 15.

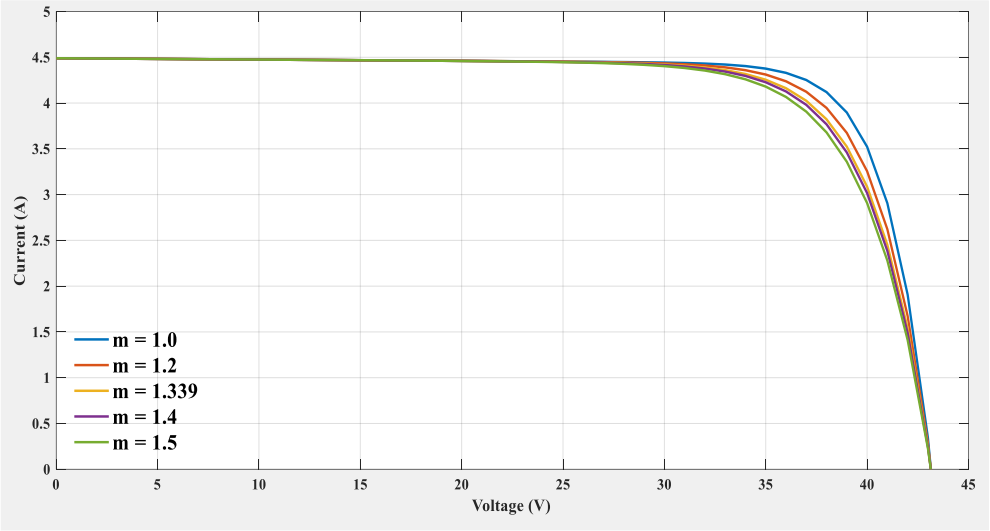

Figure 15: I-V curves with different ideality factor

b) Series and Shunt Resistances

The degradation in efficiency can be seen from these two parameters. High power dissipation across the parallel resistance (R_{sh}) under non-uniform irradiation, also some power lost in series resistance (R_s) and hence the efficiency of the PV panel is decreased. When the PV cell is ideal then R_{sh} has an infinite value and R_s tends to zero, also there is not an alternate path to current flow that causes loss power. Figure 16 displays the relationship between these two resistances. If decreasing R_{sh}

and increasing R_s that will change the shape of the I-V curve and the result of reducing FF as well as P_{max} delivered to the load. [41].

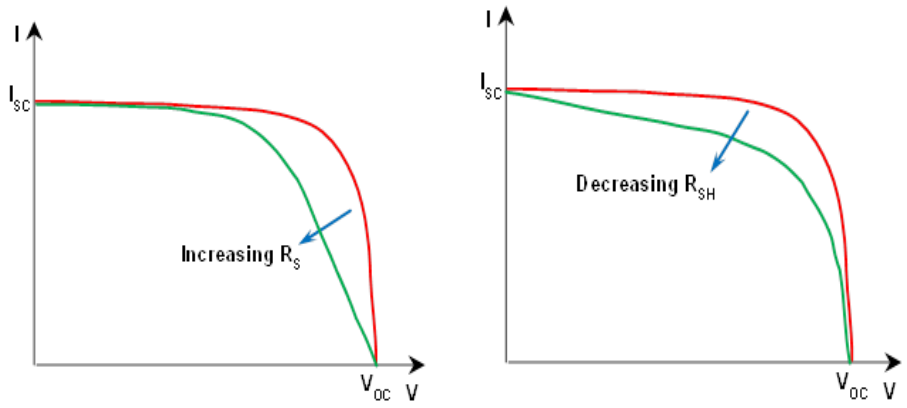

Figure 16: The influence of R_{sh} and R_s on I-V curve [40]

Several ways have proposed determining these resistances mathematically. Having mathematical equations seems to be useful to estimate these parameters. Any formula for shunt and series resistances must rely on experimental data analysis.

In literature, some researchers state that varying series resistance in an iterative method, increasing the value of R_s until the curve of current-voltage tends to the experimental results and then change shunt resistance in the same way. This method is weak and missing the accuracy in order to fit experimental data, because both resistance may not be set individually if a suitable current-voltage curve is reached. This work suggests an approach for adapting R_s and Rsh based on the maximum points found by manufacturer datasheet specifications that give $P_{max} = V_{mp}*I_{mp}$ at the maximum point of the I-V curve. Many research methods found in the literature proposed an approach to evaluate parameters that ability to adjust the I-V curve and don't care about the P-V curve. Therefore, two curves must fit the experimental data at the same time and at the same operating points. The

method in [42] indicated to match the P-V curve, but with different ways. In [42] for instance, the authors neglect the Rs value.

The relation between both resistances may be calculated by adjusting $P_{max,m} = P_{max,e}$ (model and experimental) and solving by the iteration method. The following two formulas can be used for evaluating the maximum power and then the shunt resistance.

$$P_{max,m} = V_{mp}\left\{I_{ph} - I_o\left[\exp\left(\frac{q}{KT}\frac{V_{mp}+R_s I_{mp}}{m\,N_s}\right)-1\right]-\frac{V_{mp}+R_s\,I_{mp}}{R_{sh}}\right\} = P_{max,e} \quad (3\text{-}9)$$

$$R_{sh} = \frac{V_{mp}+I_{mp}\,R_s}{V_{mp}\,I_{ph}-V_{mp}\,I_o\exp\left[\frac{V_{mp}+I_{mp}\,R_s}{N_s m}\frac{q}{KT}\right]+V_{mp}I_o-P_{max,e}} \quad (3\text{-}10)$$

Formula (3-10) indicates that both resistances vary at the same time to give the matching equalization between $P_{max,\,me}$ and $P_{max,e}$ in order to produce an accurate I-V curve cross the maximum point. The estimation process of both resistances that operates at the maximum point of the mathematical power-voltage curve agrees with the experimental maximum point. This needs iteration process until reach $P_{max,m}=P_{max,e}$. Each iteration step gives new values of R_s and R_p up to build the best I-V and P-V curves. Two initial values are needed for both resistances so the initial value of R_s is zero and the initial value of shunt resistance is calculated by:

$$R_{sh,min} = \frac{V_{mp}}{I_{sc,ref}-I_{mp}} - \frac{V_{oc,ref}-V_{mp}}{I_{mp}} \quad (3\text{-}11)$$

Figure 17 describes the flowchart of the iterative method algorithm that used in this study.

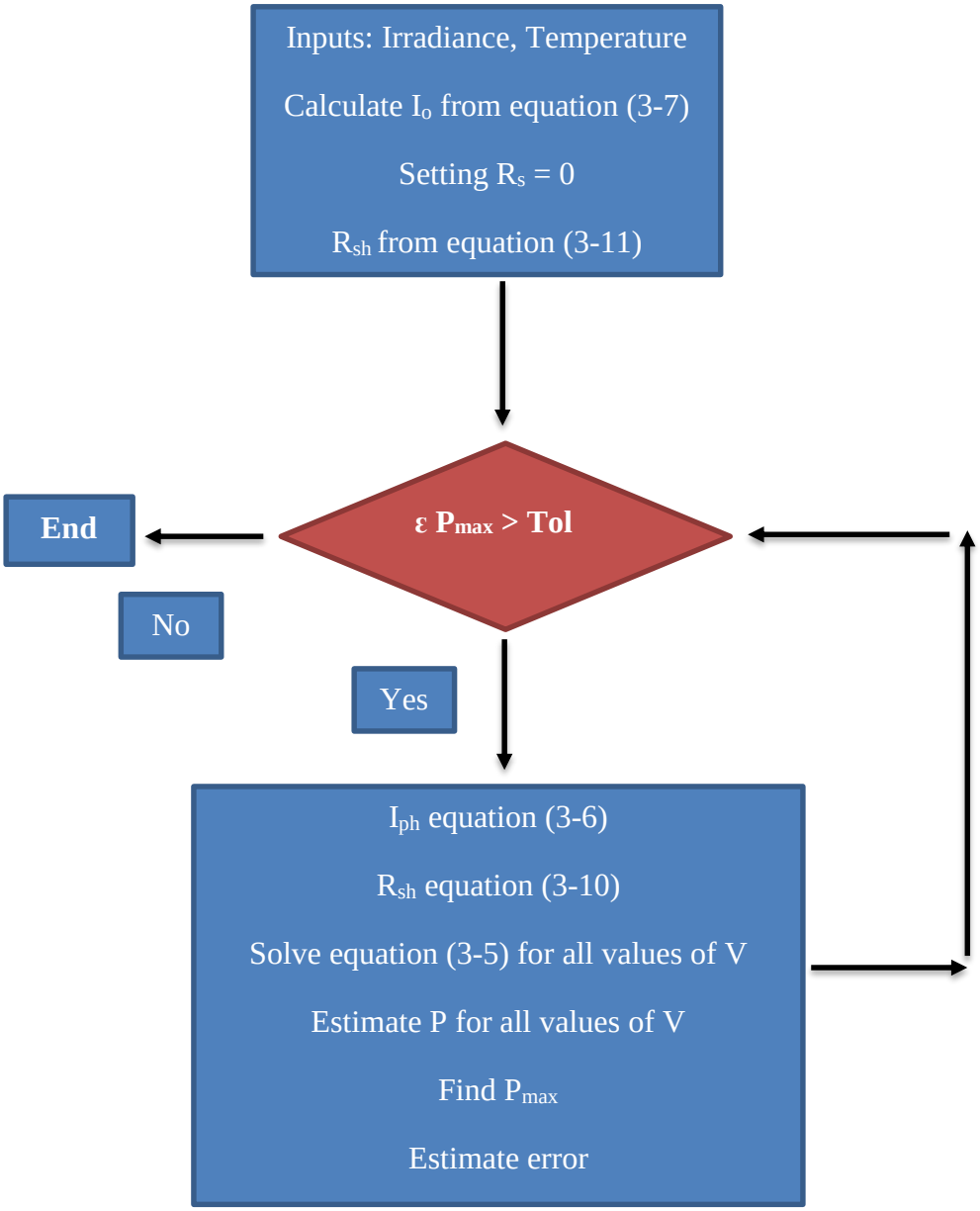

Figure 17: Flowchart algorithm of the proposed approach [31]

In this study, the NSS-24150MPV panel is selected for simulating and modeling in MATLAB / Simulink. In NSS-24150MPV, there are 72 monocrystalline silicon cells connected in series and its P_{max} 150 watts. Table 1 summarizes NSS-24150MPV panel electrical specifications.

Table 1: Electrical specifications of NSS-24150MPV panel at 25 ^{o}C, 1000 W/m^2

N_S	72
I_{mp}	4.16 A
V_{mp}	36 V
$P_{max,e}$	150 W
I_{sc}	4.49 A
V_{oc}	43.2 V
K_V	- 0.2 V/K
K_I	$3.15e^{-05}$ A/K

The iterative approach written by Matlab M-files gives the solution for both resistances is dependent on the proposed method. These values have satisfied the condition of maximum points corresponding to the maximum power. The following table includes the solution of the iterative process with five PV parameter model.

Table 2: Five parameter estimation of NSS-24150MPV panel at 25 ^{o}C, 1000 W/m^2

I_{ph}	4.49 A
m	1.34
R_{sh}	693.73 Ω
R_s	0.074 Ω
I_o	$1.21e^{-07}$A
V_{oc}	43.2 V

Figures 18 and 19 describe both curves of the NSS-24150MPV panel modeled with the proposed approach. The three remarkable points provided by the manufacturer are matched by two curves exactly: V_{oc}, I_{sc} and the maximum point of voltage and current.

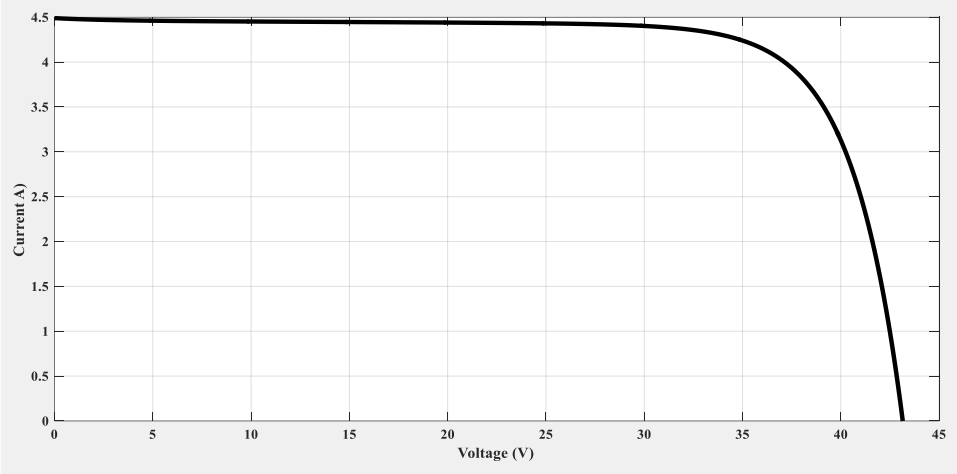

Figure 18: I-V curve of NSS-24150MPV panel

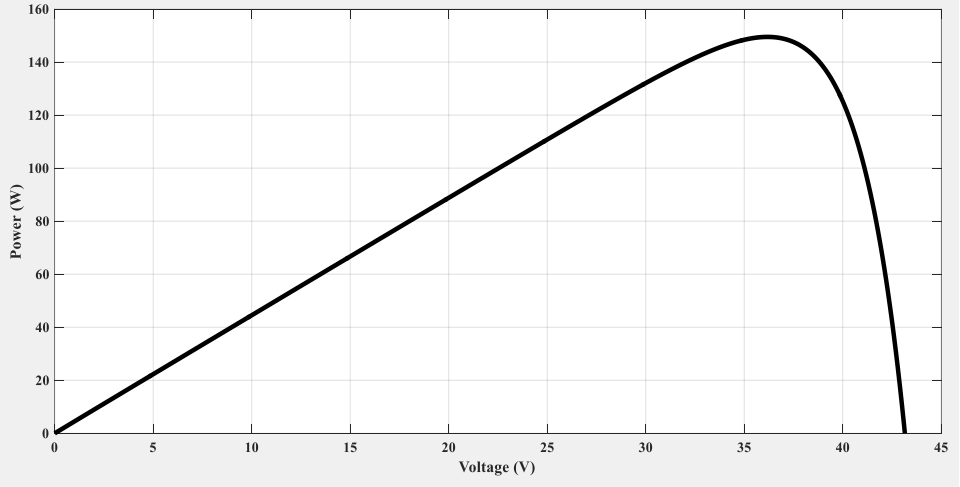

Figure 19: P-V curve of NSS-24150MPV panel

Figures 20 and 21 describe I-V and P-V curves for NSS-24150MPV panel working at a nominal temperature of 25 ˚C and five levels of illumination: 1000 W/m^2; 800 W/m^2; 600 W/m^2; 400 W/m^2; and 200 W/m^2.

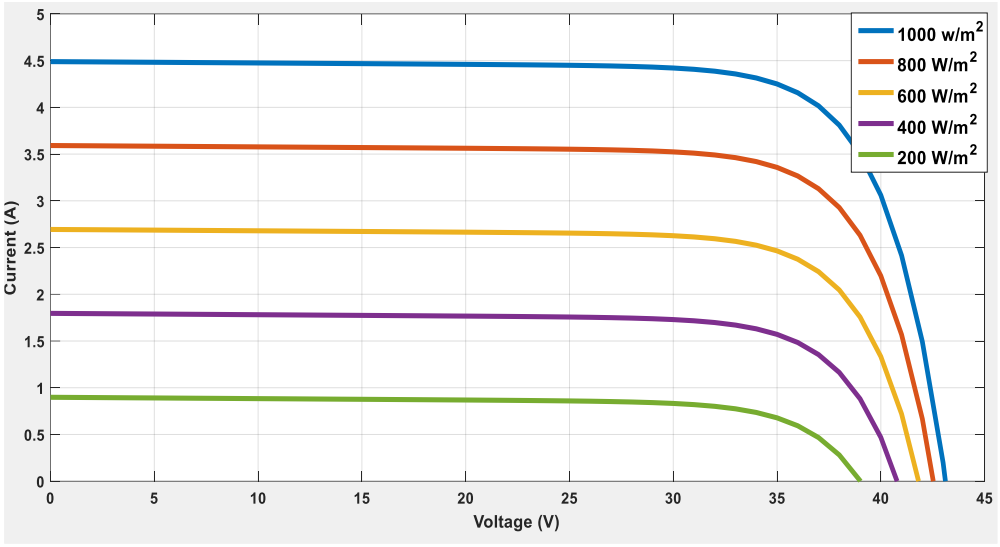

Figure 20: I-V curve of NSS-24150MPV panel at five levels of illumination

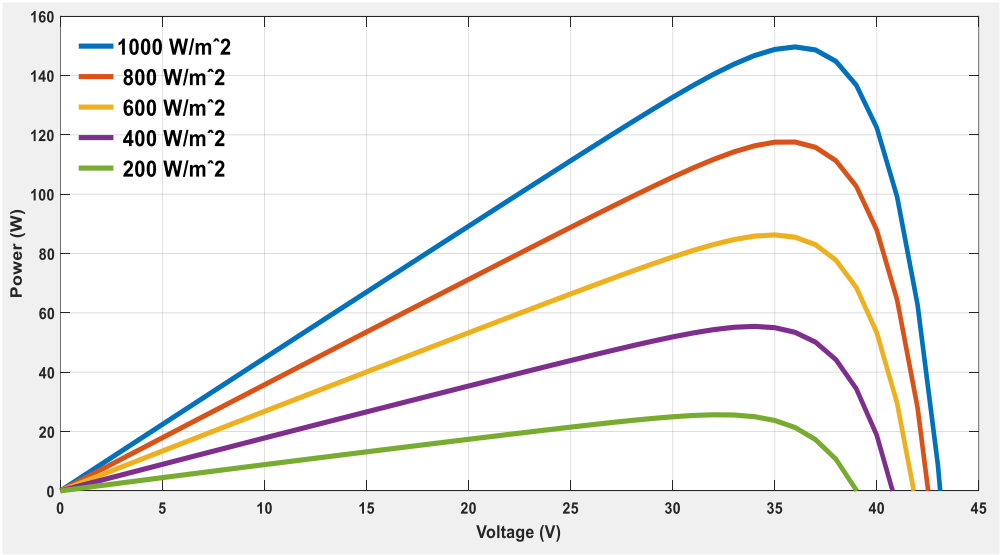

Figure 21: P-V curve of NSS-24150MPV panel at five levels of illumination

Figures 22 and 23 show both curves for NSS-24150MPV panel working at five different temperature conditions: 0 ˚C; 25 ˚C; 50 ˚C; 75 ˚C and 100 ˚C and at the illumination of 1000 W/m^2.

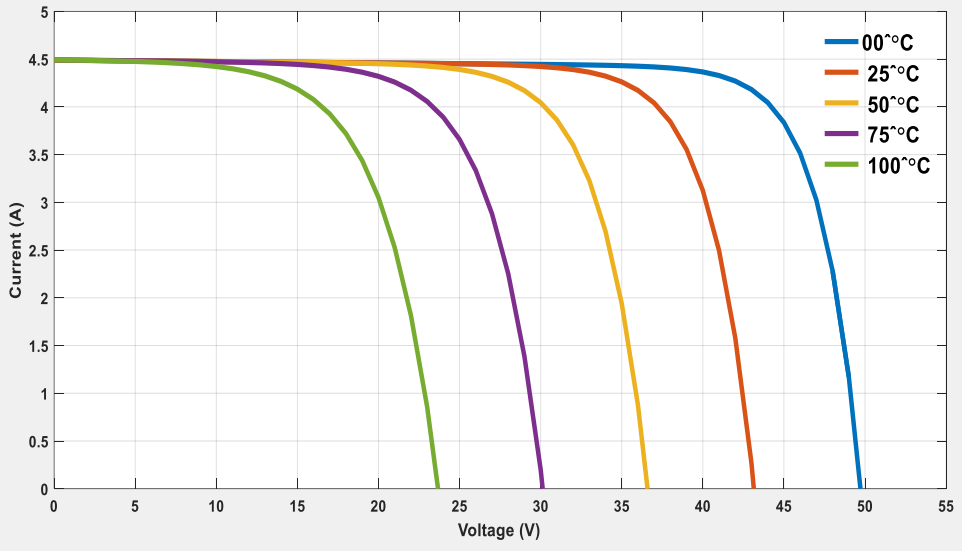

Figure 22: I-V curves of NSS-24150MPVtemperaturesive different temperature

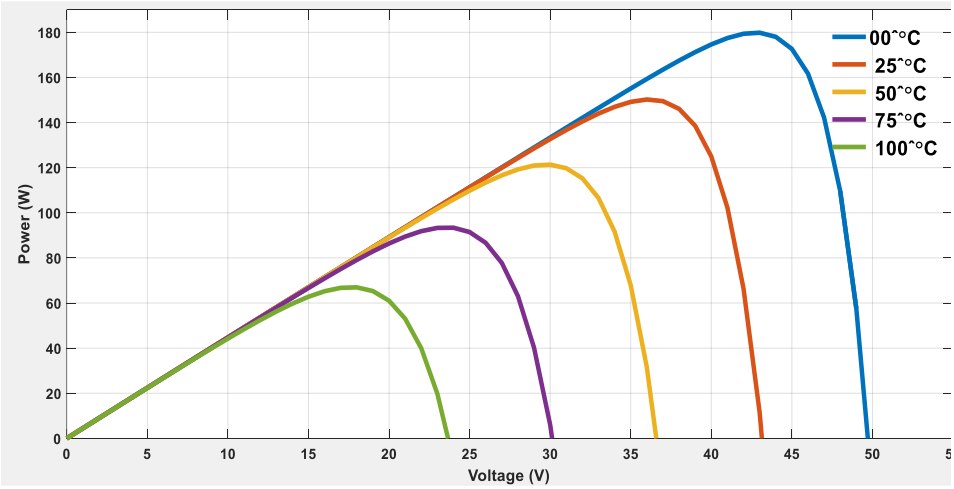

Figure 23: P-V curves of NSS-24150MPVtemperaturesive different temperature

Figures 20, 21, 22 and 23 demonstrate that characteristic curves dependent on irradiance levels and various temperatures for a sample panel. The behavior demonstrated from these figures, is that the strong effect of irradiance variations on I_{sc} and the temperature variations on V_{oc}.

Appendix A contains all Matlab M-files scripts that used to obtain the variety of irradiation and temperatures on the characteristics of PV panel. Also, scripts used to extract five

parameters of the PV module from datasheet values depending on algorithm explained in the flowchart in figure 17.

3.4 Temperature of Solar Cell

As the ambient temperature change, the cell temperature also changes, therefore the changing reflect on the behavior of the cell as well as changes in the power amount transferred to the load. Formula (3-12) evaluates the temperature of solar cell [43].

$$T = T_{amb} + \left(\frac{NOCT - 20\,℃}{.8}\right) G \tag{3-12}$$

Where NOCT indicates to the nominal operating cell temperature given by the datasheet of the panel, T_{amb} is the ambient temperature and G refers to the irradiation.

NOCT is known as the temperature achieved by open circuited cells in a panel under the conditions as depicted below: [73]

1. Irradiance = 800 W/m^2
2. Ambient temperature = 20°C
3. Speed of wind = 1 m/s

In this study, NOCT is selected equal to 45 ^{o}C, this value is found from the range of the NOCT in the market that lies between 44 and 48. The best modules have low NOCT around 32 ^{o}C and the worst case has 55 ^{o}C. Then it's a really significant tip to check the NOCT values [73].

In the next chapter, the hot spot phenomenon is explained and studied, it will understand that how the shunt resistance is playing an essential purpose in creating and developing the hot spot problem and what happened due to the fluctuations of the shunts in the reverse bias region.

CHAPTER 4

HOT SPOT PHENOMENA MODELING AND SIMULATION

4.1 Literature Survey

Hot spotting phenomenon in a series string of PV panel is a result of the mismatch. As the PV string working under partial or full shading may cause the panel destruction and power degradation.

IR image is taken of the PV string under non-uniform illumination. Figure 24 displays hot spotting problem in a part of the affected cell. Very high internal temperature resulted and has the ability to damage and destroy the whole panel, which decreases solar cells output power [44].

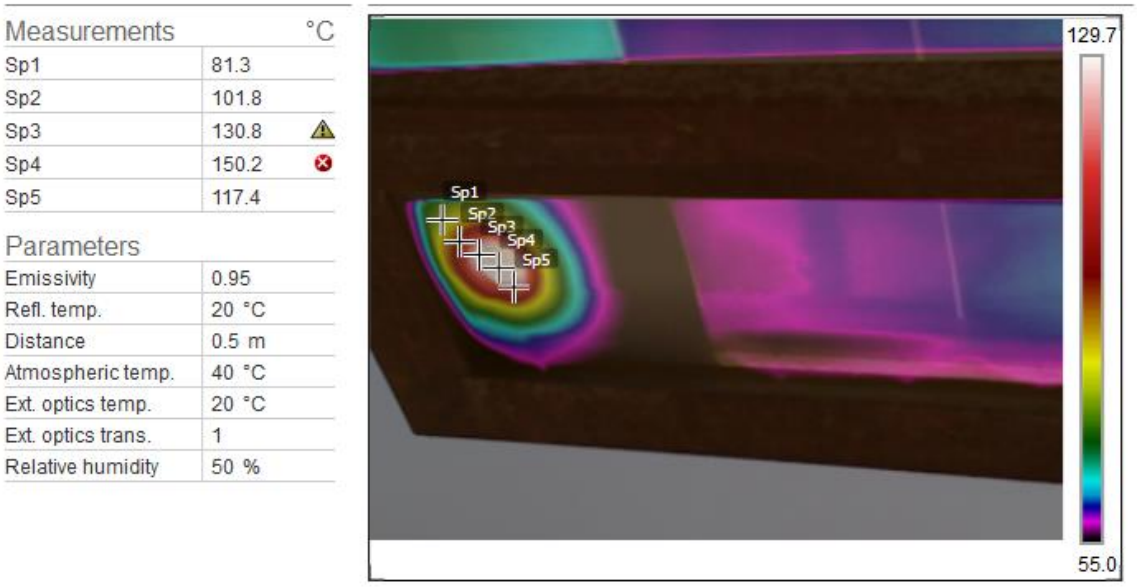

Figure 24: Thermal image of hot spotting

Several methods have been proposed to detect hot spots. Authors in [45] suggest sensor that was able to send a signal to the monitor or system operator, therefore, that sensor has the same inclination of cell angle. The function of that sensor is submitted feedback signal

if the hot spot occurred in the defective cell but this approach is very expensive. Another detection procedure of the hot spot is established in [46], which monitoring the behavior work and energy produced by the PV panels and submit the data to a system operator that analyzes data and directly identify the hot spot locations in the modules.

Reference [47] emphasize the avalanche breakdown of the PV cell, therefore, a cell is working in the reverse bias region and reaches breakdown voltage, so a part of the current passes across the defective cell. A phenomenon can happen called second or thermal breakdown as a cell temperature increase [48].

In paper [49] authors study and monitoring the localized shunt in a solar cell, resistive solder bonds in field aged panels, bypass diode functionality of the panel, the hot spot phenomenon, temperature distribution curve through the panel and charging process of batteries.

Reference [50] presented the hot spot analysis of a solar cell with a type of crystalline silicon with a new method to enhance the reliable and fast testing that can be used as a final test in the module production. The hot spot effect is identified by IR thermography and depends on climate variations, wind velocity, and irradiance. Leakage current density is a function of the maximum temperature of fully and partially shaded cell. The maximum temperature takes the leakage current density as a linear dependence correlated with hot spot and this reverse current reflects a much better evaluation of the hot spot risk that can damage the cell during its operation.

Paper in [51] showed that cracks, poor cell matching, localized soiling and shadowing can cause hot spots. Bypass diodes are encouraged to protect the cells by reducing the reverse voltage between cell terminals to less than - 10 V. When the bypass diode fails to work,

the hot spot can occur. When the shunt resistance is very low the overheated occurred at -10 V before the diodes turn on.

Reference [52] authors proposed a model able to detect host spot risk and isolate the abnormal panel directly by using electronic relay circuit until shading removed then the panel back to work. The panel parameters are tested and achieved three conditions: (i) full illumination, (ii) partial / total shading without isolation (iii) partial / total shading with isolation. This method protects the panel from permanent damage and improves the reliability and efficiency of output power.

Paper [53] discussed some procedures used to estimate the overall output power of PV panels. IR image camera hanged on quadrocopter and used for monitoring the installation of PV panels, thus a quick method to observe hot spots in large PV plants.

Researcher [54] investigated a new approach to detect a hot spot in real time by a method depends on the two fixed values of PV panel. These values are voltage and hot spot index. The current change rate formula is derived to determine hot spot and normal cells of the PV system.

Paper [55] proposed a method using image processing algorithms (Gaussian filter, median filter, and edge detection) to analyze the IR image of PV cells. This method helps to obtain the temperature increasing locations of the cells and to detect the affected hot spotting cells.

Reference [56] represented a model describes the reverse bias mode of PV cell. The study of avalanche mechanisms helps to establish this model. PV cells with reverse bias are dominated by both avalanche mechanisms and shunt resistance.

In paper [57] authors studied the thermal behavior of PV cells and established the model of the hot spot condition. The model is capable of dealing with the temperature increased

and evaluated a cell temperature, thus estimate the degradation of output power. A fully and partially shade cases are applied to the proposed module. A partially shaded is more dangerous than fully shaded affected PV cells.

Paper [58] observed 200 affected panels. Many tests are accomplished to investigate hot spot locations. Visual and IR image inspection, electroluminescence, peak power and operating voltage methods are performed. Experimental results based on IR inspection emphasized that the irradiation should be greater than 700 W/m^2 and analysis performed in the summer semester with the highest ambient temperature and write the linear relationship between temperature and irradiance.

4.2 Hot Spot Phenomenon Formation and Principle

4.2.1 Effects of Shunt Resistance of PV Cell

Many types of research show that a low parallel resistance affects the efficiency, fill factor, voltage, and current [59]. A fixed series resistance and different values of the shunt resistance lead to different effects on the I-V curve characteristics of the panel. Figure 25 describes the drop in the panel's voltage as the shunt resistance, reduced of the NSS-24150MPV model. However, if the shunt resistance lost its highest numerical value, the degradation accelerates the hot spot development over the whole panel due to the current flow in the shunt path.

The relation between shunt resistance and output power of the NSS-24150MPV panel is shown in figure 26. The same figure shows that the efficiency dropped as a shunt resistance decreased. In conclusion, the total power dissipated with very low shunt resistance [59].

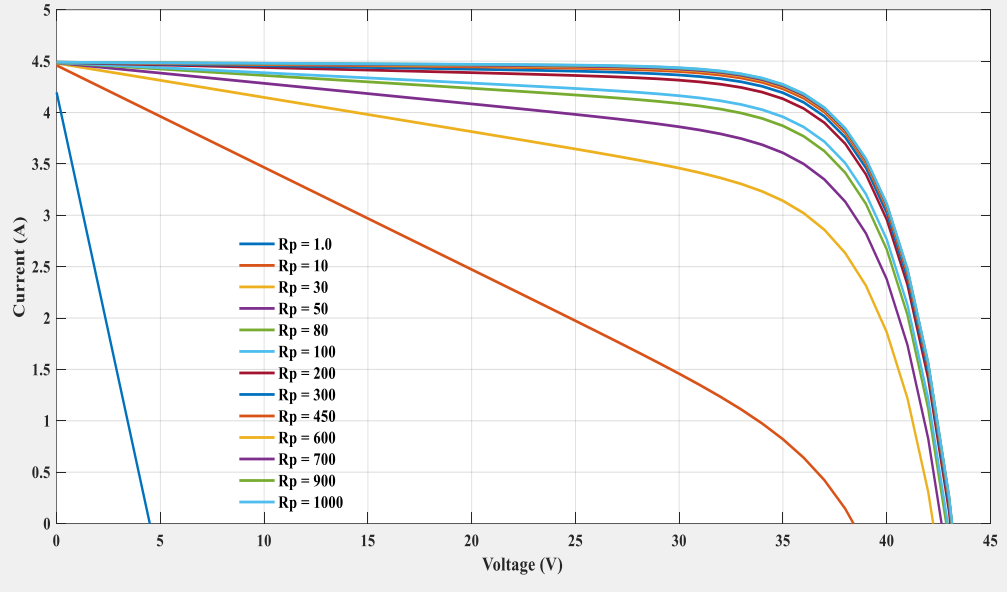

Figure 25: I-V curves with various shunt resistance

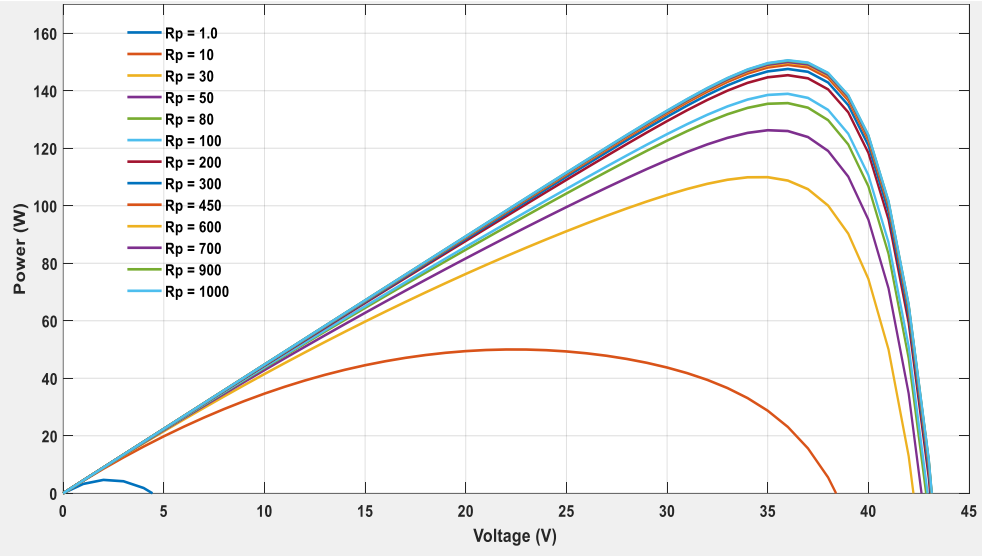

Figure 26: P-V curves with various shunt resistance

4.2.2 Hot Spot Principle

In the PV systems, the hot spot phenomenon happens when one cell or more of series connected cells in a string is working in the negative region. Physically, it happens when a single cell as shown in figure 27 is covered by an external object and produced current not

equal to the string current, thereby gives less than the string's current that leads to localized heat up area consequently the defective cell behaves as internal resistive load and consumes an amount of power [60].

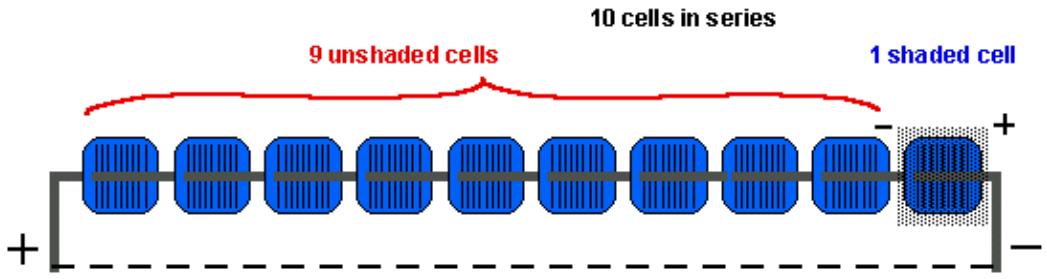

Figure 27: A string with one shaded cell [61]

This type of mismatch has occurred when any cell of the string is shaded and leads to produce less current of a string and can cause breakdown voltage of the defective cell and structural problems such as glass surface broken as shown in figure 28.

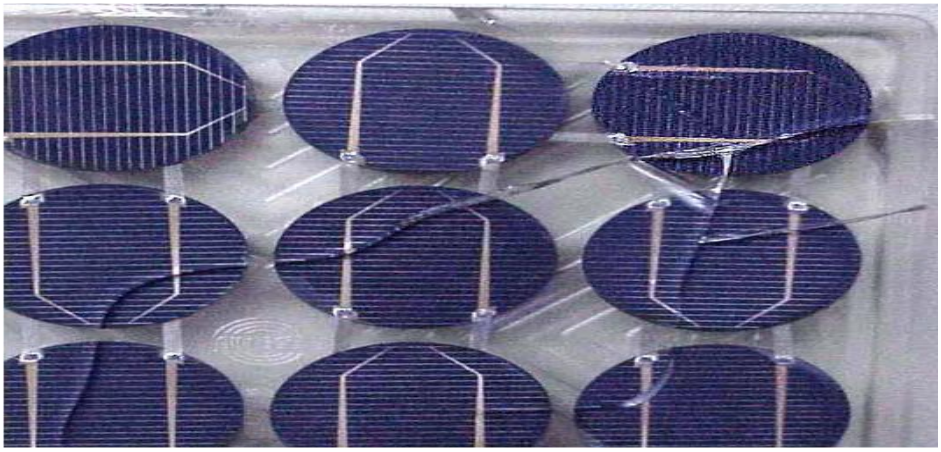

Figure 28: Glass broken due to a hot spot phenomenon [61]

4.2.3 Reverse Bias and Breakdown Voltage Model

As the shading effect continues over a long time duration and not removed, the cell starts work in the dangerous mode called reverse biased region. It is too much stress and may reach the breakdown voltage on the negative side so the shaded cell is operated at the

reverse bias, leads to dissipate more power as a heat in the shunt resistance and the total power will be reduced. In the worst case, the output power delivered to the load will be zero [62].

In reverse biased region of the current passing through the shaded cell is locally concentrated in the shunt resistance and heats up the shaded cell location that can damage the cell encapsulation [63].

The shunt resistance R_{sh} reduction has a profound impact on the I-V curve and causes a strong influence on the whole I-V curve of the module.

Figure 29 illustrates the shaded cell working in the negative region and the breakdown voltage of protection bypass diode. It can be seen that the breakdown voltage is reached to -13 V, and this represents the maximum negative operating voltage of the shaded cell in the presence of bypass diode. So when the bypass diode is disconnected, the breakdown voltage increases and reach up -30 volts, besides the high increase in junction temperature due to the breakdown current passing across a shunt resistance which leads to thermal stress of the shaded cell [64]. This causes a hot spot and burns the panel.

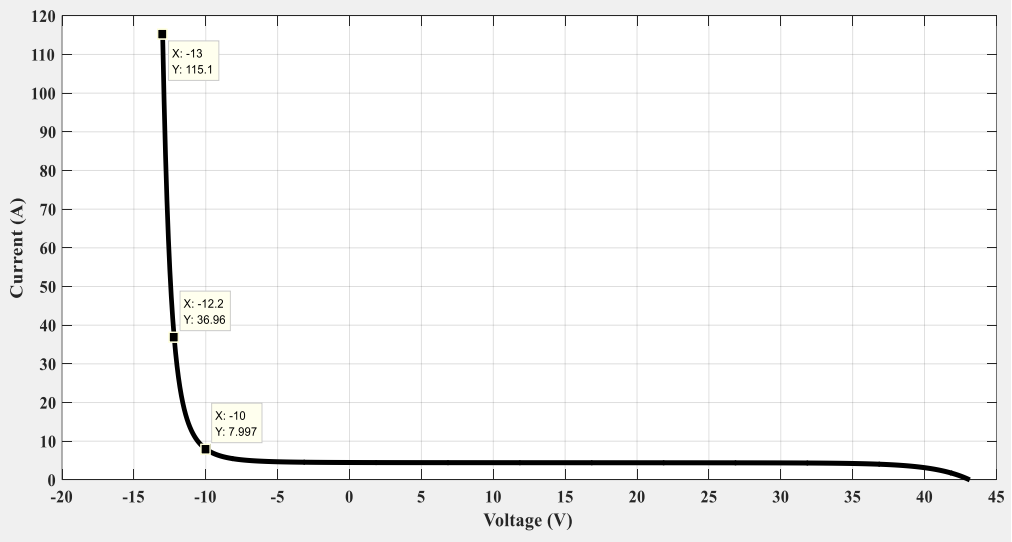

Figure 29: Reverse bias characteristics of NSS-24150MPV panel

The reverse characteristic was implemented by J. W. Bishop in 1988 [65], and it can be modeled inside the PV cell module. Figure 30 shows the solar cell with forward and reverse characteristic. However, it does include additional multiplication term M(Vj) for the reverse current which is inserted in the shunt branch so it connected in series with a parallel resistance. According to this circuit, currents distribution inside each branch can be written as follows:

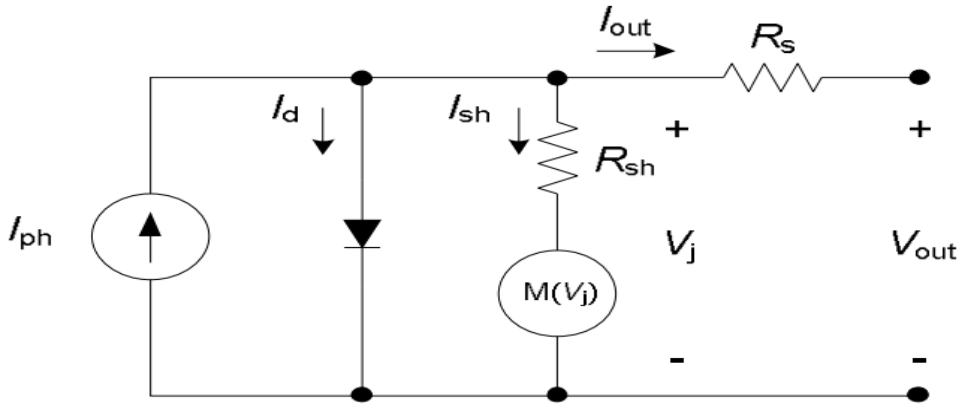

Figure 30: Solar cell equivalent circuit with reverse bias term

$$I_{sh} = \frac{V_j}{R_{sh}} \left[1 + a \left(1 - \frac{V_j}{V_{br}}\right)^{-n}\right] \quad (4\text{-}1)$$

$$I_{out} = I_{ph} - I_o \left[\exp\left(\frac{q\,V_j}{m\,K\,T_{cell}}\right) - 1\right] - I_{sh} \quad (4\text{-}2)$$

$$V_{out} = V_j - I_{out}\,R_s \quad (4\text{-}3)$$

$$V_j = V_{out} + I_{out}\,R_s \quad (4\text{-}4)$$

Where V_{br} is the breakdown voltage, V_j is the voltage across the shunt term, a is the fraction of ohmic current involved in the breakdown voltage, n is the avalanche breakdown exponent, I_{ph} is the photo-current, I_o is the diode saturation current, q is the electron charge, m is ideally factor, k is Boltzmann constant, and T_{cell} is the temperature of the cell in kelvin.

In this study, the following three parameters a, n and V_{br} are selected equal to .01, 3 and -14.4 V respectively, and these values are used in reverse biased characteristics graphical representation in figure 29 where it depicts the whole I-V curve of all working regions. The curve is implemented according to the Bishop's model [65]. As illustrated in the full illumination mode, if the solar cells connected in series basically generating power until the voltage reach to its open circuit voltage. On the other hand, the I-V curve has the reverse region if the solar cell under non-uniform illumination. The curve goes on until reaching the breakdown voltage of the diode (V_{br}) which has a range between -12 to -20 volts in polycrystalline solar cell and -30 volts in the monocrystalline solar cell [60].

Figure 29 also describes three modes of the cell's behavior. It can be seen that a linear relation between voltage and current (0 V to -10 V) lies in the reverse voltage mode due to the leakage current which passes through parallel resistance. If the leakage current increased, then the breakdown point happened in a quick manner. As known in the literature, the shunt resistance R_{sh} indicates to the defects and impurity in the cell material. As these impurity concentration are increased, the shunt resistance, reduced, so the breakdown point can happen at lower negative bias voltages. Close to the shaded cell position, the emphasis of current exceeds, therefore causes destruction in the cell due to the principle of overheating.

In conclusion, in the forward bias, low shunt resistance leads to decrease maximum power (P_{mpp}), so the fill factor of the cell will affect ($FF = P_{mpp}/(V_{oc}*I_{sc})$) and reduced. Also in the reverse bias, low shunt resistance speeds up the thermal stress damage [60]. More power loss with lower values of parallel resistance in reverse bias condition, so the operation of the shaded cells with a high shunt resistance reduces the current passes in the string and

hence the power loss as a heat in those covered calls are much less than the case of low shunt resistance values where the shunt current is high.

The shading level effect on solar cells with low and high parallel resistance can be seen in reference [61]. In the case of the high shunt resistance, the most severe case (power dissipation will be large i.e. worst hot spot effect) occurs at a low shading level and more current is passed ingoing the covered cell. On the other hand, the dangerous case happens when the low shunt resistance and the high shading level is applied, where the reduction of irradiation will cause huge leakage current and thus more imposed reverse voltage with high power dissipation.

4. 3 Hot Spot Formation Mechanism in Solar Cell

As the power degradation proceeds in the shaded cell, deterioration may be extended to the non-defective cells if the protection process is failed, that means the bypass diodes are not able to conduct in the suitable time. When the module current is greater than I_{sc} of the covered cell, then the shaded cell worked as the internal resistive load and operated in a backward biased region, so it dissipates power besides the power generated from the rest cells in the same string [66]. The whole power of that string is wasted as the heat in the parallel resistance of the shaded cell and the surface of the solar panel became stressed and heats up to the high temperatures.

4. 3.1 Currents and Voltages Distribution in PV String under Hot Spot Condition

The main risk associated with hot spot phenomena should be studied is thermal stress and the increasing in temperature degrees especially in the desert environment. It is recognized that the ambient temperature climbs up in the hottest days in summertime, so the risk increased in the cells affected by hot spots.

To examine the mechanism formation of a hot spot in PV cells, let's consider two cells connected in series as illustrated in figure 31, one cell is under partial shading.

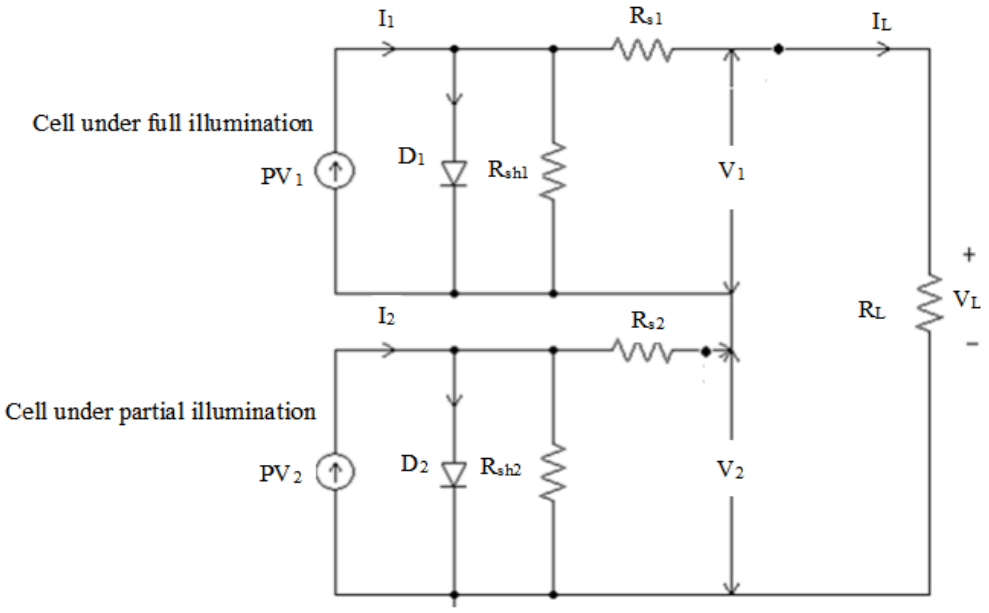

Figure 31: Two cells connected in series under non-uniform illumination

As shown in the previous figure, the first solar cell is exposed to the full irradiance while the second under partial illumination. In this case, PV_1 produced I_1 that always greater than the current produced by PV_2 (I_2) and greater than the current delivered to the load I_L. However, I_2 may be less or greater than load current I_L depending on the load resistor value. The solar cell diode D_2 has two operating regions. The first region is in the forward and occurs when the photo-current (I_2) is greater than the load current (I_L) so the defective voltage cell V_2 has a positive value even though the PV panel is under partial shading. The second case occurs when the load impedance is changed by decreasing itself. The output current (I_L) will be greater than the cell current (I_2). So the difference current (about I_L-I_2) is representing the negative or leaked current passed through the cell under partial shading. The reverse bias of cell 2 leads to make V_2 negative, so the dissipated power in the shaded

cell causing a hot spot risk. The degradation of the solar panel because of the fact that the shunt current through cell 2 is severely limited, so the current through the string is significantly limited by the shaded cell current [67]. More power degradation and fast hot spot formation occurred that making harmful stress on the panel terminals.

Voltages Distribution in PV String under Hot Spot Phenomenon

Voltages across the shaded and unshaded cells distributed based on the connection of bypass diodes. Commercially PV factories inserted bypass diodes for every group of cells. Figure 32 shows the voltage division of the string. So the voltage across the unshaded cells can be measured by the following expression:

$$V_{n-1} = \left(\frac{n-1}{n}\right) V \tag{4-5}$$

Where:

n: number of cells connected in series

V: output voltage of the panel

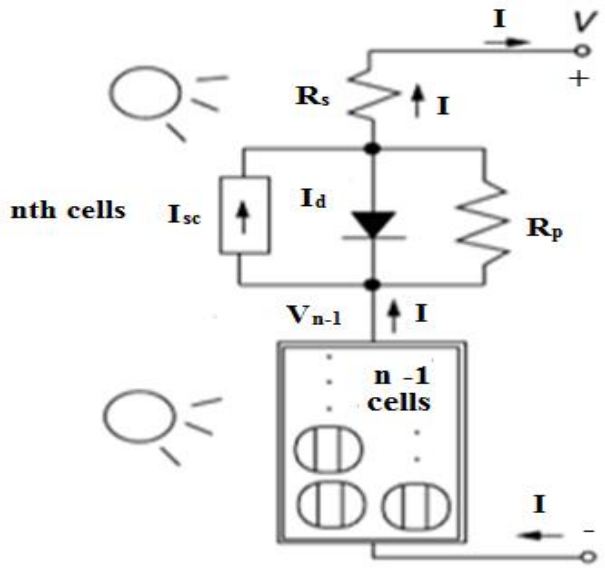

Figure 32: Schematic diagram of n cells connected in series

When some cells are under partially or fully shading effect, the voltage is divided between them as illustrated in figure 33.

Let's consider having a string with one cell under fully shading (i.e., $I_{ph} = 0 = I_{sc}$) as illustrated in figure 33. Since the string current I pass through fully illuminated cells and travels across a parallel resistance R_p, the shaded cell works in the reverse biased region, so the negative voltage across the shaded cell can be estimated by the following formula:

$$V_{sh} = I\left(R_p + R_s\right) \tag{4-6}$$

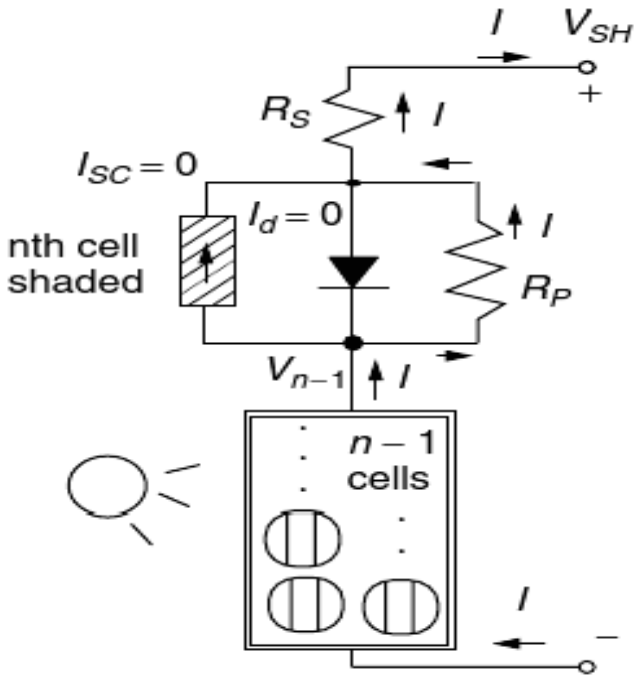

Figure 33: Schematic diagram of n cells with one shaded cell

The following expressions can be used to calculate the total voltage across the string:

$$V_{SH} = V_{n-1} - I\left(R_p + R_s\right) \tag{4-7}$$

Using the formula (4-5) in the formula (4-7) we get:

$$V_{SH} = \left(\frac{n-1}{n}\right) V - I\left(R_p + R_s\right) \tag{4-8}$$

Figure 34 describes the bypass diode operation during inhomogeneous irradiation and the switching point to convert the diode from off to on depends on the shading rate, the string's current, and the module current. It can be seen that as the load increased from zero impedance to infinity, the currents of the module, string and bypass are changed, and the operating point is switched from off to on. The diode shift to off mode when the load is open circuited and no current flow in bypass diode that means the reverse voltage across the diode.

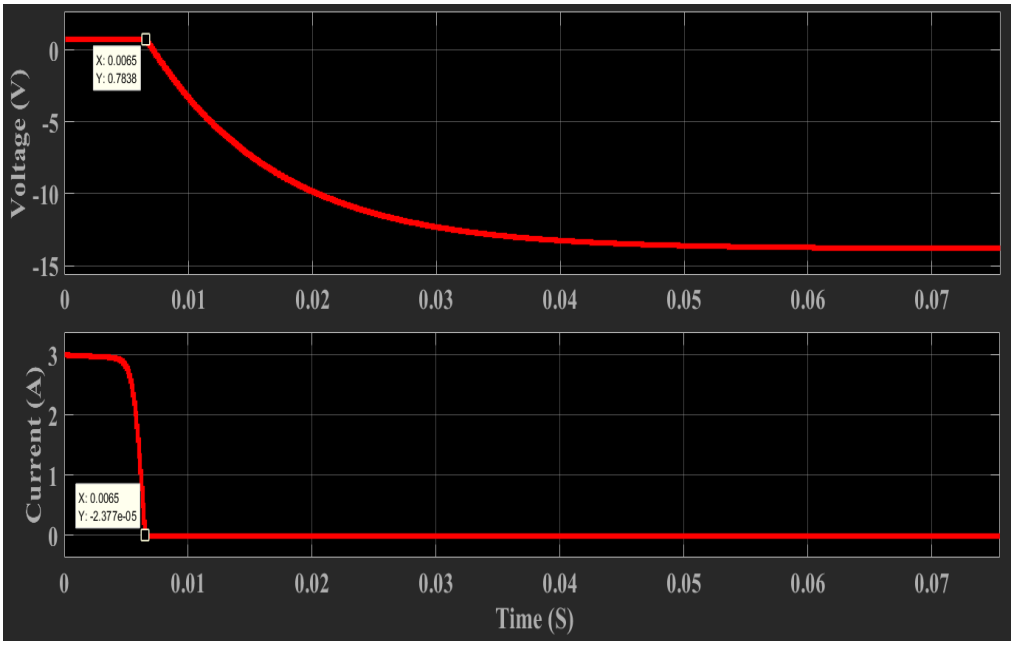

Figure 34: Bypass diode operating point under shading effect

Currents Distribution in PV String under Hot spot Phenomenon

After illustrating the voltage division of the shadowed and illuminated cells inside the same string, it is necessary to demonstrate how the current flows through the same string. Figure 35 shows the current distribution through three branches: string, bypass diode, and load. The current distribution is necessary to understand the working process of the panel under non-uniform irradiation.

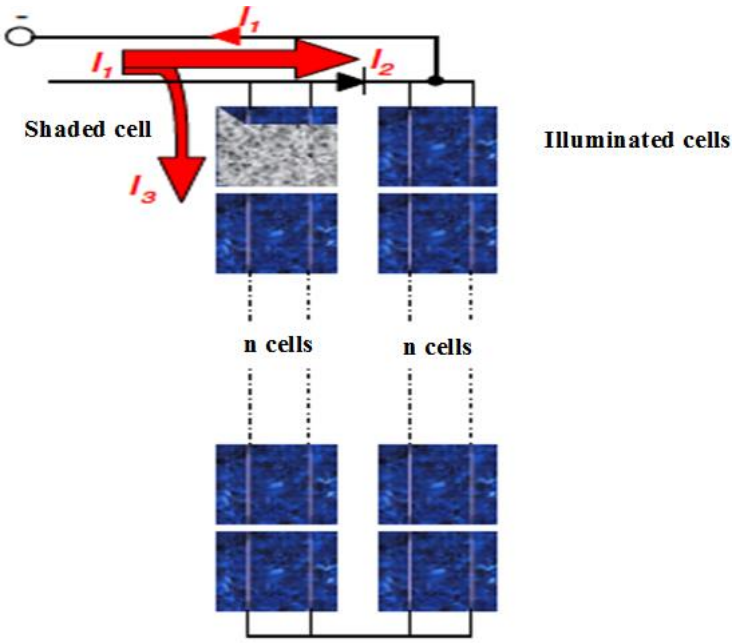

Figure 35: Currents distribution inside the string under shading

As shown in the previous figure, currents I_1, I_2, and I_3 flow in the three branches can be written as:

$$I_1 = I_2 + I_3 \tag{4-9}$$

Where:

$I_1 = I_{module}$ Module current.

$I_2 = I_{bypass}$ Bypass diode current.

$I_3 = I_{string}$ String current.

$$I_{string} = I_{sh} + I_{ph} \tag{4-10}$$

$$I_1 = I_{module} = I_{bypass} + I_{sh} + I_{ph} \tag{4-11}$$

$I_{sh} = I_{shunt}$ Shunt or leakage current, according to the Bishop's model explained in figure 30.

I_{ph} in equation (4-11) Indicates to the photo-current of the shaded cell. If there is more than one cell under the shade effect at the same time in the same string, equation (4-11) is applied on the worst / extreme shaded cell percentage level.

For example: if two cells work at two shading levels with 200 W/m^2 and 800W/m^2 respectively, the cell with lower irradiation has a photo-current that used in equation (4-11). However, the second cell behaves like a normal cell. So 200W/m^2 shaded cell, in a string with full illuminated cells, can cause significant power dissipation in the whole solar panel. The covered cell is able to reduce the string's current to almost its limited current depends on the irradiance level.

4. 4 Matlab Modeling for Hot Spot Evaluation

It is known that the voltage across a shaded cell has a negative polarity, the leakage current flow increased quickly, and a mismatch happened, therefore, the reduction in power is the latest result. This phenomenon is described by several names: avalanche breakdown, hot breakdown, nonlinear shunt resistance, dark current breakdown, or reverse breakdown voltage [68].

The model of the hot spot phenomena of PV panel has been performed in MATLAB/ Simulink environment as described in figure 36 that includes the whole module with all parts such as the load, the number of cells connected in series, the number of bypass diodes, current / voltage meters, and the Bishop circuit.

The main basic parameter of the Simulink model is represented by the equivalent circuit of solar cell described in figure 37. The irradiance and the temperature are required as input data. The simulation is able to give full details about reverse and forward bias modes for each cell individually of the whole module, allows getting both electrical characteristic

curves, and also show the current distribution in the shaded and illuminated cells and the currents flow in the bypass diodes and each string of the module.

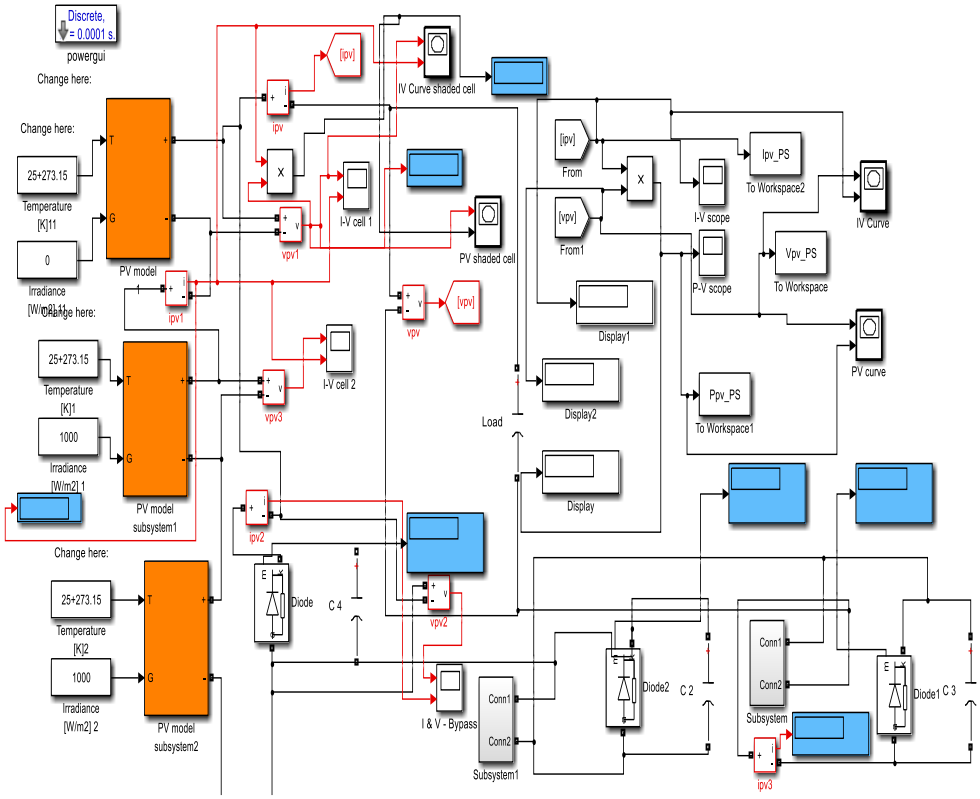

Figure 36: A Matlab / Simulink model of PV hot spot

The simulation allows to estimate I_{ph}, I_o, I_{string}, and I_{sh}, for each solar cell individually and I_{bypass} for bypass diodes and finally I_{module} of the panel.

Inside each solar cell of the model, a schematic circuit can be seen with full mathematical formulas that estimated the current flow.

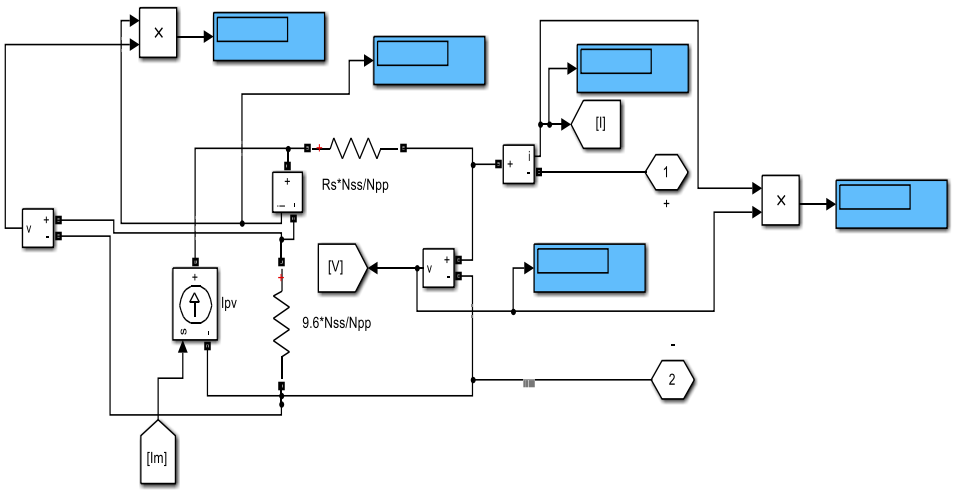

Figure 37: Simulink block of a solar cell

Figure 38 (a and b) describes the Simulink block diagram for estimate the diode saturation current (I_o) at any operating conditions of illumination and temperatures.

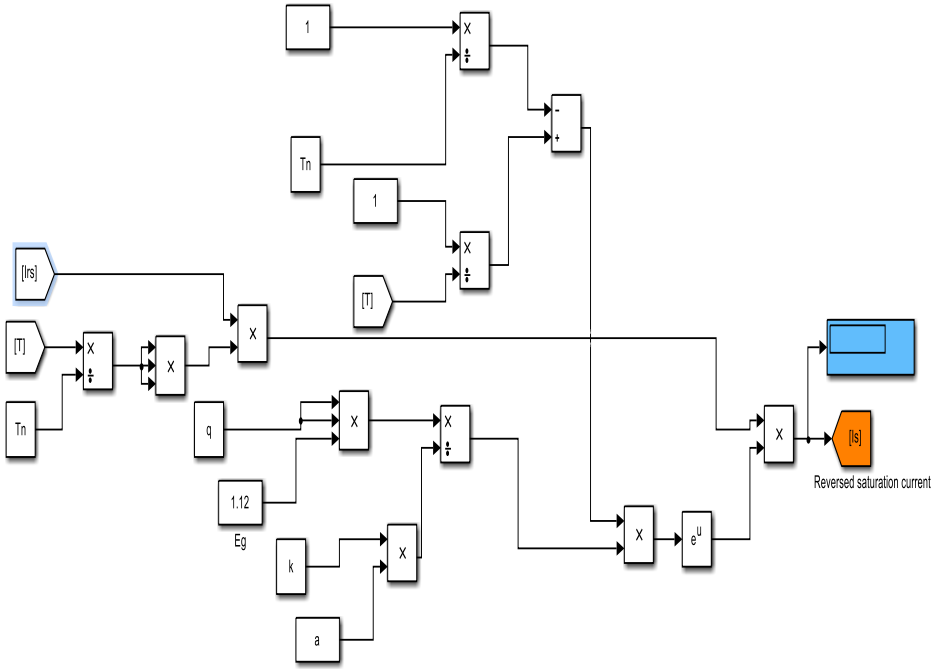

(a) Simulink blocks for calculating saturation current

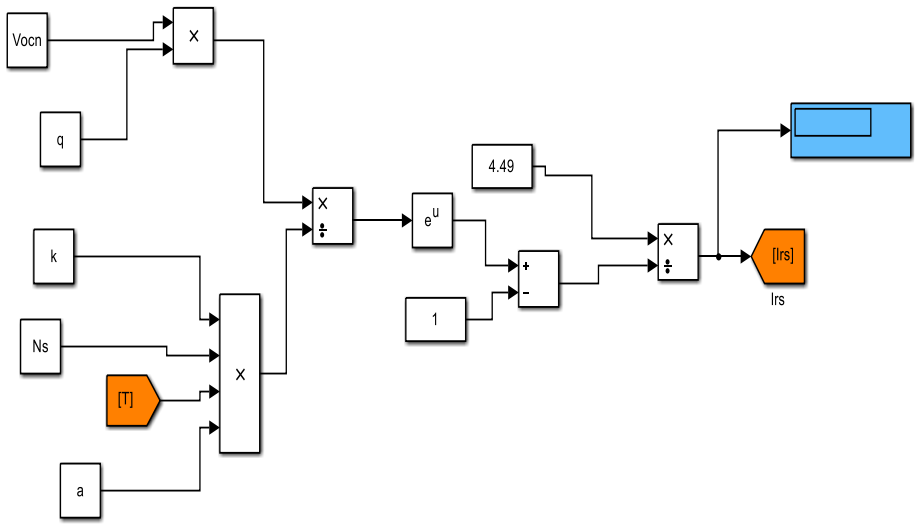

(b) Simulink blocks for calculating saturation current at normal conditions

Figure 38: Simulink blocks for calculate I_o

Figure 39 describes the Simulink blocks diagram for the photo-current (I_{ph}) at the nominal illumination level and temperature.

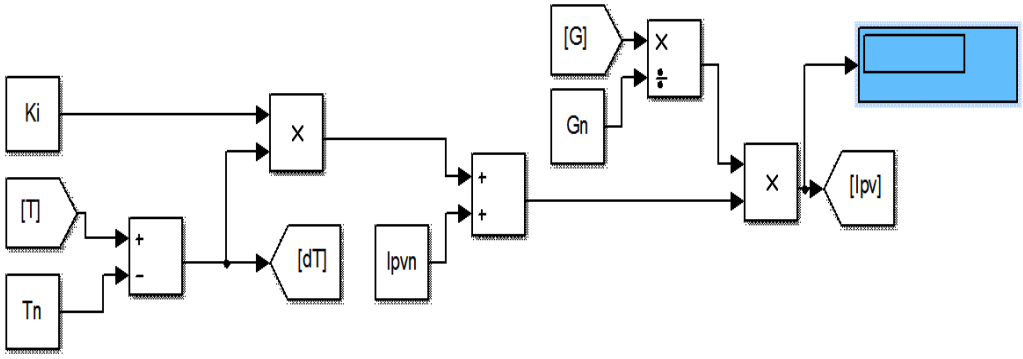

Figure 39: Simulink blocks for calculating I_{ph}

Figure 40 describes the Simulink block diagram for the current (I_m) passes through shunt and series resistances of the cell at the nominal illumination level and temperature. Series resistance current represents the string current that flows in all cells connected in the same string.

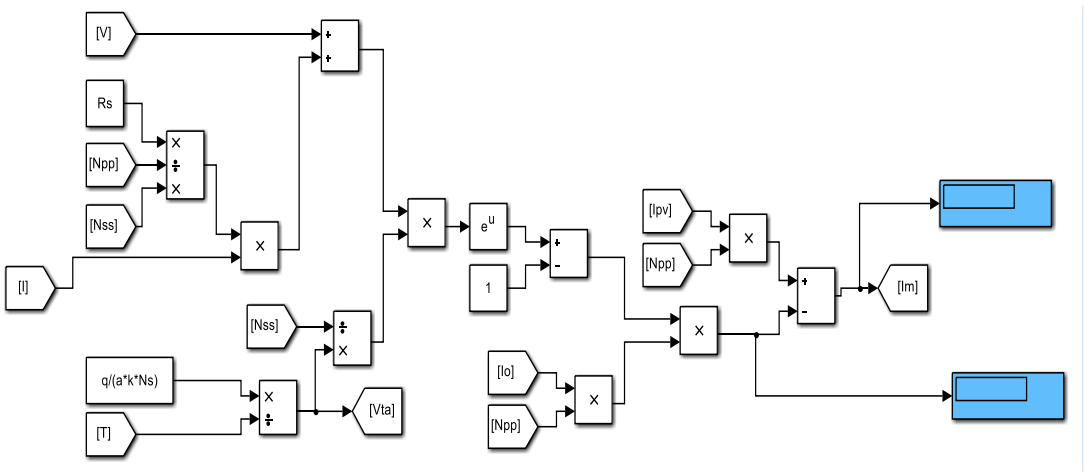

Figure 40: Simulink blocks for calculating current of shunt and series resistances

Figure 41 describes the Simulink block diagram for the leakage current passes through a shunt resistance during the shading condition for the non-uniform illumination level and the nominal temperature. This current represents the Bishop's model with breakdown voltage term.

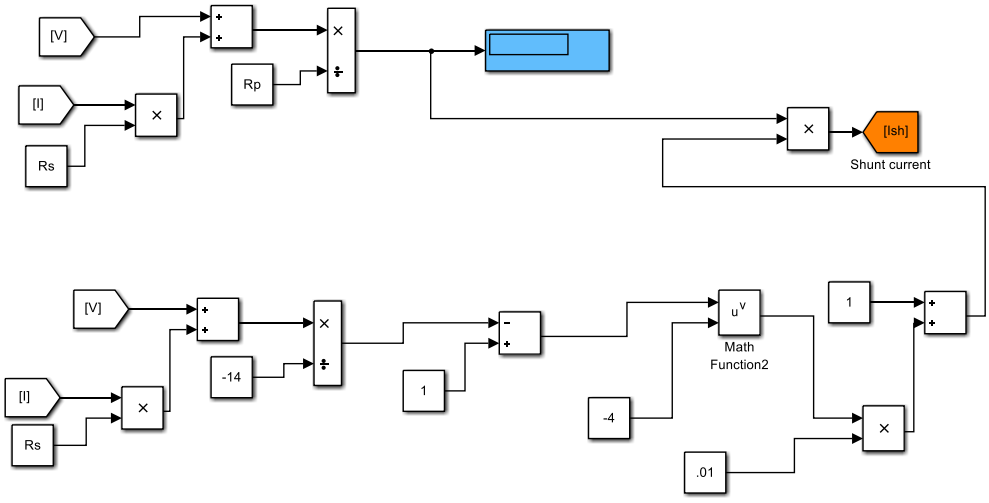

Figure 41: Simulink blocks for Bishop's model with reverse bias term

4.5 Evaluation Methods of the Hot Spot Phenomenon

In this study, three methods are used to evaluate and observe the formation and creation process of hot spots in the defective cells. The first method is dealing with the power

reduction that can read from the online power curve delivered to the fixed load. The second method is concentrated along the current behavior inside the defective and non-defective cells in the same string of the PV panel. And the last method is done by investigating thermal stress and rising temperature in the shaded cells, this method is performed by the thermal IR imaging technique. In the following subsections, the first two methods will be covered and explained with the simulation results and then validated these methods by experimental works using the third method which we shall study and learn from the next chapter.

4.5.1 PV Panel Characteristics in Study

The module that used for three methods has three strings contain 72 mono-crystalline cells serially connected. Figures 42 and 43 illustrate the PV photograph with configuration details of cells, strings, and bypass diodes. The panel is divided into 24 cells for each string with the parallel bypass device.

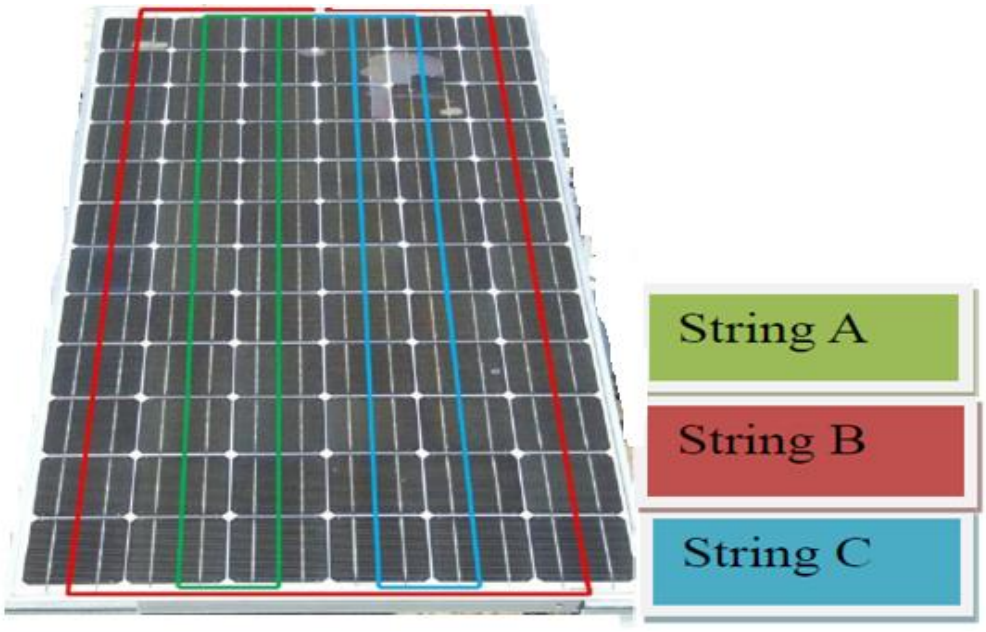

Figure 42: Picture of PV panel under study

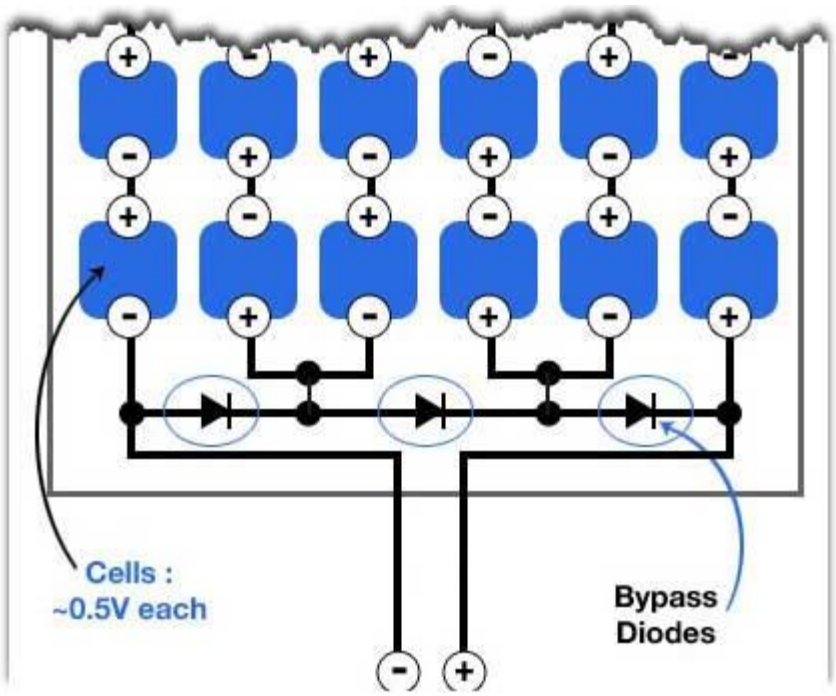

Figure 43: Configuration diagram of strings and bypass diodes

This panel has a maximum power output of 150 W with I_{sc} of 4.49A, V_{oc} of 43.2V, I_{mp} of 4.1A and V_{mp} of 36V. The effects of degradation and bad cells on the panel's I-V and P-V curves are investigated using the following methods.

4.5.2 Method 1: Reduction in Power - Online Output Power Profile (OOPP)

In this method, a fixed load is connected to the PV panel and study the shading effect during a period of time such as 24 hours. At least if one cell is shaded, out of a series connection with full illuminated cells, can induce a huge power dissipation in the whole panel output. The covered cell is capable of reducing the string and module currents to almost its limited current that proportional to shading rate. For illustration, if one cell is working under different sunlight levels, connected in series with 23 full illuminated cells worked at 1000 W/m^2, as described in figure 44.

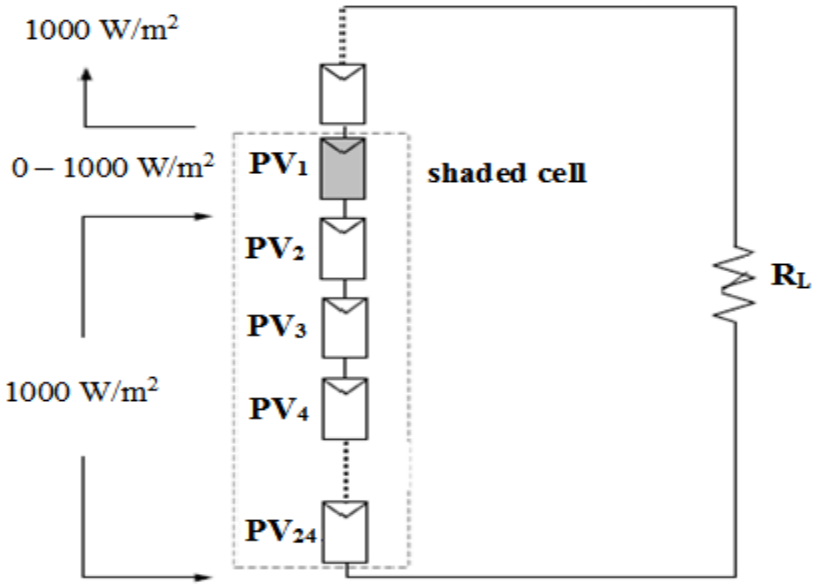

Figure 44: A string contains 24 cells with one shaded cell

Characteristic curves of the whole PV panel with one shaded cell can be shown in figures 45, 46, 47, 48, 49, and 50. Both curves are plotted simultaneously for variable impedance with various shading levels (0 to 1000 W/m^2) of the shaded PV_1 and the current is changed from zero A to the I_{sc} of the panel.

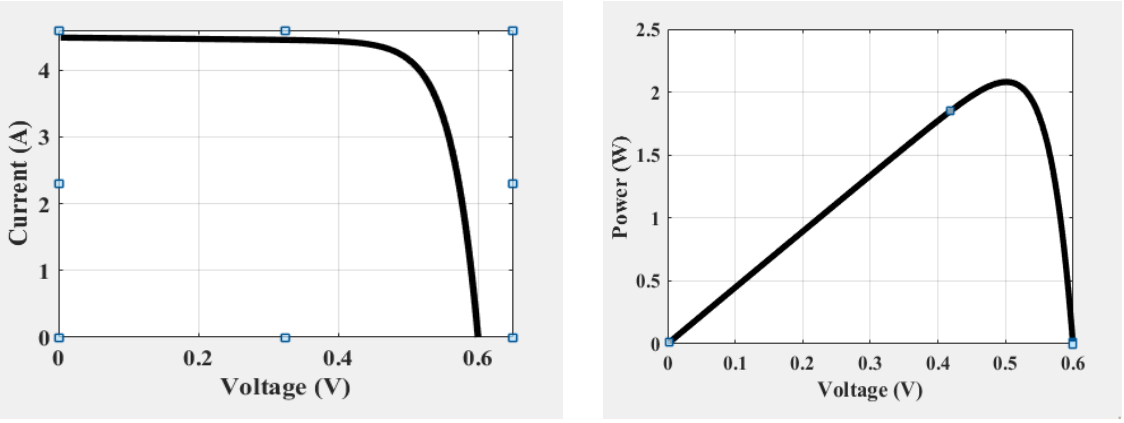

Figure 45: I-V and P-V curves of PV_1 at 1000 W/m^2

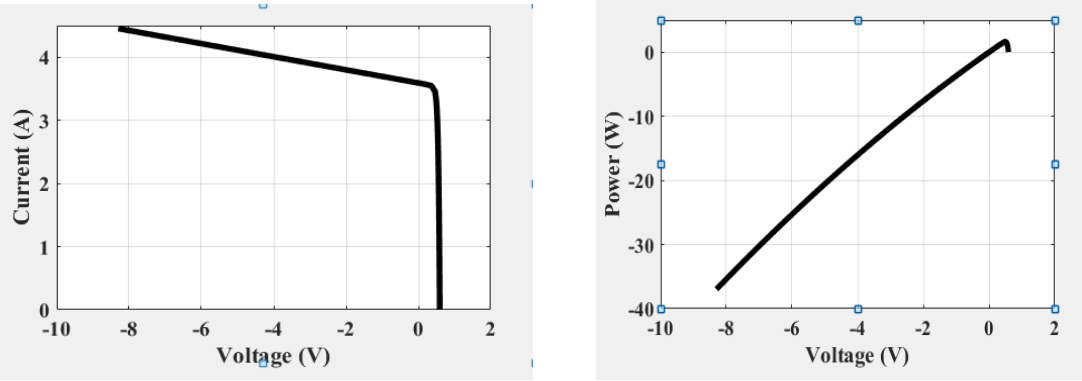

Figure 46: I-V and P-V curves of PV_1 at 800 W/m^2

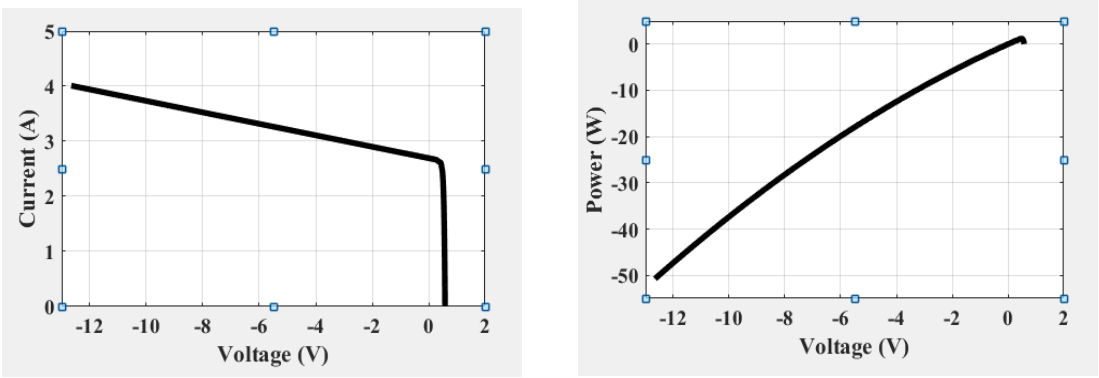

Figure 47: I-V and P-V curves of PV_1 at 600 W/m^2

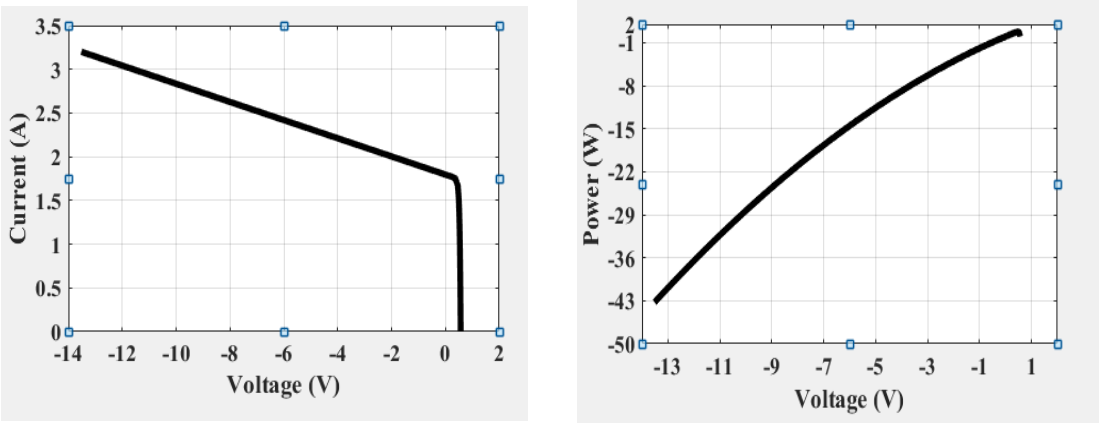

Figure 48: I-V and P-V curves of PV_1 at 400 W/m^2

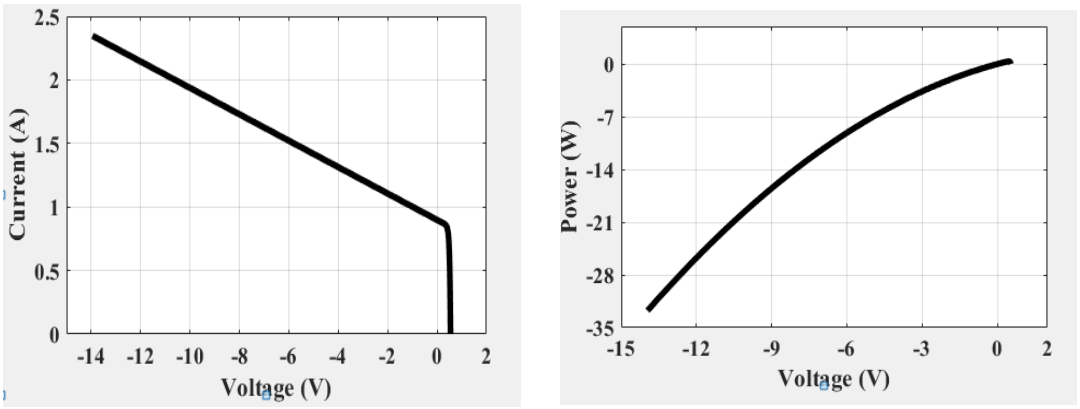

Figure 49: I-V and P-V curves of PV_1 at 200 W/m^2

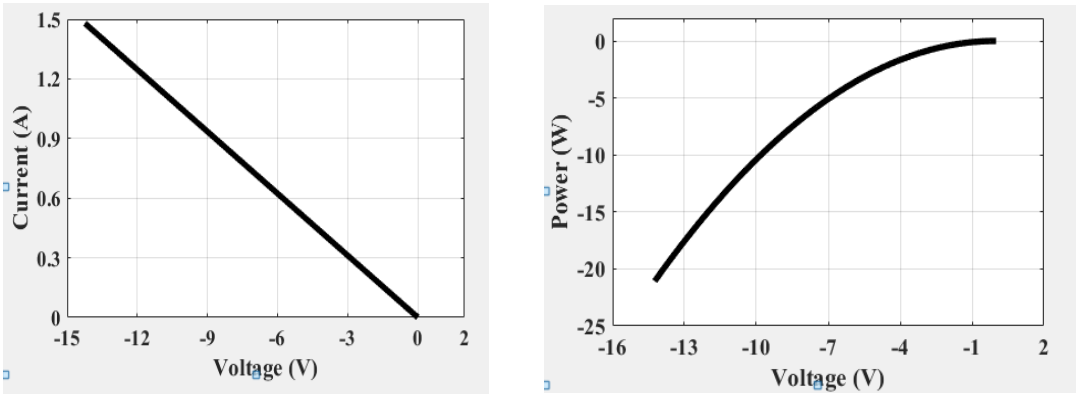

Figure 50: I-V and P-V curves of PV_1 at 0 W/m^2

It can be observed that at full illumination level 1000 W/m^2 (zero shading), the whole I-V and P-V curves are lying in the positive mode because there is no cell working in reverse bias. However, the remaining curves (figures 46-50) under different levels of irradiance lie that between 0 and 800 W/m^2 have the shaded cell operated in a reverse biased mode. As the shading level increased the negative voltage across the shaded cell increased and the current of the string decreased, thus more applied shadow level causes a more negative voltage across the defective cell.

The P-V curves on the right side of previous figures are very necessary to investigate and analyze the power reduction and the hot spot areas appeared in the shaded cell. For example, in figure 47 a cell has a reverse voltage of -13 V so huge amount of power -50 W is lost in the covered cell if the irradiance 600 W/m^2 compared with irradiance level 0 W/m^2 where power dissipated at this case about -22 W. In conclusion, a little shaded solar cell is more exposed to the hot spot risk because this amount of power is concentrated in the smallest defective areas in the cell.

From algebraic equations of voltages around the string that includes 23 full illuminated cells and one shaded, when the string voltage is zero, which means the equalization between the reverse voltage across the shaded cell and summation of the positive voltages across 23 illuminated cells. But the worst case occurs with extremely shaded cell because the impact on the other cells was huge and the panel could lose the whole contributed power that can deliver to the load.

The online power profile can detect the power reduction during the time if the shading takes place. In this study, real data are collected for the weather conditions, i.e. irradiation and ambient temperatures for three days and simulated by the hot spot model in Simulink. Figures 51 and 52 show the irradiance data during three days also the temperature profile for the same period. Figure 53 shows the power, voltage, and current across the load during three days. It can be observed that they take the same shape of input data and they are tracing each point of data during the operation process of the panel so if shading occurs, the online profile will reflect the location and the time of that problem exactly.

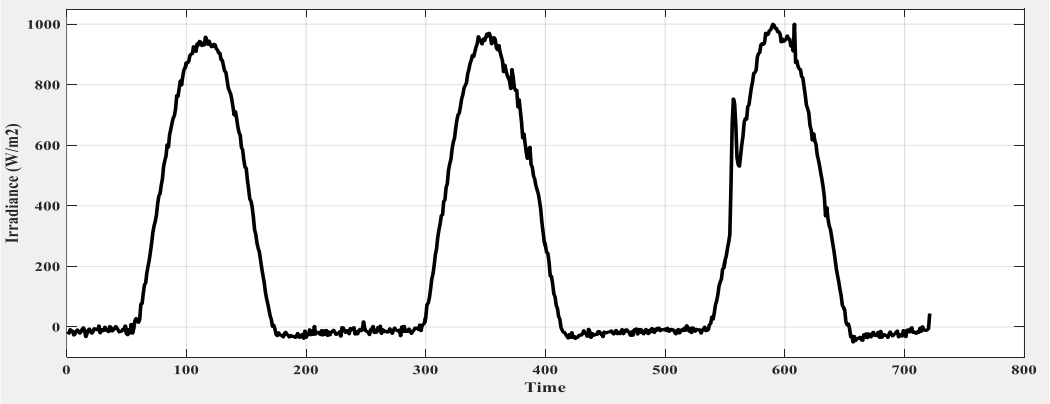

Figure 51: Irradiance data during three days

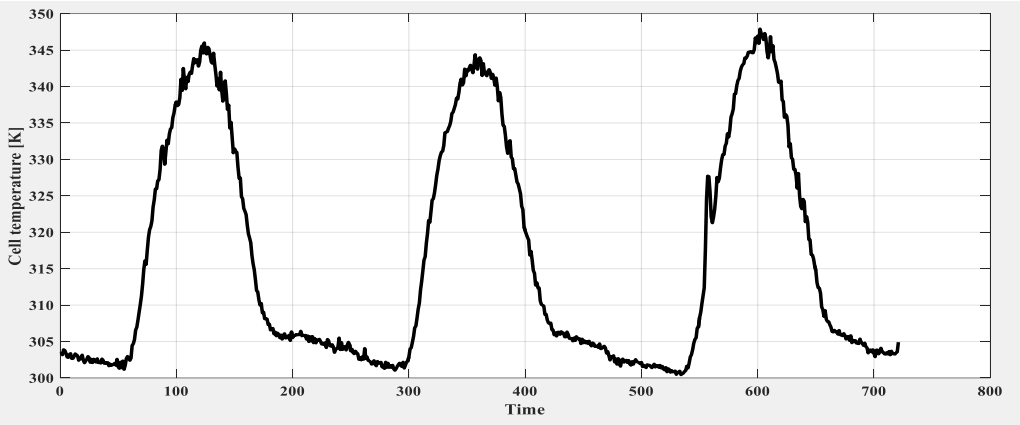

Figure 52: Cell temperature data during three days

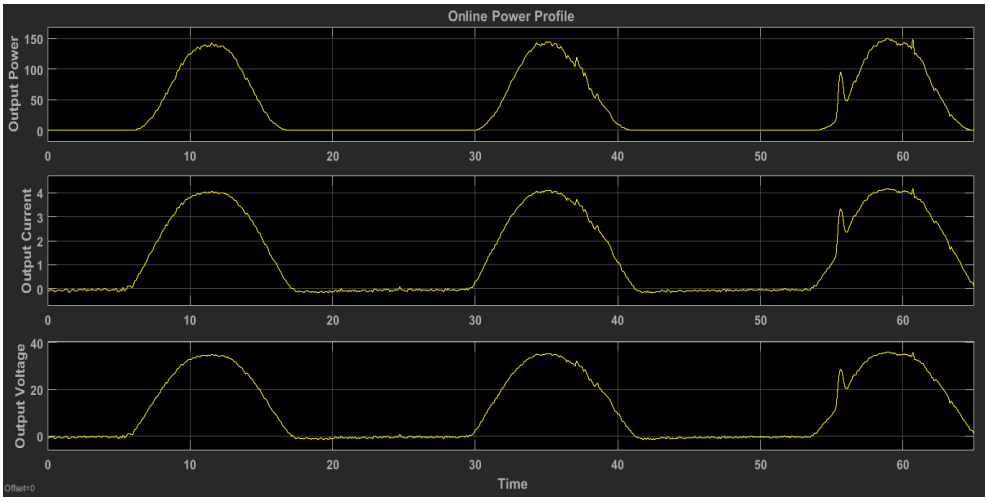

Figure 53: Online profile of power, voltage and current during 3 days without shading

If any external object caused a shading force on the surface of the PV panel during daylight hours, at least one cell shaded, a severe reflection will happen in the operation of the panel and hence the output power is affected. Hence from the online power curve, it's very clear to see the degradation in power and extracts how much force is lost during shading time, and this mismatch could cause hot spot risk if the shading object isn't removed and kept for a long time.

Figure 54 shows the online power, voltage and current profiles across the load if the shading effect occurred in the middle of the first day. Completely shading has happened on the first day for one cell only, so the power dissipated in the shaded cell leads to localized heat stress and raise the temperature degree of the rest cells in the same string. That raise in temperature creates hot spots risk in the entire string which potentially has the failure of transferring power to the load. It has been noted that the load in this situation is considered to be fixed and adjusted to 8.6 Ω ($R_{Load} = V_{max}/I_{max}$). Also, the cell temperature is considered, so the maximum power delivered to the load can be estimated by both output current and voltage.

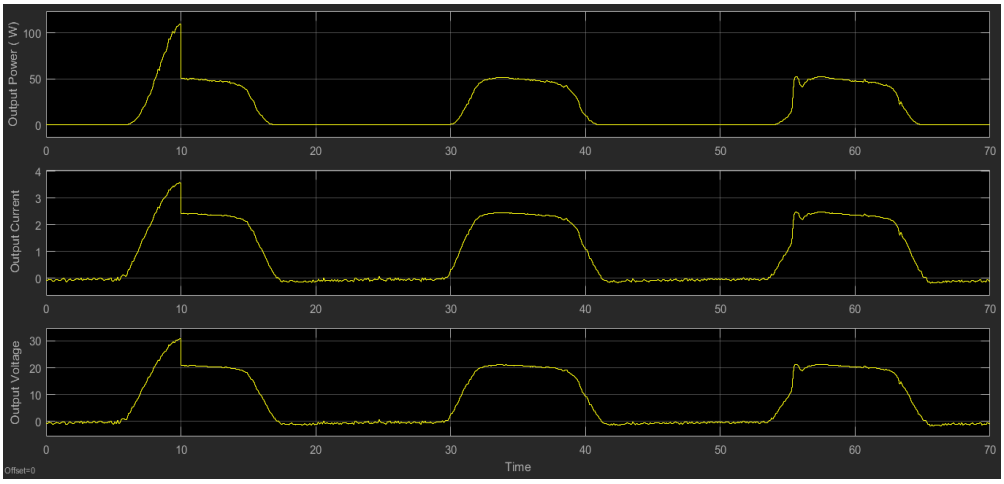

Figure 54: Online profile of power, voltage and current during 3 days under shading

It can be seen that the location, the time of energy drop and the amount of power loss compared to the normal case at the same position. For instance: in the reference situation the output power was 110 W before the shading time, and this value became 50 W after shading. This amount of power dissipation accelerated the hot spot formation in the defective cell.

Figure 55 shows the shading effect on the individual cell during three days, it's obvious that how the full shading can reduce the whole output power, current, and voltage of the system.

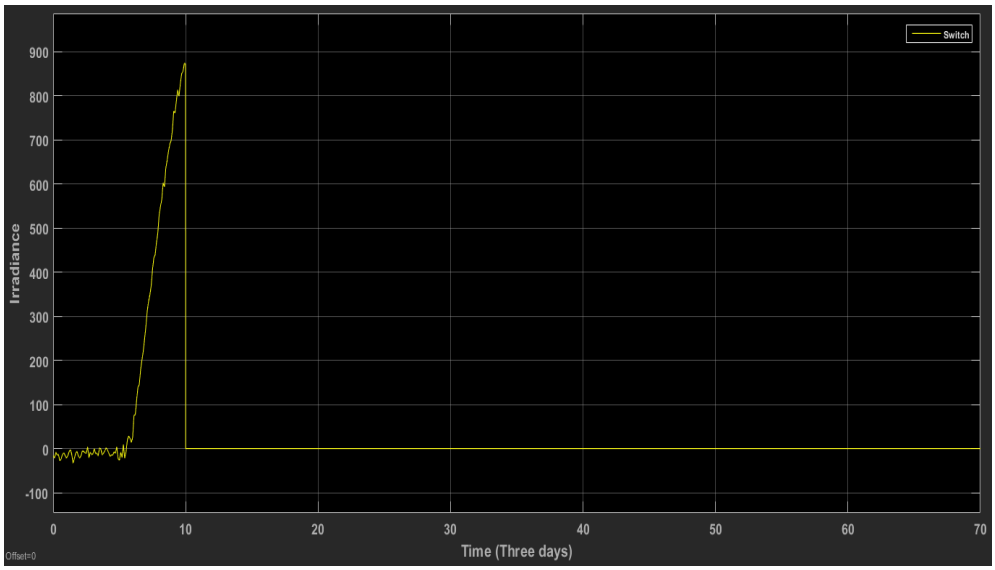

Figure 55: Online shading profile for one cell

Bypass diodes are working to reduce the hot spot effect, so they can bypass the cells included in the same affected string before the shaded cell reached the breakdown region. This operation of bypass just reduces the thermal stress on a single cell, but hot spot risk can still happen [69, 70].

4.5.3 Method 2: Currents Distribution in the Hot Spotting Area

In this method, the connection between the leakage current in the shaded cells and the shading level is seen. It can be seen that the leakage current passes through the shunt resistance depends on the shading levels applied to a cell or group of cells operates in the reverse bias region.

As a result of shunt current the output power deterioration accelerated rapidly while shading level increased so the shunt current has a linear relation with shading level and increased proportionally. Figure 56 illustrates the relation between illumination level and shunt current for one cell.

Figure 57 shows the relationship between the rise of the shunt current and the corresponding power dissipation in shunt resistance. Moreover, in this situation a higher shunt current flows through shunt resistance, the hot spot risk has a big impact on the shaded cell and speeds up the panel damage.

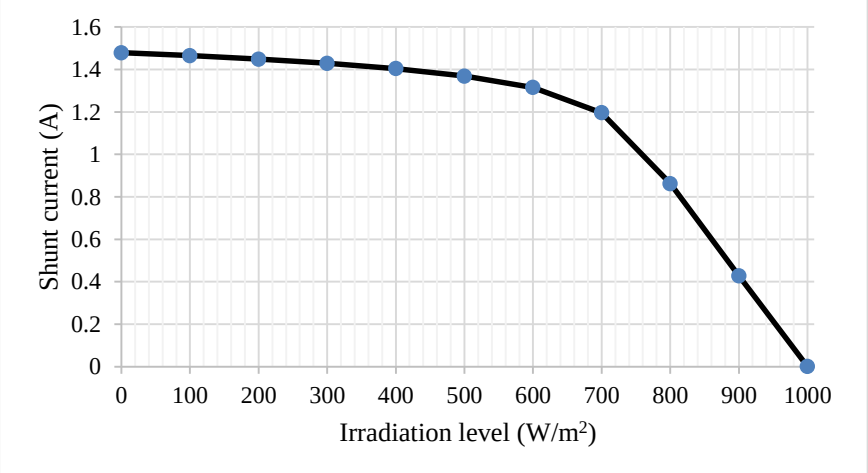

Figure 56: Relation between shunt current and irradiation level

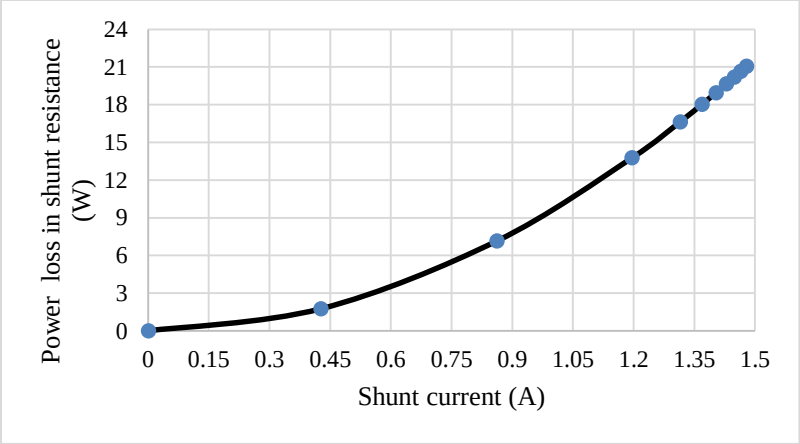

Figure 57: Relation between shunt current and power dissipation in R_{sh}

To investigate the hot spot current details, two case studies were considered. The first case is when the panel is short-circuited and the second case is when the panel is operating at full load condition; in both cases, the panel temperature is kept at the standard of 25 ^{o}C but the considered cell for experimentation is subject to the different level of irradiation. During both study cases, all other cells in the considered string or on the other panel strings are always subjected the standard irradiation level.

Table 3 : Case study to investigate hot spotting situations at short circuit condition

Irr. (W/m^2)	I_{shunt} (A)	$P_{diss\_shaded\ cell}$(W)	P_{diss_Rsh}(W)	I_{string} (A)	I_{bypass} (A)	I_{ph} (A)	$I_{module} = I_{ph} + I_{bypass} + I_{shunt}$ (A)
1000	0.001	0.46	0.01	4.47	0	4.49	4.47
900	0.427	18.42	1.76	4.46	0	4.04	4.46
800	0.861	36.97	7.15	4.45	0.023	3.59	4.47
700	1.17	49.97	13.77	4.34	0.13	3.14	4.47
600	1.32	50.47	16.64	4.00	0.45	2.69	4.47
500	1.37	47.64	18.04	3.61	0.86	2.25	4.48
400	1.41	43.24	18.96	3.20	1.27	1.79	4.47
300	1.43	38.18	19.65	2.78	1.68	1.35	4.46

200	1.45	32.73	20.20	2.35	2.12	0.89	4.47
100	1.47	27	20.66	1.92	2.56	0.45	4.47
0	1.48	21.07	21.06	1.48	2.99	0	4.47

Table 3 explains that the sunlight current has a stable value and increases as shadowing rate decreases. It can be seen that with smaller shadowing levels the power dissipated inside the covered cell still high. Hence it is clear that the total power loss is controlled by the photo-current.

If the shadow rate was very low as cleared in table 3 (illumination levels = 900 W/m^2) the bypass diode could not switch on and conducts current because the voltage drop in forward bias is lower than the operating voltage of the bypass diode, which leads to the hot spot risk at the location of the shading and lastly damages the PV panel. So the conduction time of bypass diode is controlled by the leakage current and the shading level.

From table 3 it can be observed that the power dissipated in the shaded cell is gathered from the power contributed from the rest cells connected in the same string. For instance: in the case of fully shading, The dissipated shaded cell power equal to 21.06 watts, if this value divided by the number of the resting cell (23), then it gives the same amount of power generated by each fully illuminated cell around 0.92 watts.

The dissipated total shaded cell power start to increase with the shading level rise to reach a maximum then declines while the shading level continues to reach darkness. If the shading level did not reach, the required amount needed to switch the diode from backward bias to forward bias, the diode current remains zero, but the dissipated power has been already initiated.

In the second case study, the same test is applied, but the load is adjusted to maximum operating condition, i.e. $R_L = V_{mp} / I_{mp} = 8.6\ \Omega$. All results are achieved for a single cell, with various illumination levels and working at the standard temperature 25 ^oC and recorded in table 4.

Table 4: Case study to investigate hot spotting situations at normal load condition

Irr. (W/m^2)	I_{shunt} (A)	$P_{diss\_shaded\ cell}$(W)	P_{diss_Rsh} (W)	I_{string} (A)	I_{bypass} (A)	I_{ph} (A)	$I_{module} = I_{ph} + I_{bypass} + I_{shunt}$ (A)	P_{load} (W)
1000	.05	2.08	.026	4.17	0	4.49	4.17	149.3
900	.06	2.34	.03	4.10	0	4.04	4.10	144.7
800	.33	12.38	3.16	3.92	0	3.56	3.92	132.2
700	.59	21.03	3.30	3.73	0	3.14	3.73	119.6
600	.83	28.20	6.65	3.53	0	2.69	3.53	107
500	1.07	34.19	10.30	3.32	0	2.25	3.32	94.67
400	1.31	39.06	16.47	3.11	0	1.79	3.11	82.95
300	1.43	38.06	19.68	2.78	.23	1.35	3.01	77.76
200	1.45	33.97	20.21	2.44	.57	.99	3.01	77.69
100	1.47	27.11	20.76	1.92	1.09	.45	3.01	77.69
0	1.48	23.50	20.95	1.66	1.27	.18	2.92	73.41

From table 4, it is clear that in the loaded case, the total power dissipation in the defective cell presents similar behavior in the short circuit case where the dissipation rises to reach the maximum then declines.

The bypass diode needed heavier shading level to conduct while the hot spot is growing in heat dissipation. One the bypass diode is turned on, the power delivered to the load remains almost fixed at 77.6 W while the shading level continues to increase. The shunt current also continues at an almost at a fixed value of 1.45 A, but the photo-current changed at each new level of irradiation that leads to change in the string and consequently bypass

diode currents. On the other hand, in the cases when the irradiation lies between 1000 and 400 W/m^2 the bypass diode remains off and can't conduct the current however the shading applied, this causes a real danger on the panel because the protection represented by the bypass diode is not active and the heat dissipation is going on.

The rated transferrable power to the load at STC is 150 watts that can be seen in the table at 1000 W/m^2 and this value starts to decreases as the illumination level dropped from 1000 to 0 W/m^2 .The power lost represent the dissipation across the shunt resistance and shaded cell inside the panel and lead to localized heat that means this heat could crate hot spot risk and damage the panel.

Figure 58 shows the relation between irradiation intensity and the power deliver to the load.

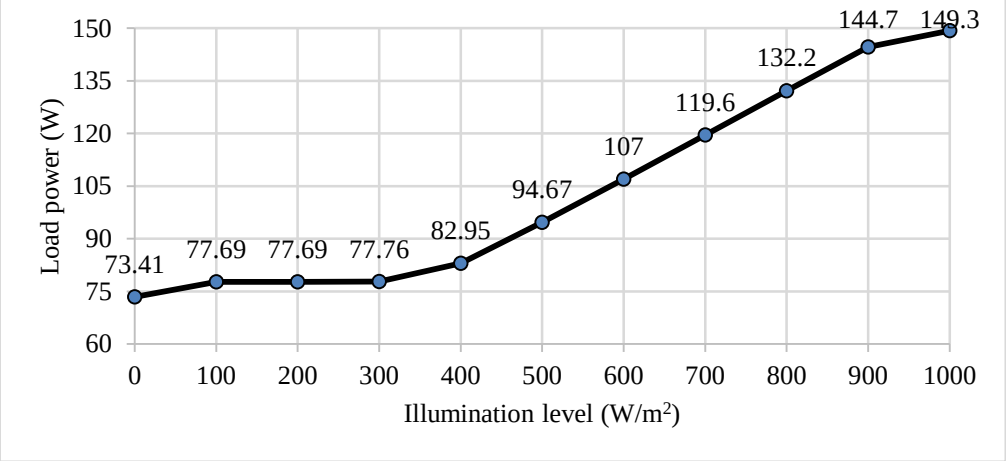

Figure 58: Irradiation level and the load power

To get interpretation and accepted discussion, it is clear to say that under short-circuit current test the worst case of the highest degradation of power inside the shaded cell of the panel. By measuring all currents, it is proved that the range of the power dissipated in the string depends on reverse current and corresponding reverse bias voltage across the cell. The negative voltage value is the summation of voltages across the unshaded cells in the string and the operating voltage across the bypass diode. Moreover, the short-circuit test of

hot spot detection investigated that at full shading case the shunt current becomes high as shown in table 3 but the photo-current has the highest values at a lower shading levels as appeared in previous table 3.

Figure 59 summarizes the behavior of the power dissipation in the shaded cell as the function of irradiation level variation in the short circuit test. The irradiation level is directly related to the photo-current. The dissipated power reaches a maximum of 50.47 W dissipate at the shaded cell. On the other hand, figure 60 shows the behavior of shunt power dissipated with the level irradiation at the affected cell.

The same conclusion for the second case is achieved as the panel is loaded, and the maximum power dissipation across the shaded cell occurred at 400 W/m^2 as seen in table 4.

By evaluating the power dissipated for the shadowed cell and shunt resistance at different irradiation levels, it was proven that hot spot is connected up to the power dissipation in the shunt resistance and the affected part of the cell and that increases internal temperature and so leading to thermal stress. This will be studied in the third method by means of thermal distribution on the cell's surface.

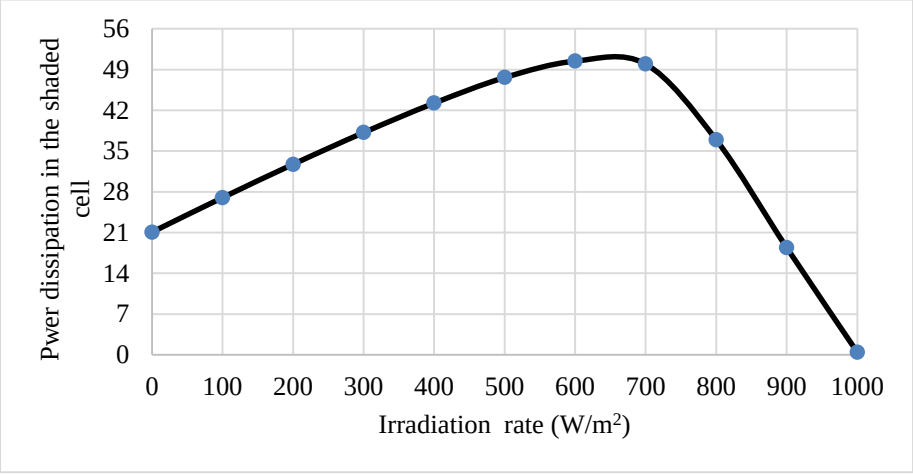

Figure 59: Power dissipation in shaded cell

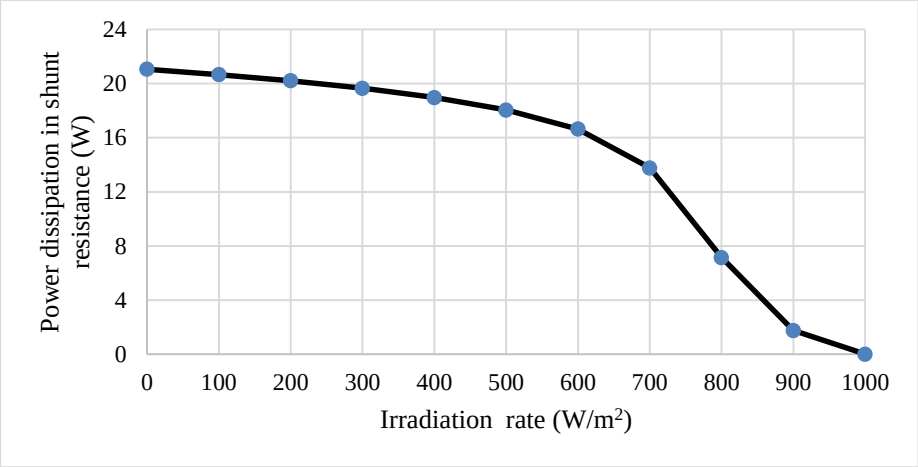

Figure 60: Power dissipation in shunt resistance

4.5.4 Method 3: Infrared Image Technology in PV Panel

Thermal image processing or thermography, is a very important measurement approach in the industrial area. This technology provides time saving, real, accurate information, and fast detection of defective devices.

IR image camera has the ability to detect a small electromagnetic spectrum lies between 9,000–14,000 nanometers in the IR range. According to the black body radiation law, any object above absolute zero will transmit IR radiation, thus the temperature can be measured. The variations in temperature of the objects can be evaluated and analysis by this method. Advancements of IR technique, detection can be used to investigate the shunt resistance that causes the hot spot in solar cells.

In 1990, the first studied with IR thermography used to observe the behavior of shunts in solar cells under reverse bias [71].

A reverse bias was detected with an IR camera. As higher temperature the cells have a strong current passing through shunt resistance, then hot spots are created and formed. Figure 61 shows thermography image captured by a forward-looking infrared radiometer

(FLIR) brand system camera to detect the abnormal panels over the large area of solar systems.

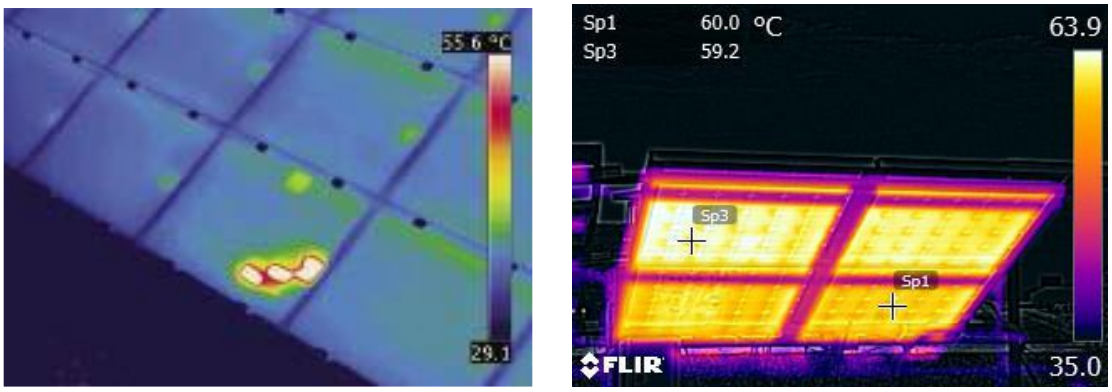

(a) Hot spot (b) PV panel from the back

Figure 61: Thermography images taken by a FLIR E60 camera

As shown above, a thermal image has a capability of discovering the abnormal and defective areas that are suffering from high temperatures. Hot spot locations can give information about shunts, especially in solar cells of crystalline silicon material, depending on the location and shape. For example, bypass diode operation can cause bypassed string to heat up thus increasing the temperature of that string and affected the whole module efficiency. Shunts, cracks, and shadowing in solar cells appear as hot spot phenomena. The most advantage of thermography cameras is giving the temperature distribution inside each cell of the panels in PV systems during working.

It is necessary to estimate the cycle life and thereby the performance of PV panels in order to evaluate the cell temperature at the same time of estimating the voltage across the cell and current flow under hot spot risk.

During irradiation, the current will flow in the panel, and the heat stress is rapidly generated, especially in the hot days according to the highest temperatures. If any mismatch

occurred during the operation cycle of the panel, the inhomogeneous irradiant reached the cells and as a result, the temperatures will be different from one cell to another. So the IR camera has the ability to display the temperature profile of all cells during the module is producing power.

In this study, the thermography image processing and a suitable temperature device are used to detect the hot spotting areas during the short circuit, open circuit, maximum power point of the module and various load conditions.

The process to validate this method depends on the highest cell temperature of the module at the short circuit test and normally loaded panel test. The steps of this method apply to the panel shown in figure 62, where the panel is exposed to a radiant of ≥ 650 W/m² and forcing shading effect on some cells in each string for many hours i.e. hot spot creation, then the hottest areas will appear and cells will heat up. Using a suitable temperature instrument (e.g. Temperature gun infrared thermometer) and FLIR E60 camera as shown in figure 63.

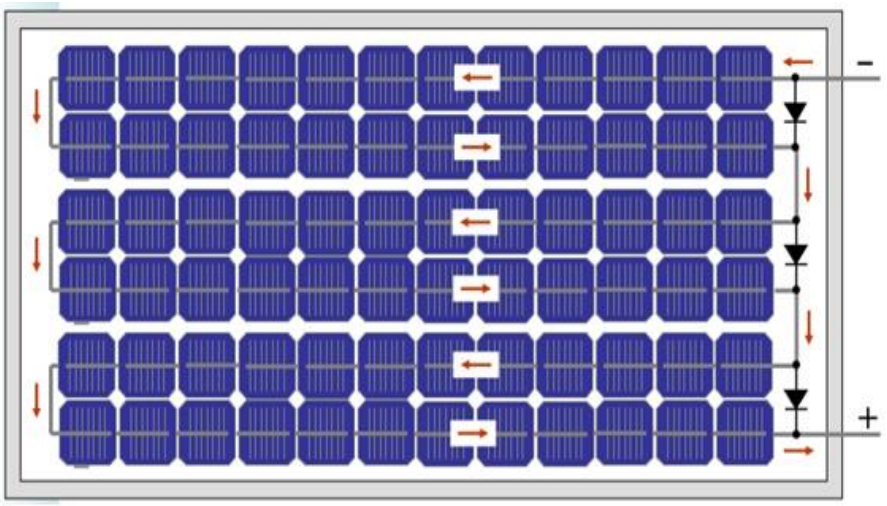

Figure 62: Typical 72 cells used in the hot spot tracking test

By creating the hot spot and recorded its temperature by the FLIR camera and measure the I-V curve of the panel under shadowed effect it is clear to say that the highest reverse current with the presence of a bypass diode indicates to defective cells.

Figure 63: FLER E60 camera

CHAPTER 5

Experimental Works and Results

5.1 Characteristics of Solar Panel and Investigation Models' Five Parameters

The solar cell model was examined for three panels, and given results appropriately with experimental datasheet supported by the manufacturer at STC of cell temperatures and irradiation levels. Modules tested in experimental works include the types of NSS-24150MPV, NSS -12100MPV and YL260P-29b PV panels.

Table 5 summarizes the specifications for three PV panels at STC and table 6 shows the calculated five parameters in Matlab M -files at STC. The simulation results for the panels under test are sensitive to the operating points of weather conditions, so to get the same values of specifications at STC could be difficult in the higher temperature areas. Without getting accurate reference conditions of irradiation and cell temperature, it is impossible to get appropriate characteristic curves with five parameters that tabulated in table 6, but it is possible for fitting the existing measures values of ambient temperature and irradiation levels and calculated the five parameters by Matlab M-files and hence plotted I-V and PV curves for each panel.

Table 5: Three module specifications at STC

		NSS-24150M PV	NSS -12100M PV	YL260P-29b PV
Operation conditions	Parameter	Datasheet	Datasheet	Datasheet
STC 1000 W/m^2 25 ^{o}C	P_{max} (W)	150	100	260
	I_{mpp} (A)	4.10	5.29	8.41
	V_{mpp} (V)	36	18.9	30.90
	V_{oc} (V)	43.20	22.50	38.90
	I_{sc} (A)	4.45	5.65	8.98

Table 6: Three PV panels five parameter estimation at STC

		NSS-24150M PV	NSS -12100M PV	YL260P-29b PV
Operation conditions	Parameter	Model	Model	Model
STC 1000 W/m^2 25 ^{o}C	I_{ph} (A)	4.49	5.65	8.98
	m	1.34	1.35	1.28
	R_{sh} (Ω)	693.73	448.60	107,132,4
	R_s (Ω)	0.074	0.001	0.304
	I_o (A)	1.20e^{-07}	8.49e^{-08}	2.48e^{-08}

Figures 64, 65, 66 and 67 describe I-V and P-V curves of NSS -12100M PV and YL260P-29b PV panels that modeled with the proposed approach explained in chapter 3. The three remarkable points provided by the manufacturer are matched by two curves exactly: V_{oc}, I_{sc} and P_{mp}.

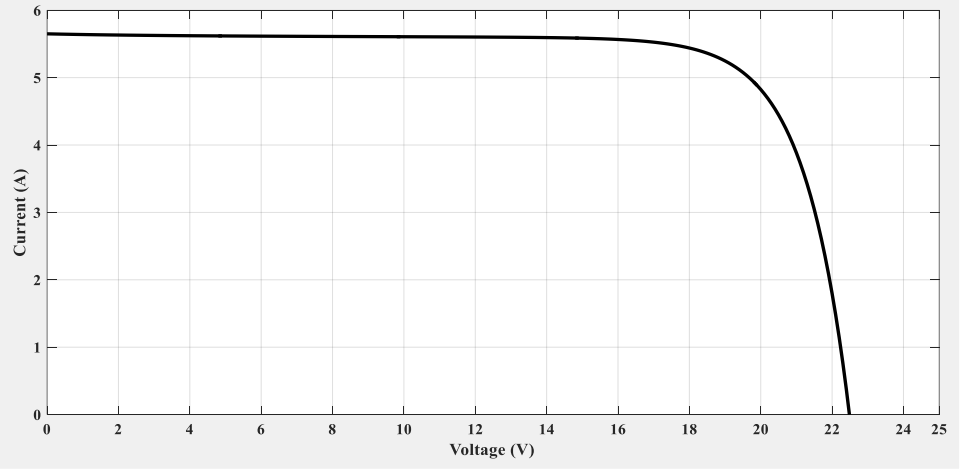

Figure 64: I-V curve of NSS -12100M PV panel at STC

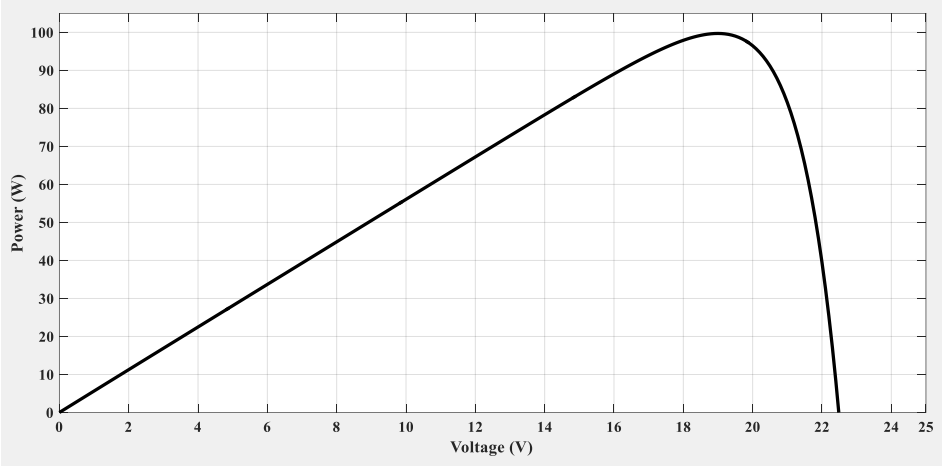

Figure 65: P-V curve of NSS -12100M PV panel at STC

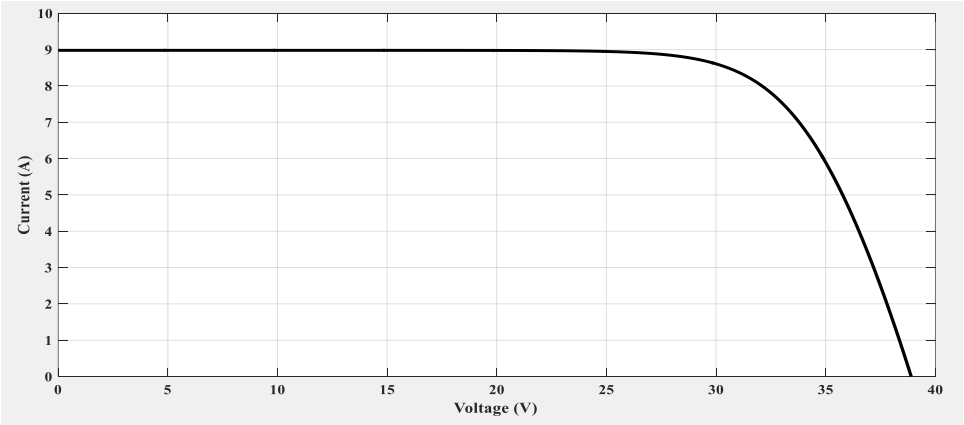

Figure 66: I-V curve of YL260P-29b PV panel at STC

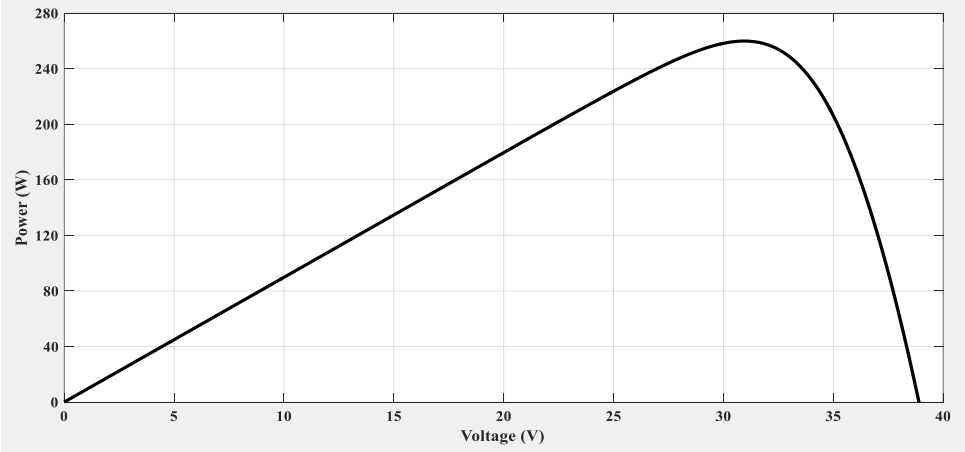

Figure 67: P-V curve of YL260P-29b PV panel at STC

The experimental works were measured by CASSY Lab configuration with its software and sensors. The outdoor test measured the I-V and P-V characteristic curve of PV modules in outdoor conditions. The experiments produced graphical results that are easily observed and identify the mismatch due to shading and dust effects.

The resistive load has a range between 0 and 100% is used to step through a range of voltages that allowed the current to measure at each step of the voltage. Thus, an accurate I-V and P-V curves for characterizing PV modules are drawn immediately. However, the resistive load is able to provide the current of zero amperes for Voc condition and zero voltage for Isc condition.

The following two tables summarize the five parameter extraction and maximum operating points for three panels under test in real operating test conditions (OTC) of irradiation and temperature.

Table 7: Specifications and five parameter extraction of NSS- type panels at OTC

Operation conditions	Parameter	NSS-24150M PV	NSS -12100M PV
OTC 1020.4 W/m^2 59 ^oC	I_{sc} (A)	4.58	5.76
	P_{max} (W)	105.99	56.40
	I_{mpp} (A)	4	4.70
	V_{mpp} (V)	26.50	12
	V_{oc} (V)	37.50	19.50
	m	2.22	2.54
	R_{sh} (Ω)	101.42	170.99
	R_s (Ω)	0.25	0.512
	I_o (A)	$1.22e^{-04}$	$3.93e^{-04}$
	I_{ph} (A)	4.59	5.76

Table 8: Specifications and five parameter extraction of YL260P-29b panel at OTC

Operation conditions	Parameter	YL260P-29b PV
OTC 833 W/m^2 66 ^oC	I_{sc} (A)	7.48
	P_{max} (W)	143
	I_{mpp} (A)	6.50
	V_{mpp} (V)	22
	V_{oc} (V)	32.50
	m	1.43
	R_{sh} (Ω)	1011
	R_s (Ω)	.84
	I_o (A)	$1.9605e^{-07}$
	I_{ph} (A)	7.48

Figures from 68 to 73 show the I-V and P-V curves of three panels using the CASSY system and then validated these plots by the Matlab M-file simulator and hot spot model in Simulink. The curves are plotted at the OTC with the specifications and five parameters illustrated in tables 7 and 8.

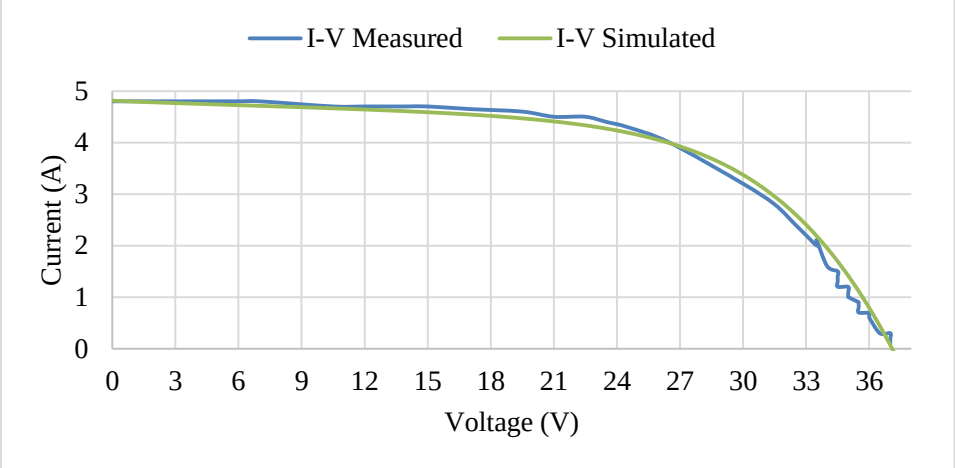

Figure 68: I-V curve of NSS -24150M PV module at OTC

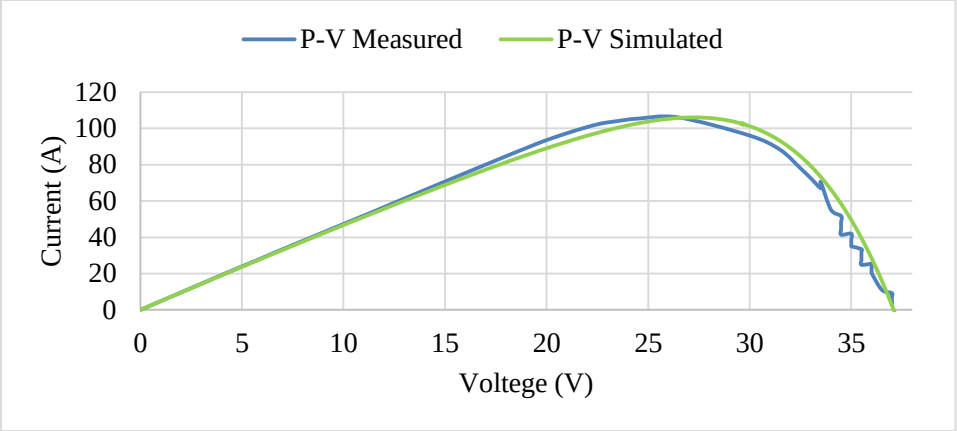

Figure 69: P-V curve of NSS -24150M PV module at OTC

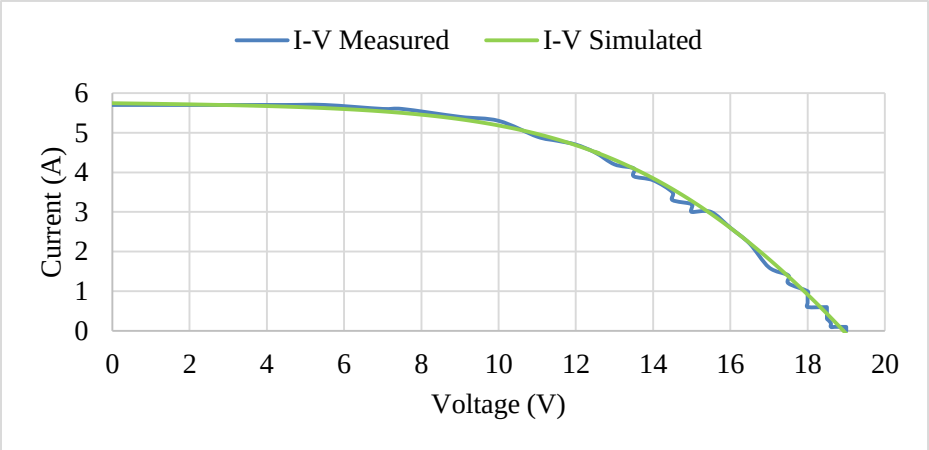

Figure 70: I-V curve of NSS -12100M PV module at OTC

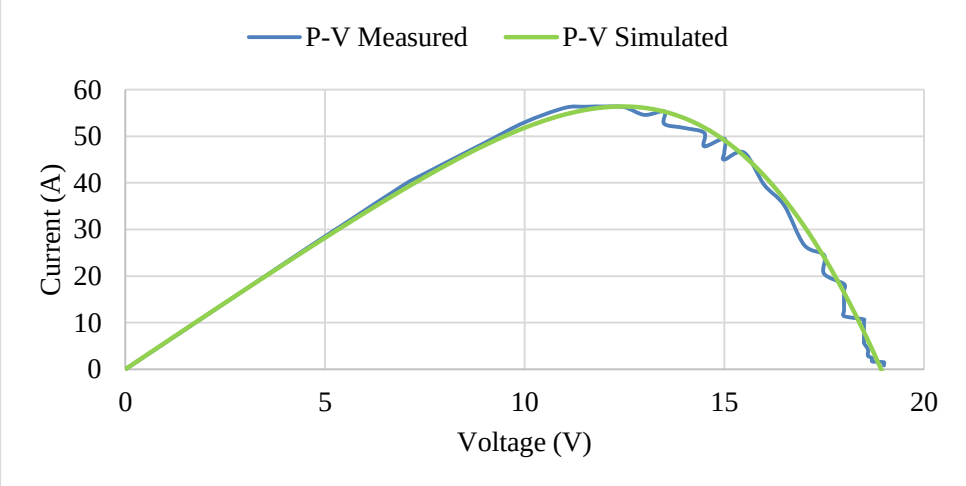

Figure 71: P-V curve of NSS -12100M PV module at OTC

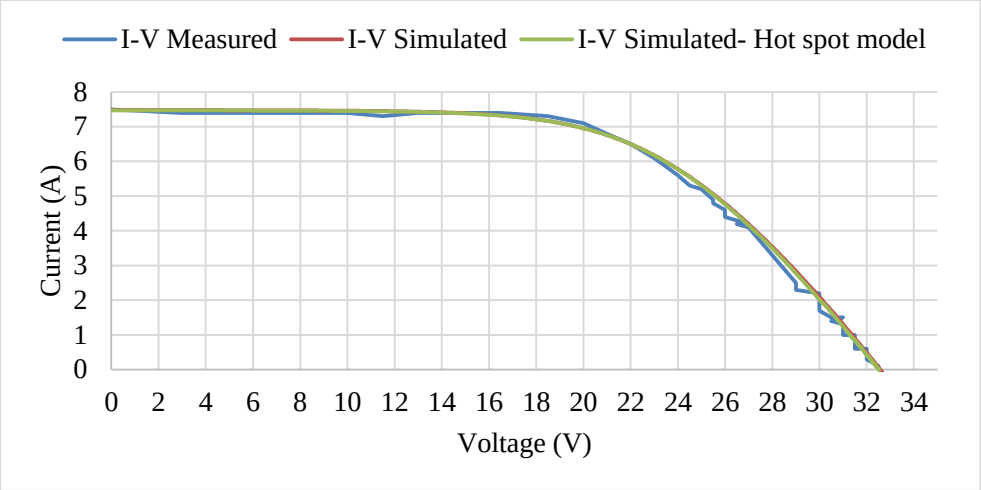

Figure 72: I-V curve of YL260P-29b module at OTC

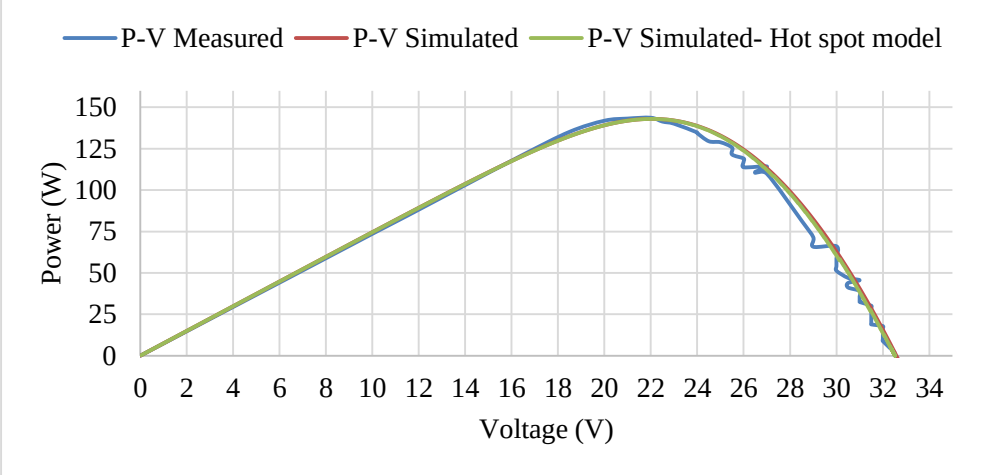

Figure 73: P-V curve of YL260P-29b module at OTC

It is clear that from previous figures the approximation is achieved between the results from measurements by CASSY system hardware and the simulator of the hot spot model. The simulation gives an accurate graphical representation of the same operating conditions because it evaluates for hundred points of voltage during the variations in the load. Figures 68 and 69 show the degradation of output power due to aging and hot spot problem of NSS-

24150M panel. The graphs demonstrate that the panel, which was used in this case is not new, and its efficiency may be weakened and refused.

From previous plots, the temperature effects should be studied carefully. Hence, when the temperature rises, V_{oc} of the panel decreases. In this study, the rated V_{oc} of the NSS-24150M panel at 25 ^{o}C is 43.2 V, and it became 37 V at 58 ^{o}C.

Besides, it's mentioned that any minor variation in the value of the parasitic resistances will change the pattern of electrical characteristic curves. A slight change in temperature will influence on all parameters of the solar cell. These parameters are considered as functions of temperature.

The reverse saturation current I_o and the band gap energy E_{gab} of the silicon material depend on cell temperature. As temperature increases as shown in all previous figures of I-V curves, E_{gab} transfers I-V curves toward the left that mean reducing the value of V_{oc} and the V_{mpp}. In other words, a large impact on the power delivered to the load while E_{gab} is changed.

Also, the increase in R_s will cause a big voltage drop of the cell as shown in all figures depict I-V curves, beside a huge impact degradation on the module voltage. A decrease in R_{sh} will cause a path to a current flow through the shunt resistance and reduces the module current, leading to lower output power. While the temperature increases the value of the ideality factor also changes and it is increased or decreased linearly depending on the material of the solar cell. This value has a strong relation with shunt and series resistances. Figure 72 shows a large reduction in the value of series resistance beside the knee of the I-V curve that affected by the value of the ideality factor.

R_s has a massive impact on the slope of the I-V curve near V_{oc}, and hence the value of R_s is determined by calculating the slope dI/dV_{oc} of the curve at the V_{oc} from the measured data for all panels. By the same way, the value of $-1/R_{sh}$ is determined at I_{sc} by estimating the slope dI_{sc}/dv of the curve.

From I-V curve in figures 68, 70, and 72, it is observed that R_s increases continuously with decreasing the irradiation level and then stabilizes with the more raise in irradiation. On the other hand, for low irradiation levels, around 700 W/m^2, R_{sh} was shown increase slightly. However, for high irradiation levels around 1000 W/m^2, it begins to increase rapidly. Increasing R_s and reducing R_{sh} will decrease P_{max} that delivers to the load and causing a large drop of FF as shown in figures 69, 71 and 73.

To get accepted discussion, it is clear to say that from figure 69, the abnormal panel suffered from a hot spot problem, and its shunt resistance is dramatically decreased and hence the performance of the panel is very poor. To estimate accuracy, the average relative error in term of peak power output so the maximum power due to empirical data has a low value around 106 W. Some considerations should be considered with an outdoor module, i.e. the performance of bypass diode operation and the adequacy of the internal wire connections of the serial cells. These considerations clearly appeared in simulated plots that reflects either the panel is working fine or has poor efficiency.

5.2 PV Panel under Shading Effect – Initial Hot Spot Study

PV YL260P-29b is a new panel used to examine the effects of shading of a single solar cell or any configuration of shading pattern and plotting the I-V and P-V curves, then decided the worst case depending on the amount of power dissipation and the reverse bias voltage applied. As explained earlier, since the solar cells are connected in series, the same current

must pass through each cell under normal operation conditions. The shaded cells operate in the reverse bias voltage, thus dissipated power that leading to heat up the affected area of the cell and cause the hot spot problem. The function of bypass diodes permits part of a module's current to flow around shaded cells, therefore, limiting the current losses of the whole panel. To verify and validate the model of the hot spot that designed in Simulink, multi real scenarios are established and applied where the module operated at various levels of irradiation and temperatures that are measured in practical experiments and then used to examine the initial hot spot for each case. For each scenario, the behavior of the bypass diode is recorded and the currents distribution between the shunt resistance and the affected string are observed. Also, the five parameters are considered as a function of temperature to get the real I-V and P-V curves.

Six scenarios are tested with a completely shaded cell. Table 9 summarizes each case with full details about currents distribution, power calculations, and the value of the parasitic resistances related to operating points of irradiation and temperatures.

In all cases, the load for the panel is adjusted to maximum conditions, i.e. $R_L = V_{mp} / I_{mp}$. The I-V and P-V curves are measured by the CASSY lab in practical experiments and the parasitic resistances are estimated from the I-V curves for each case.

Table 9: Initial hot spot study at R_{max}

Irr. (W/m^2)	Temp. ^oC	R_{sh} (Ω)	R_s (Ω)	I_{shunt} (A)	I_{string} (A)	I_{bypass} (A)	I_{module} (A)	P_{diss_Rsh}(W)	$P_{diss\_shaded\ cell}$(W)	P_{load} (W)
1000	25	1071324	.304	0	0	6.22	6.22	0	0	139.1
715	61	1007.5	0.98	.61	.61	3.66	4.27	6.21	6.22	65.67
760	61	339.4	1.24	1.79	1.79	2.53	4.33	18.23	18.29	71.18
780	65	329	1.36	1.85	1.85	2.86	4.7	18.75	18.83	75.23
820	64	900	1.1	0.8	0.8	3.41	4.21	9.6	9.8	72.58
833	66	1011	0.84	.65	.65	3.63	4.29	7.06	7.09	73.44

Each case has a different five parameters that calculated by Matlab M-file simulator. These different parameters were caused in various I-V and P-V characteristics.

The electrical characteristics of each case without shading effect are plotted by CASSY Lab during experiments and by Simulink hot spot model. Figures 74 and 75 describe the I-V and P-V curves at operating points of irradiation and temperature that mentioned in first two columns of table 9.

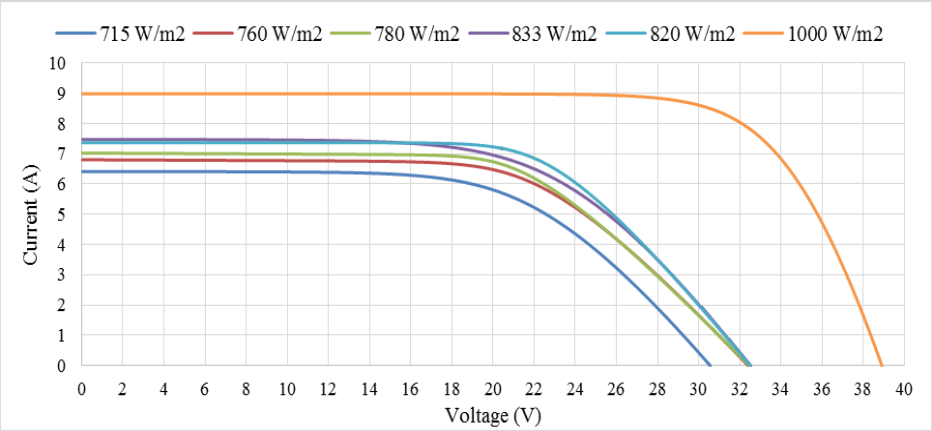

Figure 74: I-V curves of YL260P-29b module at initial hot spot study

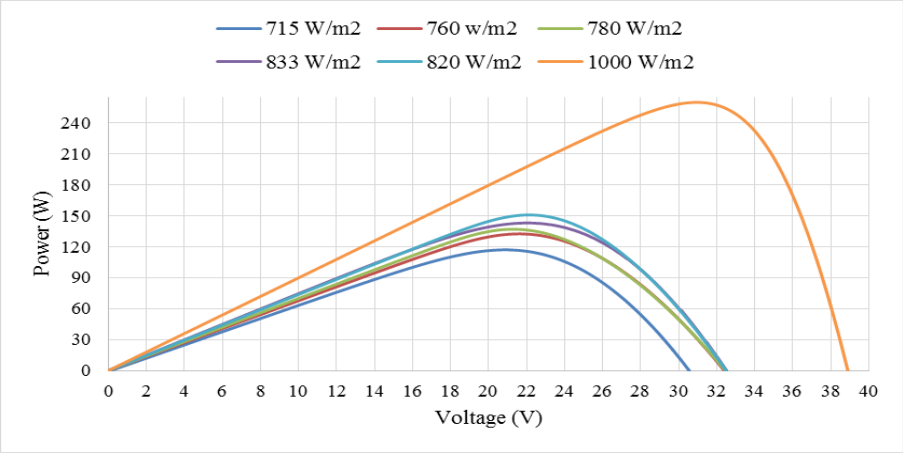

Figure 75: P-V curves of YL260P-29b module at initial hot spot study

Table 9 demonstrates the strong relation between the shunt current and shunt resistance when the irradiation level decreases. As mentioned in chapter 4, when the cell temperature

increases, then the shunt resistance reduces dramatically as a function of temperature, and the shunt current that caused initial hot spot is quickly increasing. This observation can be seen when the irradiation level reached 760 and 780 W/m^2 and the shunt resistance has a value around 330 Ω, so the dissipated power through the shunt is raised and leads to a hot spot phenomenon. Also, it is clear that, for maximum efficiency of a module, the highest R_{sh} is desired (Irr. = 1000 W/m^2).

On the other hand, when the irradiation levels are recorded at 715, 820 and 833 W/m^2, the shunt resistance has a large value around 1000 Ω however the currents are still distributed between the bypass diode and the shunt path as explained in chapter 4. In all cases, because of fully shading is applied, the photo-current is zero and hence the shunt current must equal to the affected string current.

It can be seen that from the results the bypass diode is working in the presence of shading. Bypass diode plays an important role for limit the voltage across the shaded cell from access the breakdown voltage as explained in chapter 4.

In conclusion, three factors accelerate the hot spot development: rise in temperature, the lower the irradiation hitting the cell and decreases the numerical value of shunt resistance. Deterioration in power means if one cell is shaded it has a huge influence on the module, and leads rapidly to the hot spot risk and damage the panel.

5.3 PV Module under Hot Spot Phenomenon Evaluation

This part includes the explanation of the work process of the hot spot model in Simulink. Wide Simulink blocks and details with inputs of weather data are considered as sub-modules of the model. A flowchart of the hot spot model is illustrated in figure 76.

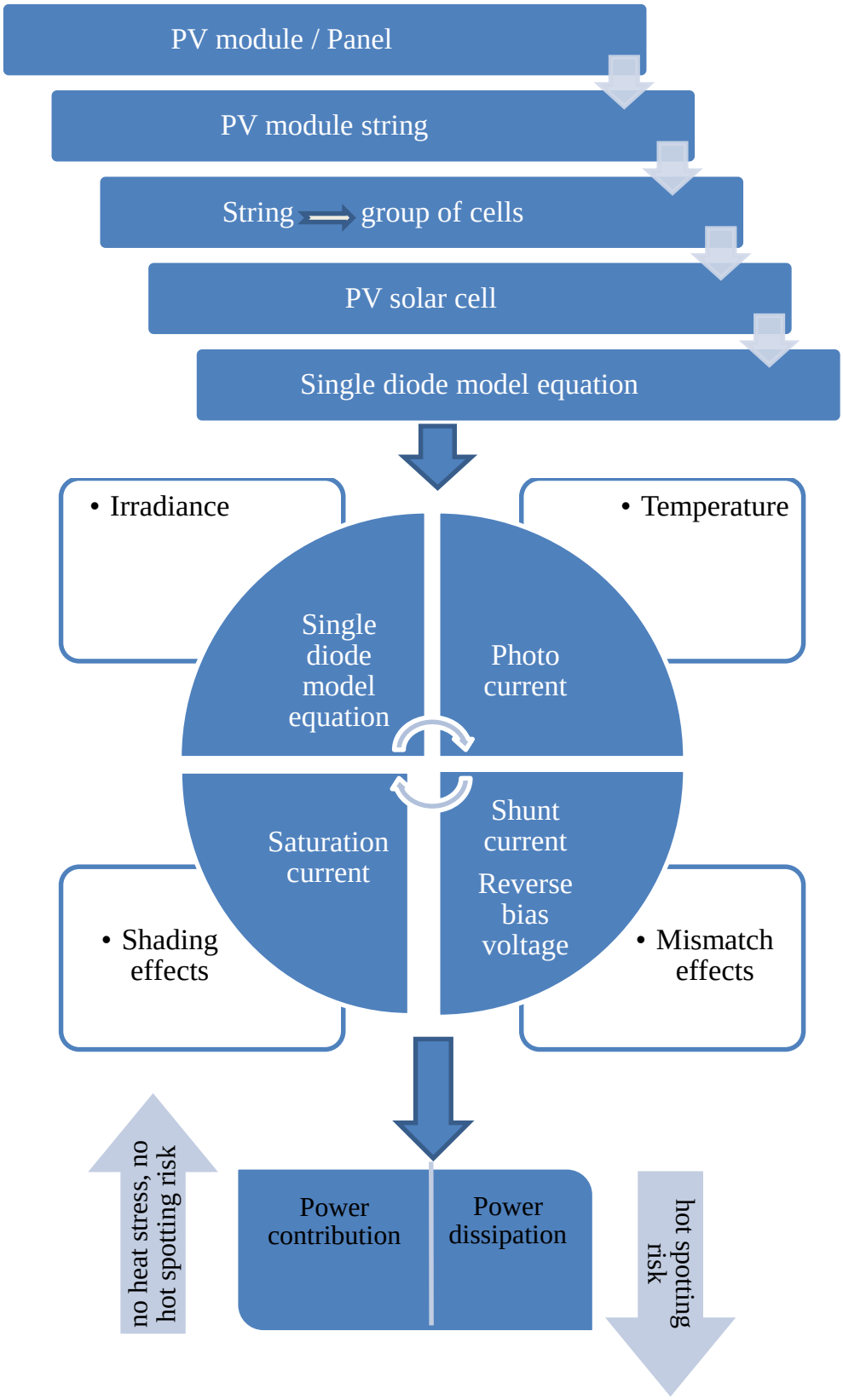

Figure 76: Flowchart explains the hot spot model structure

5.3.1 Fast Hot Spot Creation and Examination

To examine the shading effects on a PV panel, a series of laboratory experiments were carried out. In each test, different areas of the one cell were shaded, in order to investigate the effects of the shadow level on the panel. The shading was performed by black carton cover to get a completely dark cell. The various combinations of shading were implemented in the outdoor test to control the shading ratio and recording the currents and voltages across the bypass diodes by thermography technique. The obtained results were discussed in the following subsections.

First Hot Spot Point due to Shading Effect:

In this study, one cell of NSS -24150M PV module was shaded by black carton cover for two hours as shown in figure 77. NSS -24150M module has been deteriorated so the locations of degradation have appeared in the strings. The impact of this damage on the efficiency of the panel was specified by the two characteristic curves and IR technique.

The hot spot is generated quickly and its temperature reached 120 ^{o}C, however, the ambient and module temperatures were 40 ^{o}C and 56 ^{o}C respectively. The hot spot was seen by the naked eye and this situation rarely happened. Figure 78 shows the picture of initial hot spot damage taken by digital camera. This test is performed at a short circuit condition, so it represents the worst case for hot spot initiation and formation.

(a) The whole panel

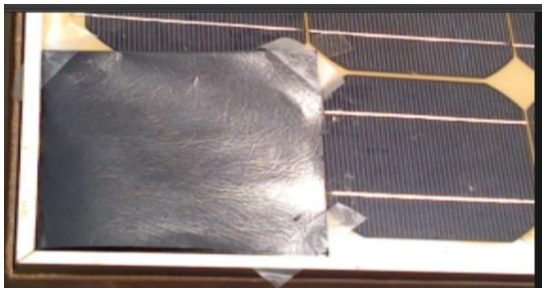

(b) single shaded cell

Figure 77: NSS -24150M PV panel with one shaded cell

Figure 78: Visualization hot spot damage at 120 ^{o}C

The former figure represents the worst case of shading that occurs when the whole cell is shaded. Low R_{sh} has localized shunt path within the cell structure. In this case, overheating happens because massive amounts of leakage current flow through a little area connected with shunt resistance. As the current path is tight, hot spot heating is very rapid.

Identifying Hot Spots by Thermal Camera:

The IR camera used for the analyses presented in this study was a FLIR E60 camera. E60 camera has 320 × 240 resolutions that gives high-quality thermal images. Its temperature ranges from –20 to 650 °C, with thermal sensitivity < 0.05 °C. These professional specifications help even a small changing of temperature to be detected and give a clear image for the hot spot phenomenon analysis.

Advanced software for image processing, schemes, and analysis is also available for the FLIR system so the captured photos can be analyzed by the FLIR software tool. FLIR tool can display both thermal and normal images side-by-side for more analysis. Figure 79 shows an IR image of the hot spot investigated by shading one cell as illustrated in figure

77. The temperature distribution was recorded within a little time (one minute) of forcing leakage current flow through the shaded cell.

In determination path and the origins of shunts, it is preferable to capture the images as quickly as possible after the leakage current flow is achieved, otherwise, the heat moves out of the defective cell to new adjacent cell and causes the increases in temperature. At 150 ^{o}C thermal breakdown has occurred in the material of the shaded cell.

In this case, the load current is equal to the value of I_{sc} in that weather conditions, which corresponds to the maximum current to be generated in the cell. Perhaps this test will lead to irreversible cell burn that could cause a variety of solar cell parameters and I-V characteristics.

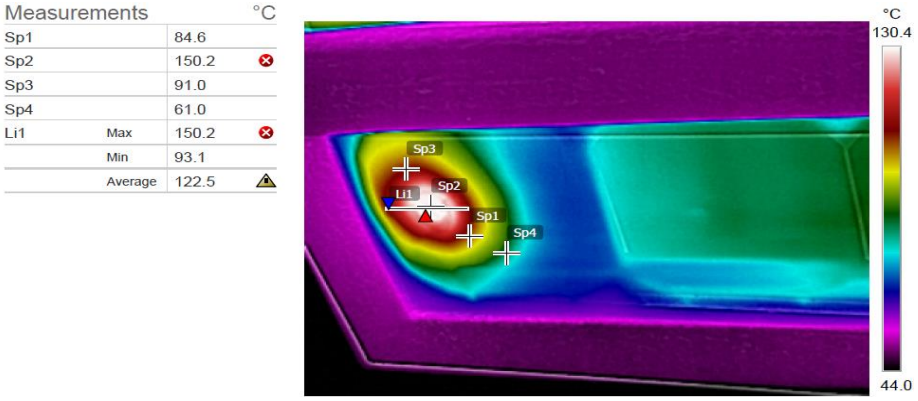

Figure 79: Thermography picture of shaded cell

Figure 80 illustrates the temperature profile generated from an IR image of the defective cell. The profile shows the temperature values with respect to the coordinates of the hot spot area. For example, the maximum temperature happened during hot spot risk has coordinates between 22 and 25. All points lie in this range has danger hot spot temperature that reached 150.2 ^{o}C, and this value has the ability to destroy the panel within few minutes. Additionally, the temperature is distributed around the defective area, depending on the

shunt paths for backward current flows in the reverse bias. IR picture in figure 79 shows the temperature of the surrounded areas of the hot spot that have a range between 90 and 150 ºC with an average value 122.5 ºC and all of these points indicate to the harmful thermal stress exerted on the cell that reduces the performance of the whole panel.

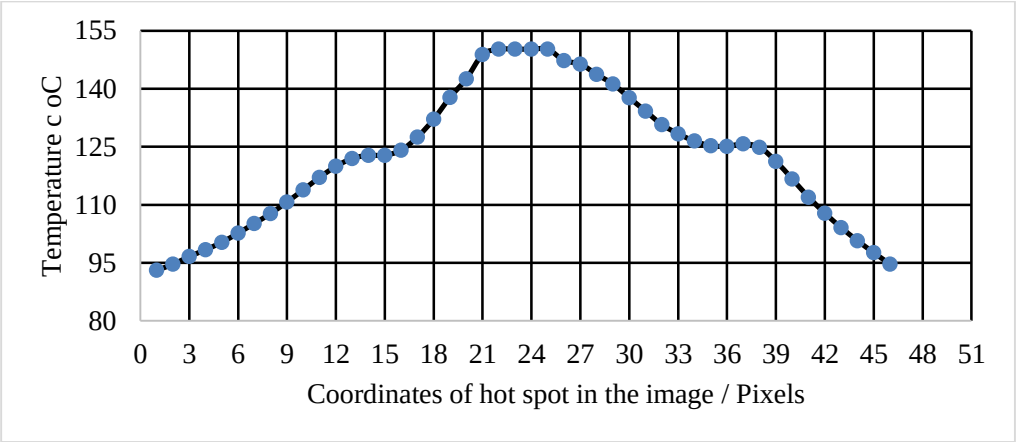

Figure 80: Temperature hot spot profile taken at Li1

Bypass Diodes Conductivity:

PV panels are usually connected with bypass diodes to protect the module against mismatch or faults resulted from the hot spot phenomenon and to limit the negative voltage (breakdown voltage).

The IR camera is used to check the operation of bypass diodes. Figure 81 shows an IR picture of the junction box that contains 3 bypass diodes. When the cell is under shading effect, the currents will be divided between the string and the bypass diode which is turned on and conducts the current, so from the thermal image, it is clear that a brighten heat around the working bypass diode so temperature increases in the diode to prove its functionality. Also from the thermal image, it's easy noted that the differences in temperature distribution between three diodes. As predicted diode 3 has the highest temperature with 57.6 ºC.

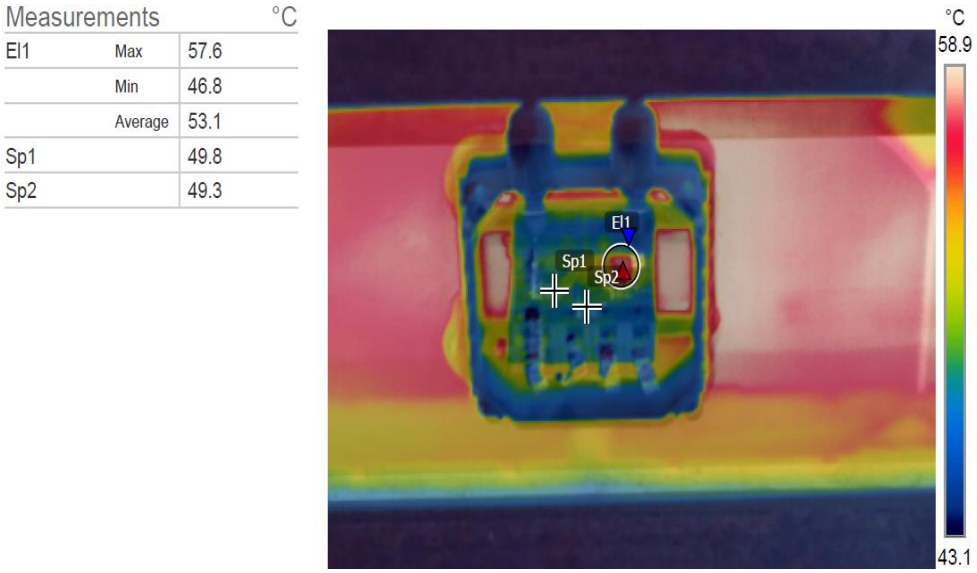

Figure 81: Thermal image of junction box

The I-V curve of the reverse bias mode and the shunt current flow for the hot spot damaged cell are shown in figures 82 and 83. It demonstrates that the shunt current circulated around the shunt resistance, however, the current passes through the defective cell is represented by the string's current so the total current of the whole module should be equal to the string current and bypass diode current as explained in chapter 4. The I-V curve of the whole module is illustrated in figure 84 that shows the activation point of the bypass diode under hot spot phenomenon.

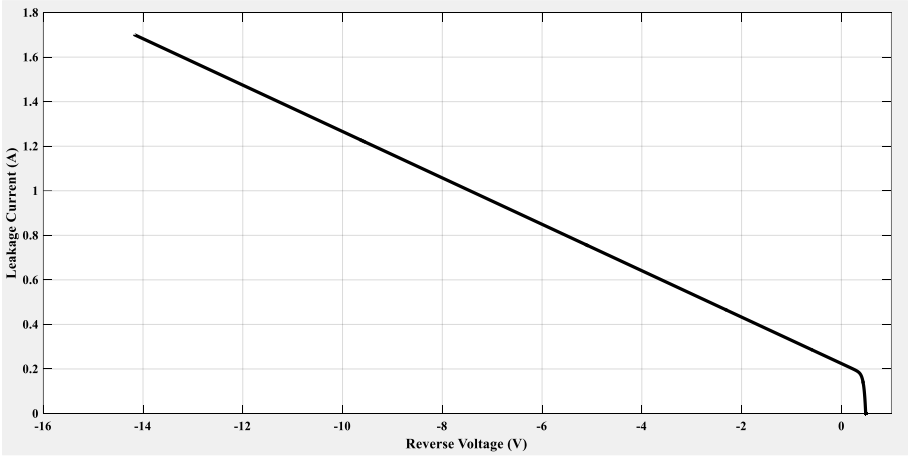

Figure 82: I-V curve of revers bias damaged cell

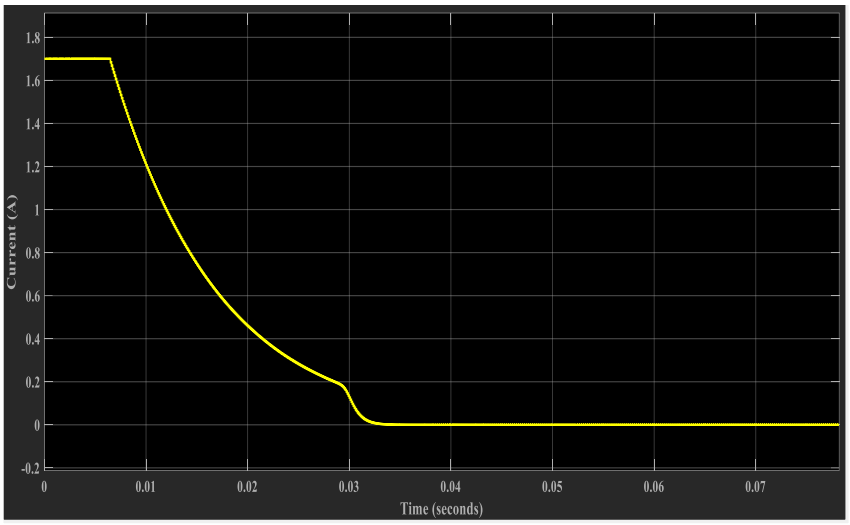

Figure 83: Shunt current flow through damaged cell

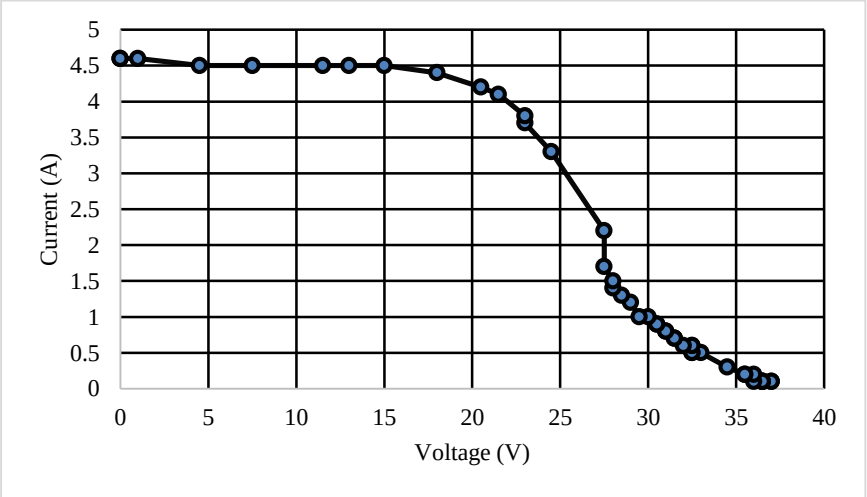

Figure 84: Practical I-V curve of the panel under hot spot damaged cell

From figure 84, it's easy to investigate where the activation process of bypass diode happens. The resistive load is changed and all currents flow are also changed until the voltage of the module became 27.5 V and at this point, the bypass diode is turned on.

5.3.2 Thermal Analysis of Hot Spot Model and Verified the Currents Distribution

In order to verify the reverse current that can cause the hot spot inside the shaded cell, the experiment is conducted by using thermal analysis to illustrate the currents flow in the bypass diode and shaded cell respectively.

The reverse current of the shaded cell appeared as a heat around the shaded locations and the bypass current also appeared as a heat around the diodes.

A description of the test:

Two conditions are established in this test, short circuit current condition, i.e. extreme case and the loaded condition, i.e. the normal case where the panel is loaded. Two cases are performed under forcing shading effect on a single cell of each string and captured IR images.

The following sequence of thermal images displayed the distribution of temperature in the whole panel, shaded cell and bypass diodes. The test is performed within 20 minutes to avoid damage to the panel.

Case 1: Short Circuit Condition

In this scenario, many images were captured to demonstrate the behavior of the hot spot and the bypass diode operation. Figure 85 from a-d shows the thermal distribution.

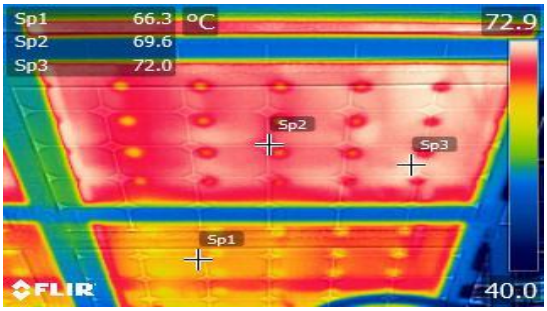

a- Whole panel- back view

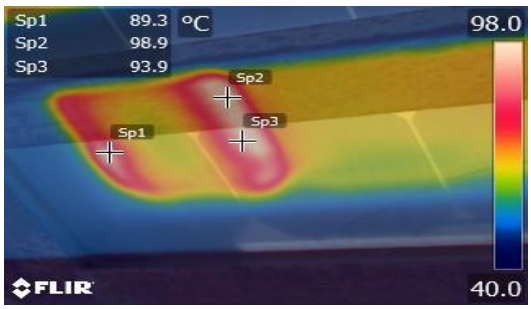

c- Shaded cell

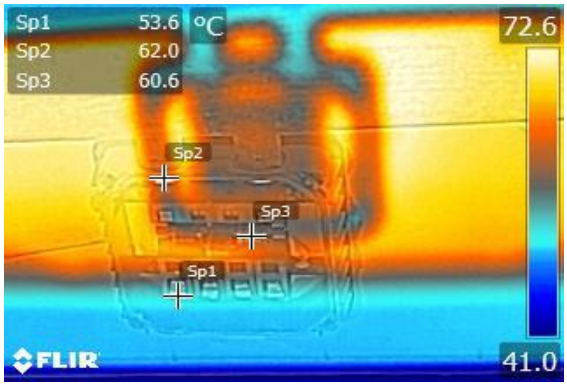

b- Junction box

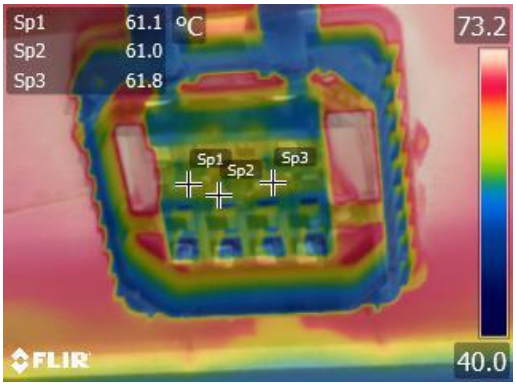

d- Bypass diodes

Figure 85: Thermal pictures of temperature distribution

From previous thermal photos, it's clear that the temperature rapidly increased when one cell is shaded and working at the 99 ^{o}C within a few minutes as shown in picture c, but the rest cells have the average temperature around 70 ^{o}C as shown in the picture a. Temperature progression of hot spot proves that in order to get the maximum hot spot temperature, the shading time should extend from 5 min to 2 hours. Figure 86 presents the relation between the hot spot location and its maximum temperature. This plot illustrates the temperature distribution over the weak area, i.e. hot spotting area. This area is illustrated by the thermal photo in figure 87 by the line that indicates the highest temperatures coordinate in the picture. As well, it becomes clear that defective cell has largest temperature degree recorded at the 110 ^{o}C until the thermal strength is achieved. This effect could be led to a narrow defect area and a higher local leakage current as illustrated at spot 1 in figure 87.

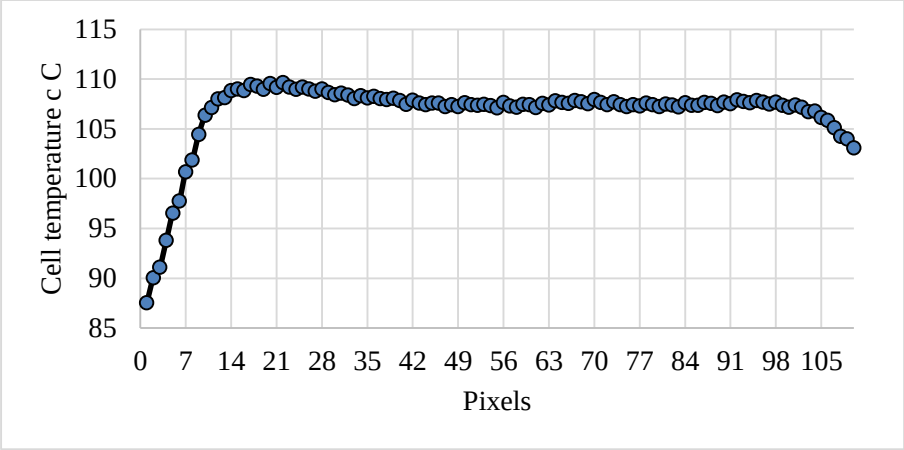

Figure 86: Temperature hotspot profile taken at Li1

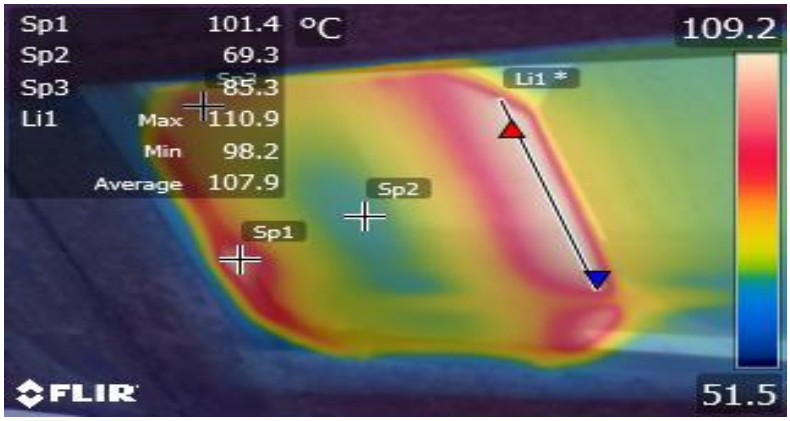

Figure 87: IR image of fully shaded cell with hottest area

From previous thermal images, it concludes that the range of heating of the solar cell is closely connected to the characteristics of the p-n junction material. As a non-uniform of irradiation reaches the cell, the shunt defects are locally concentrated and produce a path for the leakage currents.

Case 2: Loaded Panel – NSS -24150M PV module

As mentioned previously the bypass diode in the normal operation condition and no shading effects, still in reverse bias mode i.e. not working. Figure 88 shows no conductivity of bypass diodes and hence no current flow in the normal case.

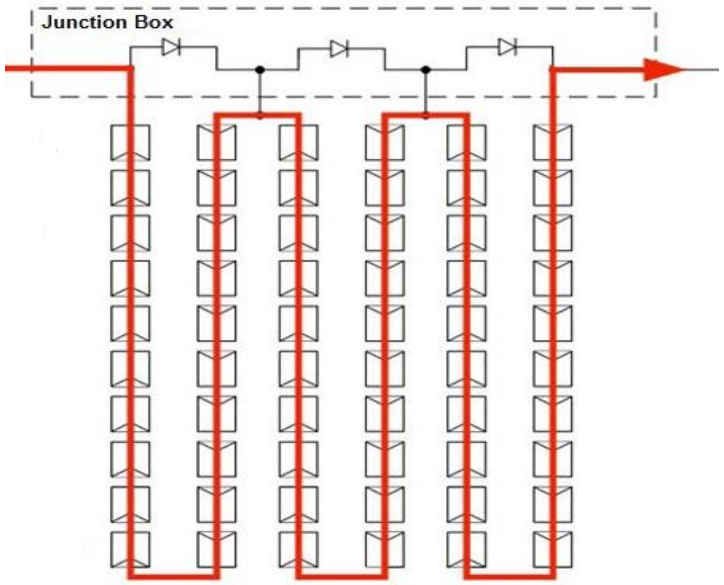

Figure 88: A connection of bypass diodes to each third of the panel without conductivity

In the case of shading and the panel is loaded, the bypass diode switch on and becomes conductive, depending on the shading level and the number of cells under shading in each string and hence decreases the voltage of panel by one-third, and the module's current will be separated between the affected string and conductive bypass diode as shown in figure 89, where the second string is bypassed and the current split between the string – two middle columns- and the bypass diode.

The thermal image in figure 90 describes the conductivity status of bypass diode - the middle diode-. It is indicated to a higher maximum temperature after conductivity operation, i.e. after shading effect. So the temperature of the middle diode is 87 ^{o}C compared to the left and right diodes where they temperatures are 69.9 ^{o}C and 62.4 ^{o}C respectively.

In this scenario, failure of bypass diode didn't happen, however the overheating usually occurred if diode p-n junction temperatures > 130 °C as seen in first hot spot point creation where the temperature reached to 140 °C so the bypass diode was damaged.

The affected string and the current flow during shading appears in thermography image 91 where it shows the typical pattern in which individual cells are much hotter than others in a third of the module. The temperature reaches to 58.5 ^{o}C in the defective string.

To analyze the poor cell suffered from the hot spot with the reverse current, it is still hotter than the other cells in the same string with reverse current flow and worked at the temperature 94.9 ^{o}C as shown in image 92.

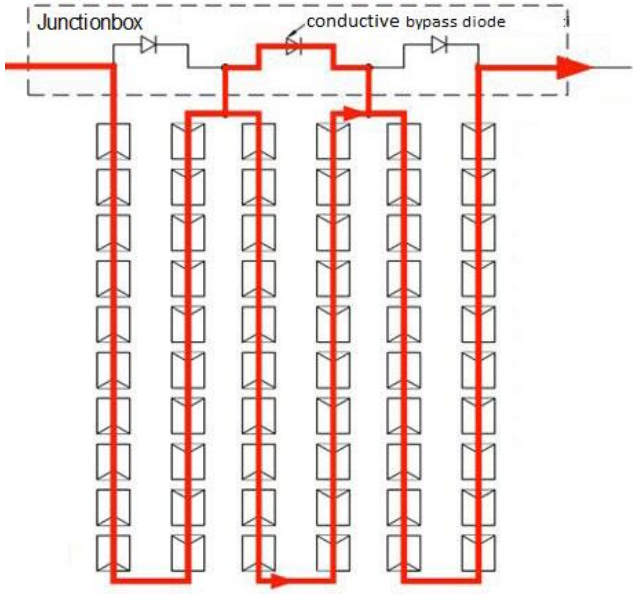

Figure 89: A connection of bypass diodes to each third of the panel with conductivity

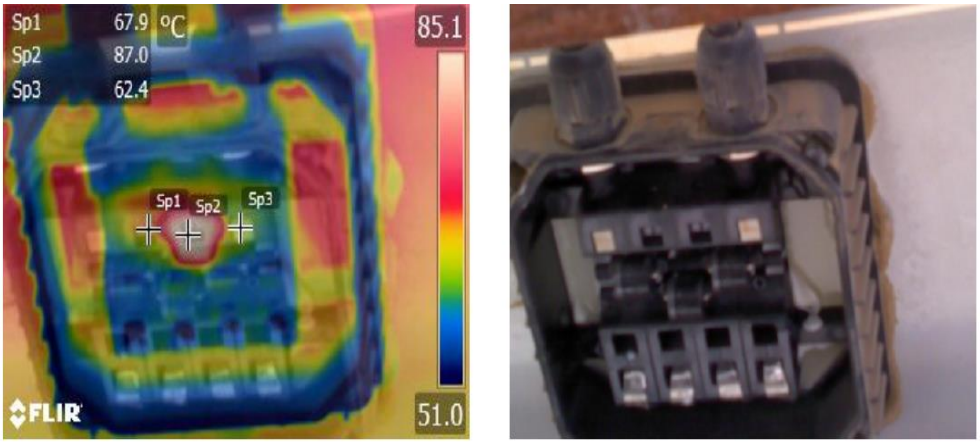

Figure 90: IR picture of middle bypass diode conductivity

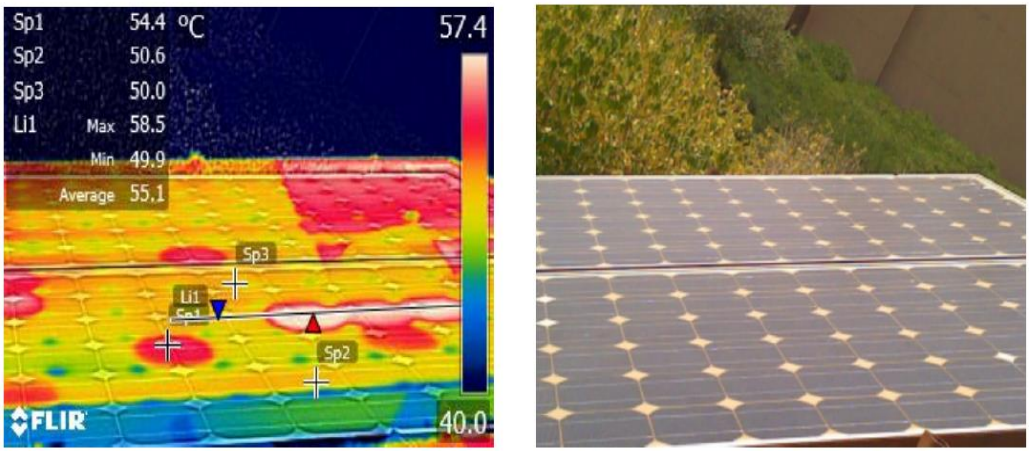

Figure 91: IR picture of middle string of the panel (left) and digital picture (right)

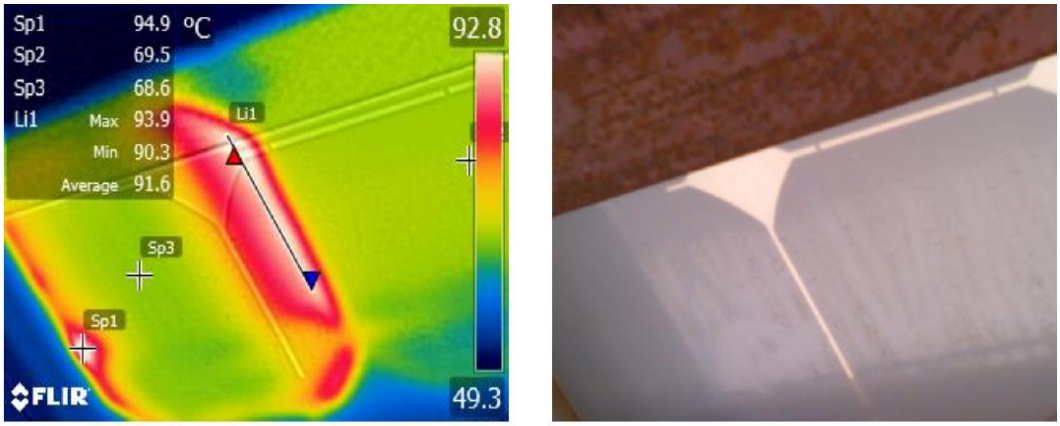

Figure 92: IR picture of hot spotting cell (left) and digital picture (right)

Figure 93 illustrates the temperature differences under hot spot phenomenon for three adjacent cells connected in two different strings. It should be noticed that the non-shaded cells have less temperature because there is no heat dissipation from these cells. For instance, the cells beside the aluminum frame of the panel tend to be with lower temperature – spot 3 at 51 ^{o}C –, while the cells beside the shaded one and junction box tend to be warmer – spot 1 at 67.5 ^{o}C –.

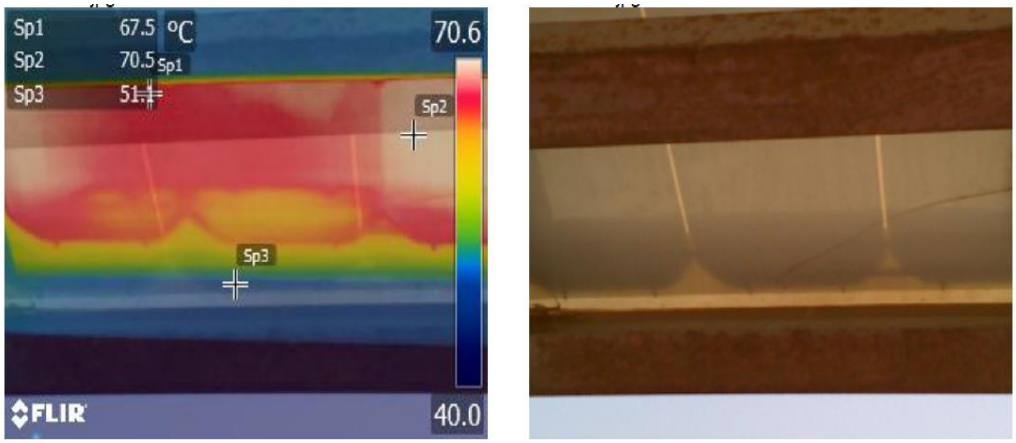

Figure 93: Cells temperature differences (left) and digital picture (right)

The same scenario applies to other strings and the same results we get. The following thermal images in figure 94 (a and b) depict the thermal behavior of bypass diode before and after shading effect and the thermal analysis measurements are summarized in table 10.

It's clear that the temperature is rapidly increased as the shading is applied and the deterioration of the output power will be huge, also the panel will lose its ability to produce energy. The hot spot risk area is extended during the time of shading and the thermal stress threatens the remaining cells, so the PV panel lifetime will be in danger.

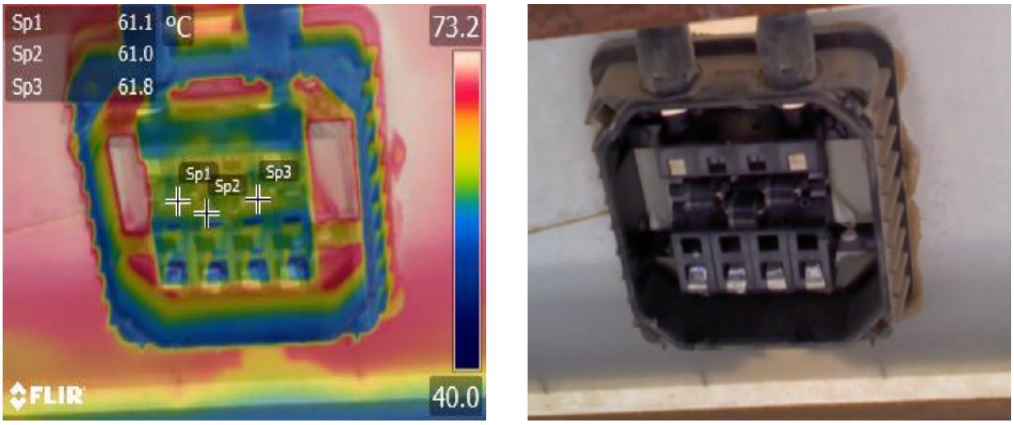

(a) Before shading

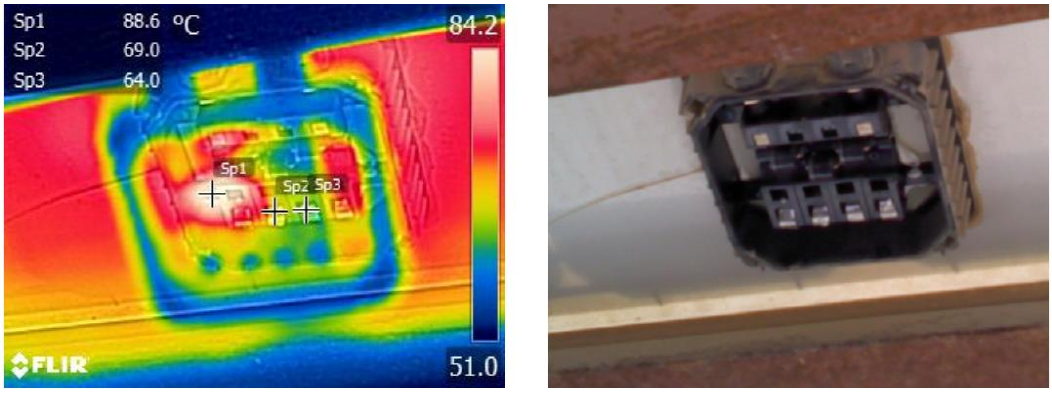

(b) After shading

Figure 94: IR picture of bypass diodes temperature differences before /after shading

Table 10: Thermal analysis of captured time before and after shading

IR image	Capture time (min.)	Spot 1 °C	Spot 2 °C	Spot 3 °C
Before shading	11 : 45 AM	61	61	61
After shading	12.04 PM	88.6	69	64
Temperature and time difference	20	+ 27.6	+ 8	+ 3

In conclusion, it's clear that from previous two images, hot spot increases quickly within few minutes. It was recorded within 20 minutes and the temperature of bypass diode that switch on is reached 88.6 °C under fully shaded cell. On the other hand, the second diode affects more than the third one because it's really close to the conducting bypass diode.

Case 3: Loaded Panel – YL260P-29b Module

In this case, a new panel is used to observe the behavior of the transient shaded cell under reverse bias voltage -13 V and noticed the currents of bypass diode and string path. It's clear that from the thermal image in figure 95 the entire string's current is forced through that cell in reverse bias. In this scenario, because of the cell is completely shaded i.e. photo-

current is zero, so the entire string's current is equal to the shunt current that can cause a significant hot spot. A bypass diode to shunt the leakage current is derived as observed in figure 96 that describes the thermal view of the junction box worked at 60.6 ºC.

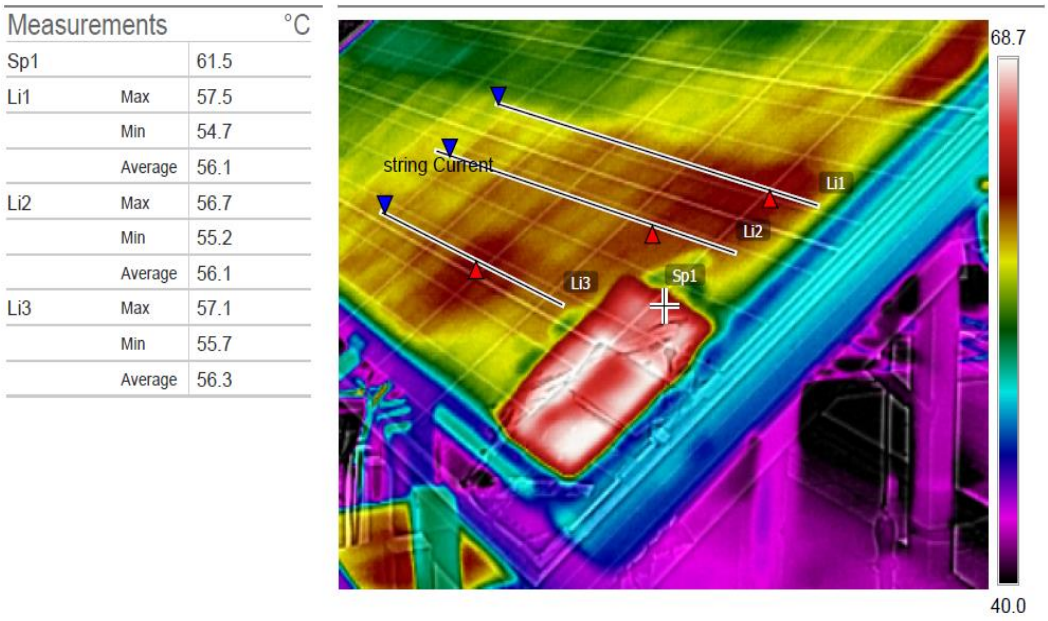

Figure 95: String current under reverse bias condition

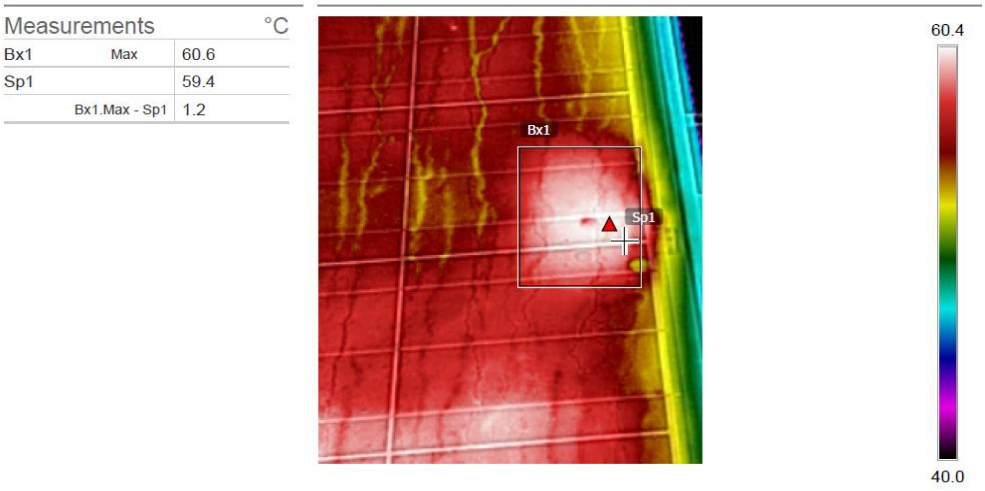

Figure 96: Junction box under reverse bias voltage -13 V

Figure 97 shows the temperature difference and the distribution on the shaded solar surface from the front and back. Initiation of hot spot location with raised temperature of about 12

ºC compared to the temperature of the rest cells from the front view as illustrated in image 97 (a). In contrast, figure 97 (b) shows the IR image on the back that presents an even higher temperature at the rest of unshaded cells with increased temperature around 4 ºC.

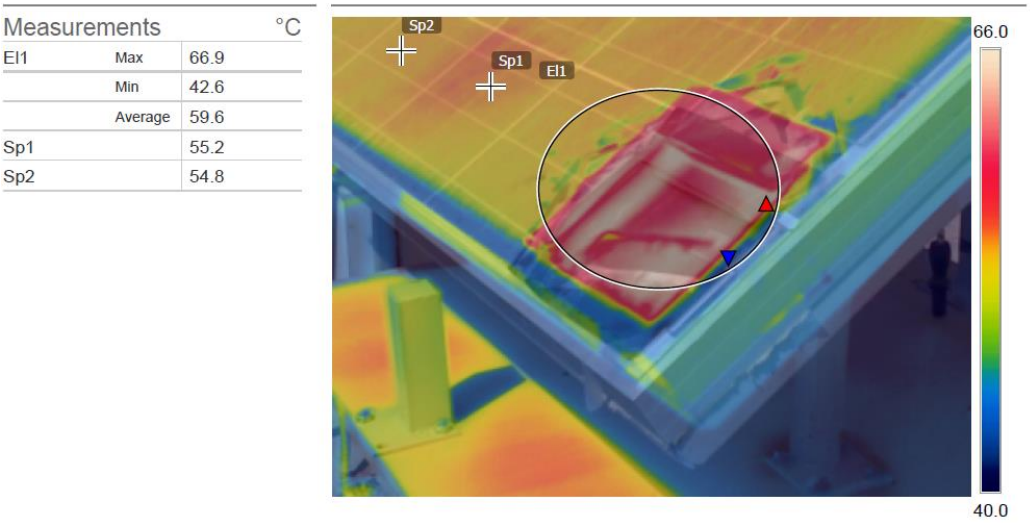

(a) IR image of shaded cell - hot spot location at the front of the panel

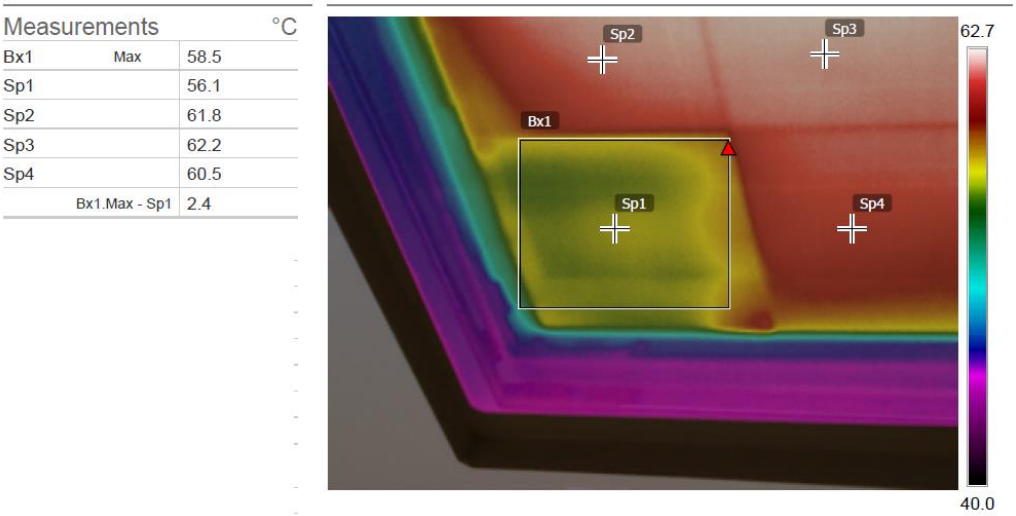

(b) IR image of shaded cell - hot spot location at rear of the panel

Figure 97: IR picture of solar panel presenting hot area location

Additionally, temperatures recorded in front of the module are spotted to be higher by about 5 –11ºC of temperatures recorded on the rear. This is due to the rise of the thermal

resistance influenced by insulation at the rear of the panel. Referred to the heat conduction law, the temperature at the back is predictable to be greater than temperatures at the front of the module.

As the shading effect has been fixed for a long time, the cell operating under reverse bias and raises the temperature will finally lead to decreasing power output.

5.3.3 Hot Spot Development and Tracing

The temperature changes in the shaded cell were observed by the IR camera. Thermal pictures were captured at 420 s period. A large part of the cell temperature remained unchanged, presenting no marks of hot spot initiation. The location is signed by the circle in figure 98 (a-e) tracked the propagation process of the hot spot temperature during shading effect duration.

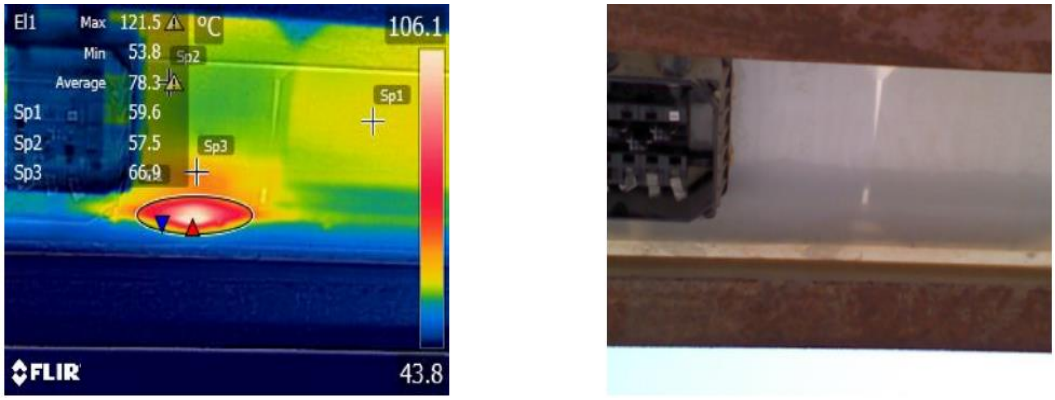

(a)

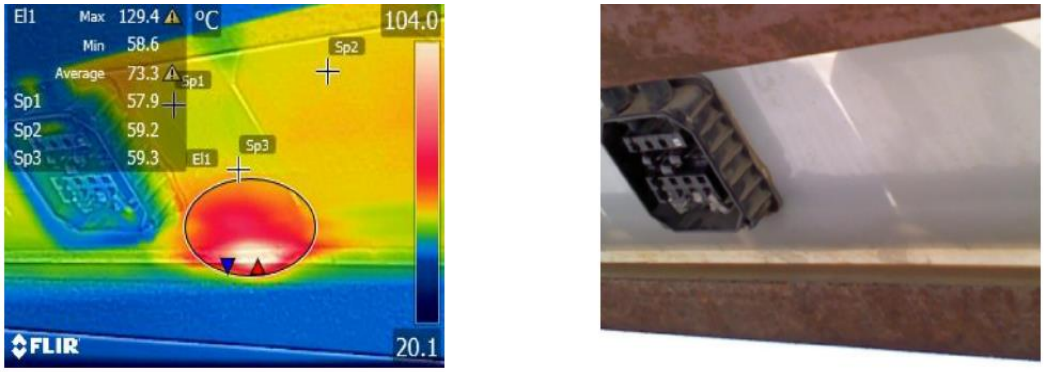

(b)

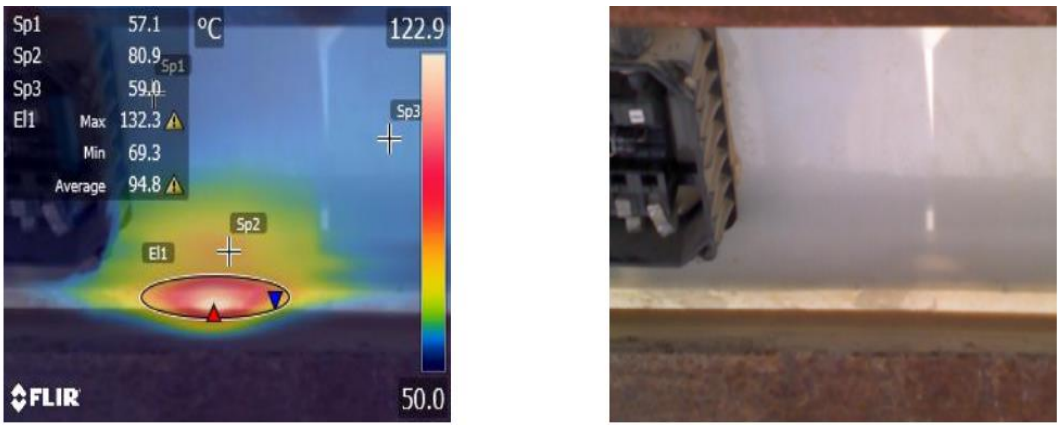

(c)

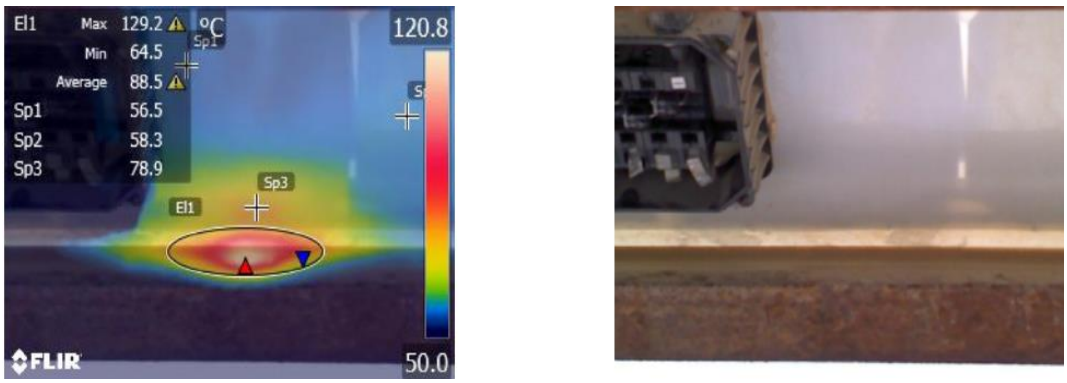

(d)

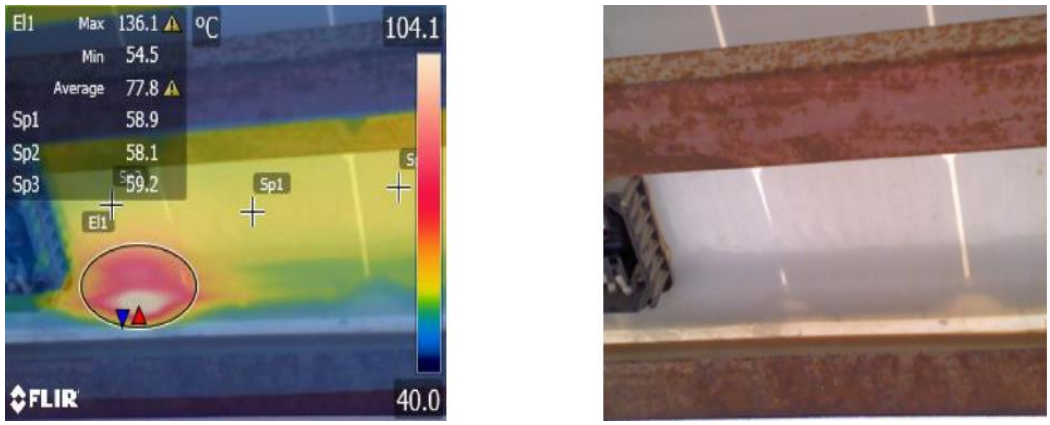

(e)

Figure 98: Thermal pictures of hot spot tracking within 7 minutes

Figure 98 illustrates the tracing process formation of the hot spot phenomenon within 7 minutes. IR photos were caught quickly because the temperature increases rapidly and threat the panel to damage or burn. It is clear that the hot spot area varies with temperature, because of the variations of shunt resistance at too high temperature. Additionally, the defects of semiconductor material of PV cell lead to extra heating in the hot spot location. From thermal photos (a and b) the temperature rises up from 121oC to 129 oC directly within less one minute, and the hot spot area expanded and propagated as clear in photo b and reaches for the adjacent cell. Reverse current usually concentrated in a narrow portion of the damaged cell and can cause very high thermal dissipated as appeared in photo c where it's working at 132.3 oC and reaches to that temperature within less 2 minutes. This temperature can damage the glass and melt the back encapsulation sheet of the cell if the shading is continued for many several minutes.

After 10 s the temperature suddenly reduces from 132 ^{o}C to 129 ^{o}C and a possible reason is that the circle of hot spotting area increases and creeping toward the adjacent cell as illustrated in photo d also the micro cracks play an important role in hot spot development and could happen between two different sides of cells and shared the risk of hot spot.

Finally, the temperature is reached to 136.1 ^{o}C as appears in IR photo e and then the shading effect is removed in order to save the module against burn. A hot spot is concentrated beside the bottom edge of the shaded cell as shown all thermal photos. The thermal breakdown has happened within the too low duration. The plot of the temperature propagation can be summarized in figure 99.

The analysis of the recorded temperatures has been illustrated. From the tracking process, it's possible to see a direct relationship between the thermal heat, the maximum

temperature portions, the leakage current, and the area of hot spot growth. The relation is proved by a narrow area of the hot spot and a high shunt current circulated inside the damaged cell that leads to a critical temperature.

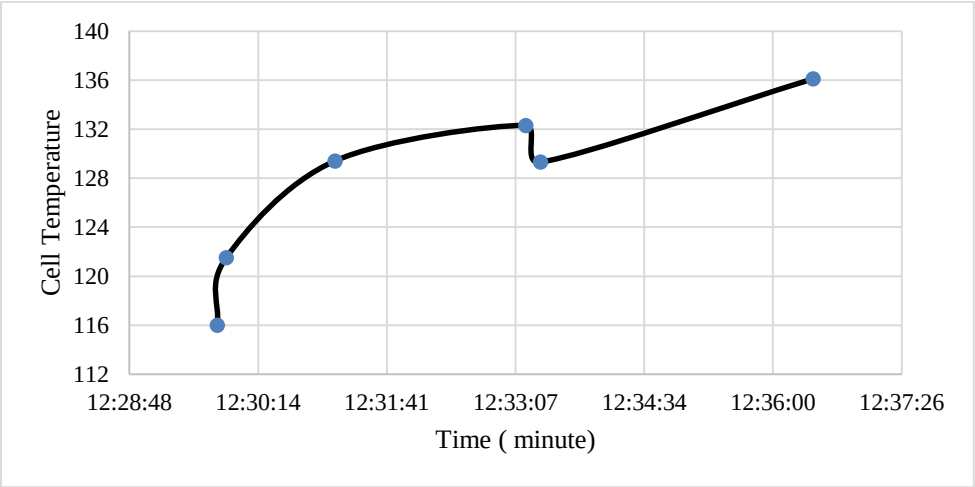

Figure 99: Hot spot temperature evolution

5.3.4 Hot Spot Observation by Online Curve and Thermal Analysis

In chapter 4, the online curve method was explained in detail. In this section, the online curve method is achieved and validated.

The same panel that used in the fast hot spot creation test was observed with one completely covered cell. The following plots in figures 100, 101 and 102 are called online curves and plotted by CASSY Lab system and hot spot model in Simulink. It can be seen that too large drops in voltage, current and consequence power. The reduction and degradation were happening within less than 10 minutes. Thermal analysis of this scenario is discussed in the following thermal photos.

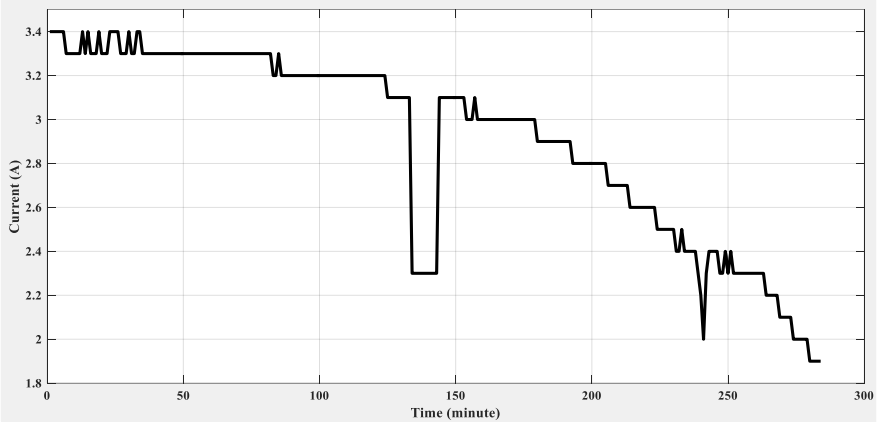

Figure 100: Online current curve of PV panel with shading

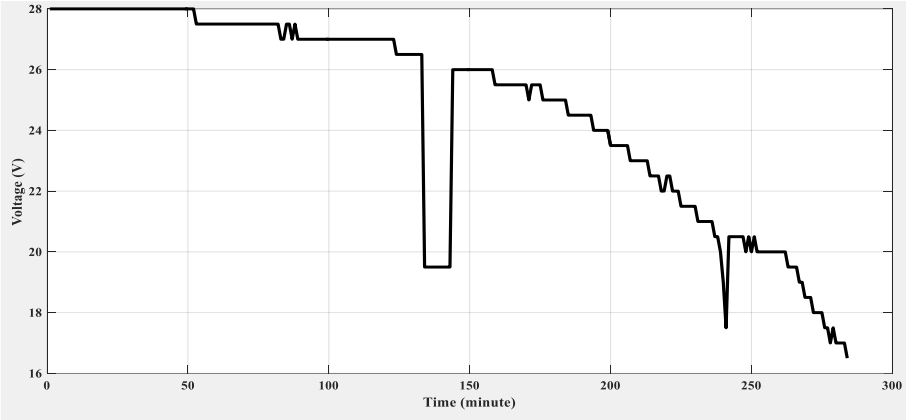

Figure 101: Online voltage curve of PV panel with shading

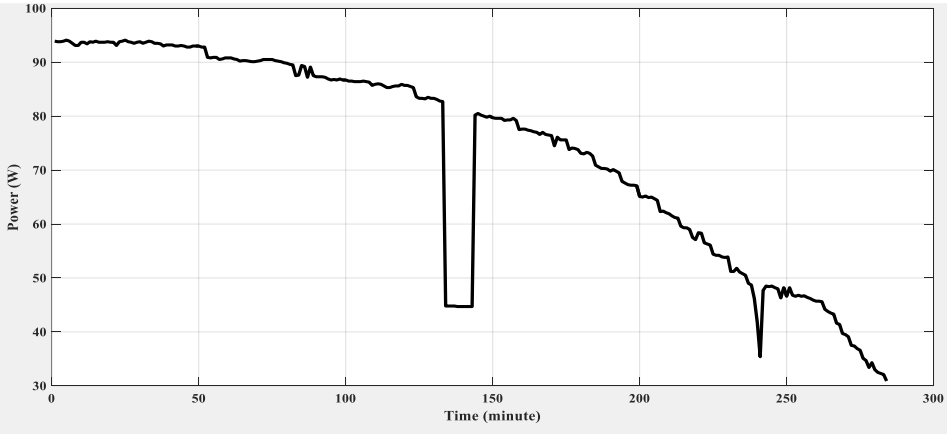

Figure 102: Online power curve of PV panel with shading

Previous three curves illustrate how the power dissipates inside the defective cell during shading. Strong reduction occurs in voltage causes high loss power as shown in figure 102 i.e. the power delivered to the external load before the shading effect was equal to 83 W and after shading it becomes 44 W. This power dissipation represents a real danger to the panel's life if the shading is not removed. The hot spot risk increases rapidly and could destroy the panel, and the bypass diode exposes to the high current flow that can damage the diode if the shading effect continues for a long time.

Thermal Analysis of Online Profile Method

The online curve, diagnostics by means of the thermal camera that has great benefits. The effect of the parallel resistance was experimentally tested by FLIR E60 camera and indicated by the leakage current passes through shunt paths as proved in preceding sections. As expected from the simulations, when the value of the R_{sh} decreases, the leakage current increases and the module current reduces depending on the number of shaded cells and the shading rate. The following thermal pictures show the leakage current passed through the defective string and demonstrate the functionality of bypass diode in forward biased. The IR pictures in figures 103, 104 and 105 are captured during recorded the online curve method.

IR images in figure 103 represent the whole panel (picture a), junction box (picture b) and defective string before the shading occurred (picture c). The panel is loaded with an external resistance load equal to 8.5 Ω and worked in a good weather condition where the irradiance was 1000 W/m^2 and the ambient temperature around 41 ^oC.

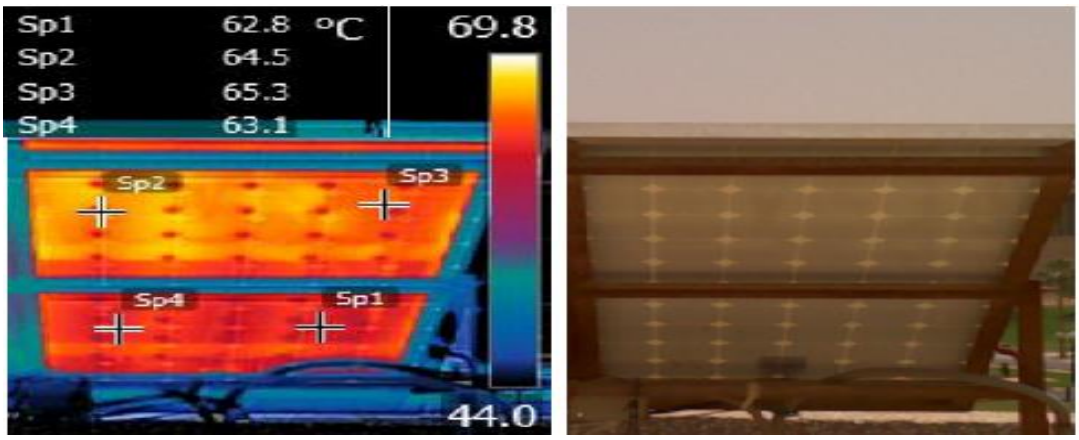

(a) Loaded panel – back view

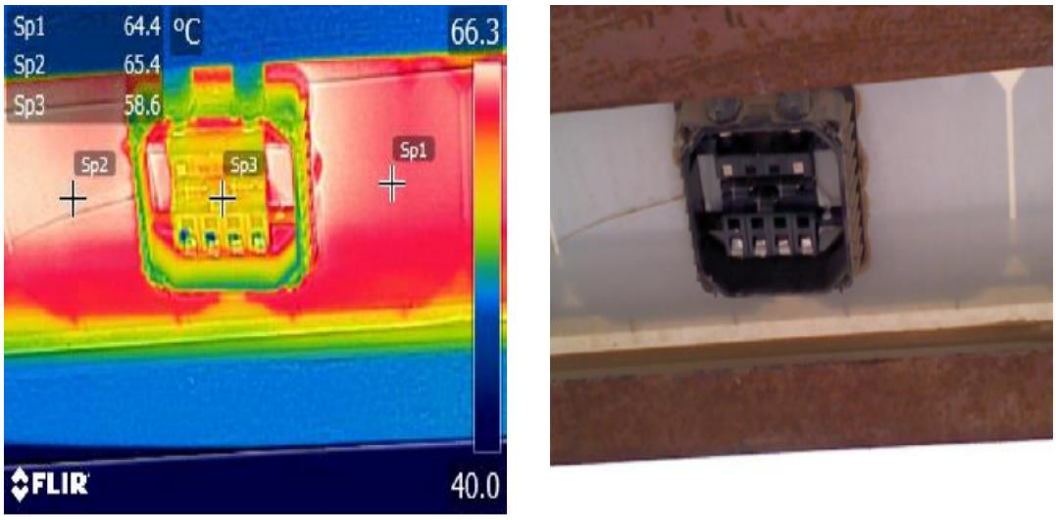

(b) Junction box – bypass diodes

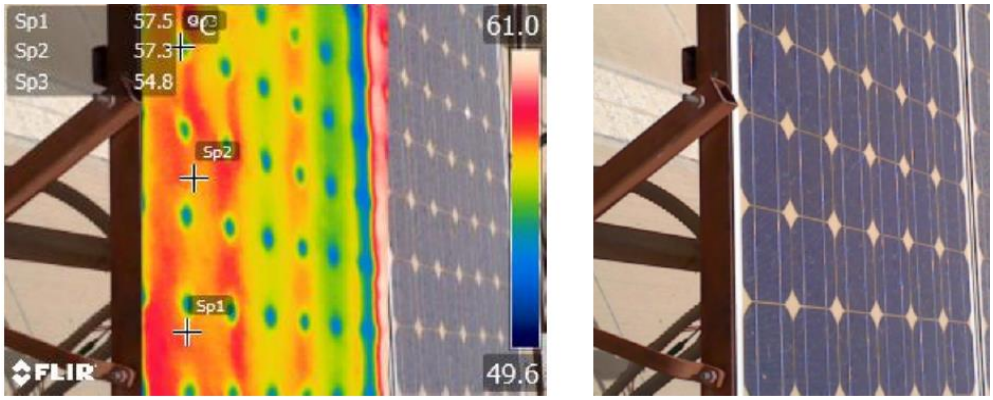

(c) Top view – strings of panel

Figure 103: IR pictures during online profile method before shading effect

IR photo in figure 104 shows the thermal distribution during the shading event. It makes clear that the conductivity of bypass diode protected third string, and its temperature reached to 79.6 ^{o}C within 5 minutes. Figure 105 displays the thermal distribution over the third string from the top view. The leakage current can be remarked in the location of warmer areas indicated by box1in figure 105. These areas have the highest temperatures compared to the rest string of the panel. The temperatures are recorded from the highest – bottom string- to lowest string 62 ^{o}C, 53 ^{o}C, and 52 ^{o}C respectively.

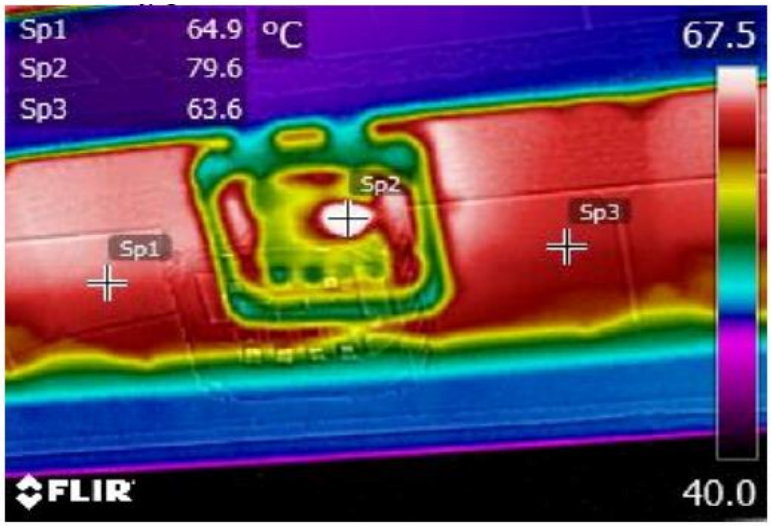

Figure 104: IR picture of bypass diode conductivity after shading

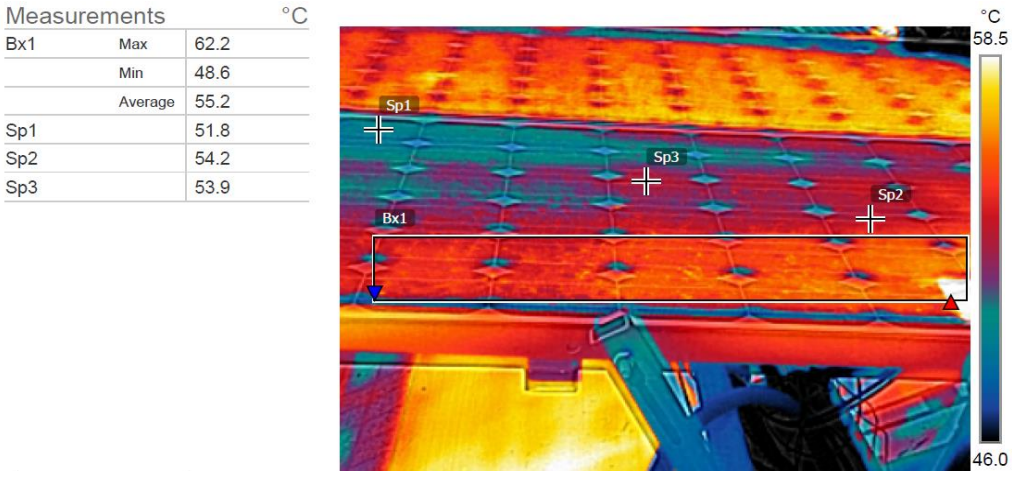

Figure 105: IR picture depicts leakage current in the third string after shading

Between 50 and 75 degrees, there was a large drop in load power from a peak of 83 W down to 44 W. The dissipated power can contribute to accelerating the hot spot risk because the shaded cell works as an internal resistive load. The whole power losses due to increase in temperature are able to damage the panel when the shading continues for extended minutes.

5.4 Emissivity and Measurements

Emissivity means absorptivity at a given wavelength, but will vary significantly for irradiation above and below the E_{gap}, of defects and hot spot areas.

In this study, the effect of surface emissivity of glass on the solar cell temperature is not included and ignored. IR imaging will give a visual profile of temperatures and the size of the hot spot during the mismatches, however, we don't look for the accurate temperature at which solar cells operate so the emissivity is not important when tracking the shunt current and observing the origins of shunts.

As long as, the temperature variations that can be measured on the panel's glass surface are little. In parliamentary procedure, for these fluctuations to be visible, the FLER imaging camera that used in this study possesses a thermal sensitivity ≤0. 05 ºC so no need to take into account emissivity.

Additionally, in order to avoid reflection of the thermal camera, it should not be positioned vertically to the panel being investigated. However, emissivity is at its highest when the camera is vertical and reduces with rising angle.

CHAPTER 6

Conclusion and Future Works

6.1 Conclusion

This research has described the effects of shading and dust on the power efficiency and characteristic curves of the solar cells in the Saudi Arabia environment. The shading effects that causes a mismatch on the solar cell performance is studied and simulated with a complete model including hot spot phenomenon. Specification techniques applied on hot spot model support data of the photo-current, diode current, series and shunt resistances, ideality factor and finally cell defects that worked in a reverse bias mode.

The full or partial shading limits the photo-current of the affected cells. This fact results in a strong current difference between the shaded and non-shaded cells of the same string forcing the bypass diodes to conduct.

Moreover, hot spot causes destruction of the panel that heating the material's area of solar cell.

I-V and P-V curves are obtained experimentally. Both curves gave information about five parameters such as photo-current, reverse saturation current, V_{oc}, I_{sc} and P_{mpp}. The cell working in the reverse bias region and suffering from hot spot problem could be seen from I-V and P-V curves when the activation point of the bypass diode leads to a step or steps in the I-V characteristic or multiple peaks of power in the P-V characteristic.

The parasitic resistances affect the behavior and control the configuration of the I-V curve. The shunt resistance has a substantial effect on the operation of the panel because it holds a relation to the leakage current.

PV module with hot spot cells was simulated by Simulink based on Bishop's model in order to measure current flow through a bypass diode, the shunt current, and the module current around the affected string. Current distribution detailed picture was reached under several test conditions.

The hot spot evaluation methods demonstrate that there is a strong relation between the powers dissipated in both shunt resistance and shaded cell, additionally a relationship among the shunt current and illumination levels during the current flow inside the module. Shunt current circulated around the defective cell and causes heat stress in the shunt resistance. If the shading effect continues for a long time the hot spot risk is extended to a new cell and hence burns the panel. Sometimes bypass diode couldn't be activated, although the high shading level is applied. In this case, the panel performance is wasted, however the hot spot development increases in a short time and the damage definitely is happening.

From simulation and results, the full shading is not the worst-case scenario.

The hot spot model has confirmed the operation of the bypass diode during the event of shading in a string. The bypass diode stabilize the panel power delivery to the load.

In many cases, the effected cell continues to dissipate power, consequently spreading heat among the panel area while the diode is switched on.

For detecting the position of the hot spot in crystalline silicon solar, the thermography technique is used to find the origins of these hot spots. The analysis, diagnostic and detection depends on the IR thermography technique used was efficient, rapid, and save efforts of the inspection of mismatch problems in PV cells. The inspection time at the outdoor fields of defective heating cells was faster with backside thermography.

The explanation of heat effects is not an easy task. There are several various electrical mismatches, which could lead to a thermal stress. Some effects are complex and compound, for instance, a hot spot can be caused by linkage mismatches or bypass diode failure.

The temperature effect is studied on the solar panel performance and the electrical characteristics. That is any small variation in the temperature leads to change all parameters of solar cells. Note that the I-V and P-V curves are measured under different cell temperature.

By IR technique, all mismatches can be investigated and the temperature distribution was reached by FLIR camera. Thus the IR technique is considered as a great support in the solar cell diagnosis by locating the hot spot areas.

Here the relation between the heat of abnormal cells and possible electrical faults can be determined. So broken cells, bypass diode short circuit, and cell internal defect can heat the whole solar panel and cause a single hot cell or multiple hot cells. In the case of multiple hot cells, the several various temperature levels can be observed that leads to the complete reduction of output power. As the temperature increases like in Saudi Arabia environment in summer days, the risk of thermal stress rises quickly.

The hot spot model in Simulink environment was validated by the thermal camera where all currents were observed as a heat in the real field.

The ambient temperature and irradiation measurement give no illustration of the rapid fluctuations of the panel electrical characteristic. But the relation connects the temperature of the defective cell and the temperature of the surrounding areas (rest cells) additionally

the power difference between the concerning cell string remain to be recognized at rapid fluctuations.

6.2 Future Works

It is necessary to understand the hot spot phenomenon properly to design the thermal part of the hot spot model. A very important parameter of the thermal part is the thermal resistance. This thermal part will serve to cover the initiation, starting point of overheating and see its effect on the affected cells.

The simulator model of the hot spot in this thesis only deals with the electrical behavior of the solar cell under phenomenon and permit the external shading. Future work should include another parameter in the hot spot model that would permit the thermal analysis of the cell under shading effect, in order to increase the accuracy of hot spot monitoring and evaluation system.

Studying the micro cracks of the cells is considered an important issue to deal with the hot spot from other aspects. The diagnostics instrument represented by thermal camera should be connected in the live stream mode of the camera in order to record the event evaluation in video mode during the shading effect. To improve the design of PV cell against the hot spot problems, high shunt resistance should be achieved. Since the shunt, products can keep high output power efficiency under low irradiation conditions. This improvement can support low reverse leakage current. Which can decrease the hot spot, secure longer panel operation, better reliability and enhance the protection process under shading effect.

To fulfill complete protection against hot spot risk, the bypass diode in panel strings should be conducting at lower values of the reverse bias voltage. Manufacturers should also supply data about the reverse bias behavior of their panels.

Appendix

Matlab Scripts that are used in this study contains all M-Files for evaluating five parameters of the solar cell, plotting both curves, under the variation of temperature and irradiation, variable of R_s and R_{sh}, and final variation of ideality factor on the characteristics of the solar cell.

A.1 Script for extracting five parameters from the data sheet and producing I-V and P-V curves.

```
clear all; close all; clc
Vocn = 43.2; % nominal Open circuit voltage
Vmpp = 36; % Voltage at maximum power point
Iscn = 4.49; % nominal Short circuit current
Impp = 4.16; % Current at maximum power point
Ns = 72; % Number of series connections
Kv = -.123;
a=1.339;
Ki = 3.15e-5;
Pmax_e = Vmpp * Impp; % max power
Np = 1; % Number of parallel connections
q = 1.602e-19; % Electron charge magnitude
k = 1.381e-23; % Boltzmann's constant
Gn = 1000;       %Nominal irradiance [W/m^2]
Tn = 25+273.15;  %Nominal operating temperature [K]
T = 25+273.15;
G=1000;
Vtn = k * Tn/q; %Thermal junction voltage (nominal)
Vt = k * T/q;  %Thermal junction voltage (current temperature)
Eg = 1.124; %for module 1 at 25 C
Rs_max = (Vocn - Vmpp )/ Impp;
Rp_min = (Vmpp / (Iscn - Impp))- Rs_max;
% Initial values of Rp and Rs
Rp = Rp_min;
Rs = 0;
tol = .001;
error = Inf;
```

```
while(error>tol)
    dT=T-Tn;
    Ipvn = ((Rs + Rp)/Rp) * Iscn;
    Ipv = (Ipvn + Ki * dT ) * (G/Gn) ;
    Isc = (Iscn + Ki * dT ) * (G/Gn);
    Ion = Iscn / (exp (Vocn/a/Ns/Vtn)-1);
    Io=Ion*((T/Tn)^3)*exp(q*Eg/(k*a)*((1/Tn)-(1/T)));
    Rs = Rs + .001;
    Rp = Vmpp * (Vmpp + Impp * Rs )/(Vmpp*Ipv - Vmpp * Io* exp((Vmpp+Impp * Rs )/Vt/Ns/a)↙
+ Vmpp*Io-Pmax_e );
    % Solving the I-V equation for several (V,I)
    V = 0:.1:Vocn;
    I = zeros(size(V));
   for j = 1: length(V)
    U(j) = Ipv - Io * (exp((V(j) + I(j)*Rs)/ Vt/Ns/a)- 1) - ((V(j) + I(j)*Rs))/ Rp - (.01↙
*(V(j)+I(j)*Rs)*(1-((V(j)+I(j)*Rs)/-14.4)).^-3) -I(j);
   while (abs(U(j))>.001)
     % Solves U = I - f(I,V) = 0 with Newton-Raphson
  U(j) = Ipv - Io * (exp((V(j) + I(j)*Rs)/ Vt/Ns/a)- 1) - ((V(j) + I(j)*Rs))/ Rp - (.01 *↙
(V(j)+I(j)*Rs)*(1-((V(j)+I(j)*Rs)/-14.4)).^-3) -I(j);
  U_div(j) = -Io*Rs /Vt/Ns/a*exp((V(j) + I(j)*Rs)/ Vt/Ns/a)- Rs/Rp-(.01*Rs*(1-(V(j)+I(j)↙
*Rs)/-14.4).^-3)-(.01.*(V(j)+I(j)*Rs).*(-3*(1-(V(j)+I(j)*Rs)/-14.4)^-4*(Rs/-14.4)))-1;
   end
   end
 P= ((Ipv- Io*(exp((V+I*Rs)/Vt/Ns/a)-1)- (V+I*Rs)/Rp)- (.01 .*(V+I*Rs).*(1-((V+I*Rs)/-↙
14.4)).^-3)).*V;
   Pmax_m= max(P)
   error = (Pmax_m - Pmax_e);
end

subplot(2,1,1)
  plot(V,I,'LineWidth',2,'Color','k')
%  plot(V,I) %Plot the I-V characteristic curve
title(' I-V curve');
xlabel('Voltage [V]')
ylabel('Current [A]')
axis([0 45 0 6])
grid on
subplot(2,1,2)
plot(V,P,'LineWidth',2,'Color','k')
% plot (V,P) %Plot the P-V characteristic curve
xlabel('Voltage [V]')
ylabel('Power [W]')
axis([0 45 0 160])
grid on
```

```
disp(sprintf(' Rp_min = %f',Rp_min));
disp(sprintf('     Rp = %f',Rp));
disp(sprintf(' Rs_max = %f',Rs_max));
disp(sprintf('     Rs = %f',Rs));
disp(sprintf('      a = %f',a));
disp(sprintf('      T = %f',T-273.15));
disp(sprintf('      G = %f',G));
disp(sprintf(' Pmax,m = %f  (model)',Pmax_m));
disp(sprintf(' Pmax,e = %f  (experimental)',Pmax_e));
disp(sprintf('    tol = %f',tol));
disp(sprintf('    Ipv = %f',Ipv));
disp(sprintf('    Isc = %f',Isc));
disp(sprintf('    Ion = %g',Ion));
disp(sprintf('\n\n'));
grid on
```

A.2 Script for generating plots of characteristic curves with different values of irradiation.

```
clear all; close all; clc
Tr=25+273;
T1=25+273; % Reference temperature in degree
S=[1000 800 600 400 200]; % Solar radiation in mW/sq.cm
ki=3.15e-5; % in A/K
Iscr=4.49; % SC Current at ref. temp. in A
Irr=1.20399e-07; % in A
k=1.38065*10^(-23); % Boltzmann constant
q=1.6022*10^(-19); % charge of an electron
A=1.339;
Eg = 1.79;
Ns=72;
V0=[0:1:45];
I = zeros(size(V0));
Rs=0.074;
Rp= 693.738192;
Vt= k * Tr/q;
for i=1:5
Iph=(Iscr+ki*(T1-Tr))*(S(i)/1000);
Irs=Irr*((Tr/T1).^3)*exp(q*Eg/(k*A)*((1/Tr)-(1/T1)));
for j = 1: length(V0)
    U(j) = Iph - Irs * (exp((V0(j) + I(j)*Rs)/ Vt/Ns/A)- 1) - ((V0(j) + I(j)*Rs))/ Rp -↙
I(j);
```

```
   while (abs(U(j))>.001)
     % Solves U = I - f(I,V) = 0 with Newton-Raphson
  U(j) = Iph - Irs * (exp((V0(j) + I(j)*Rs)/ Vt/Ns/A)- 1) - ((V0(j) + I(j)*Rs))/ Rp - I↙
(j); % function of current F(I(j))
  U_div(j) = -Irs*Rs /Vt/Ns/A*exp((V0(j) + I(j)*Rs)/ Vt/Ns/A)- Rs/Rp -1; % derevative of↙
previouse equation
  I_(j) = I(j)-U(j)/U_div(j); % next value = Xn- F(I(j))/divv(F(I(j)))
  I(j)= I_(j); % PV current.
   end
end
P0 = V0.*I;
figure(1)
grid on
plot(V0,I);
hleg = legend('1000 w/m^2','800 W/m^2','600 W/m^2','400 W/m^2','200 W/m^2');
set(hleg,'FontSize',15);
axis([0 45 0 5]);
xlabel('Voltage in volt','FontSize',18);
ylabel('Current in amp','FontSize',18);
title('I-V curves for different solar irradiance values','FontSize',18)
% legend BOXOFF
% end
hold on;
figure(2)
grid on
plot(V0,P0);
axis([0 45 0 160]);
xlabel('Voltage in volt','FontSize',18);
```

```
ylabel('Power in watt','FontSize',18);
legend('1000 W/m^2',' 800 W/m^2',' 600 W/m^2',' 400 W/m^2',' 200↙
W/m^2','Location','NorthWest')
set(legend,'FontSize',18);
title('PV curves for different solar irradiance values','FontSize',18)
legend BOXOFF
hold on;
figure(3)
grid on
plot(I,P0);
axis([0 5 0 160]);
xlabel('Current in amp');
ylabel('Power in watt');
legend('1000 W/m^2',' 800 W/m^2',' 600 W/m^2',' 400 W/m^2',' 200↙
W/m^2','Location','NorthWest')
title('PI curves for different solar irradiance values')
legend BOXOFF
hold on;
end
```

A.3 Script for generating plots of characteristic curves with different values of temperatures.

```
clear all; close all; clc
Tr=25+273;
Z=[0 25 50 75 100];
T1=Z+273;
S=1000;
Vocn = 43.2; % nominal Open circuit voltage
Iscr=4.49; % SC Current at ref. temp. in A
Vmpp = 36; % Voltage at maximum power point
Impp = 4.1; % Current at maximum power point
Rp =693.738192;
Rs =.07;
A=1.339;
KV =-.2;
ki =3.15e-5;
Ns =72;
k=1.38065*10^(-23); % Boltzmann constant
q=1.6022*10^(-19); % charge of an electron
Eg = 1.79;
V0=[0:1:55];
I = zeros(size(V0));
Vtn= k * Tr/q; %Thermal junction voltage (nominal)
for i=1:5
Vt = k * T1(i)/q; %Thermal junction voltage
Iph=(Iscr+ki*(T1(i)-Tr))*(S/1000);
Irr = Iscr / (exp (Vocn/A/Ns/Vtn)-1);
Irs=Irr*((Tr/T1(i)).^3)*exp(q*Eg/(k*A)*((1/Tr)-(1/T1(i))));
```

```
for j = 1: length(V0)
 U(j) = Iph - Irs * (exp((V0(j) + I(j)*Rs)/ Vt/Ns/A)- 1) - ((V0(j) + I(j)*Rs))/ Rp - I↙
(j);
   while (abs(U(j))>.001)
% Solves U = I - f(I,V) = 0 with Newton-Raphson
  U(j) = Iph - Irs * (exp((V0(j) + I(j)*Rs)/ Vt/Ns/A)- 1) - ((V0(j) + I(j)*Rs))/ Rp - I↙
(j); % function of current F(I(j))
  U_div(j) = -Irs*Rs /Vt/Ns/A*exp((V0(j) + I(j)*Rs)/ Vt/Ns/A)- Rs/Rp -1; % derevative of↙
previouse equation
  I_(j) = I(j)-U(j)/U_div(j); % next value = Xn- F(I(j))/divv(F(I(j)))
  I(j)= I_(j); % PV current.
   end
end
P0 = V0.*I;
figure(1)
grid on
plot(V0,I);
axis([0 55 0 5]);
xlabel('Voltage in volt','FontSize',18);
ylabel('Current in amp','FontSize',18);
title('I-V curves with different ambient tempereatures','FontSize',18)
legend('00^\circC',' 25^\circC',' 50^\circC',' 75^\circC','↙
100^\circC','Location','NorthEast')
set(legend,'FontSize',18);
legend BOXOFF

 hold on;
 figure(2)
 grid on
 plot(V0,P0);
 axis([0 55 0 190]);
 xlabel('Voltage in volt','FontSize',18);
 ylabel('Power in watt','FontSize',18);
 title('P-V curves with different ambient tempereatures','FontSize',18)
 legend('00^\circC',' 25^\circC',' 50^\circC',' 75^\circC','↙
 100^\circC','Location','NorthEast')
 set(legend,'FontSize',18);
 legend BOXOFF
 hold on;
 figure(3)
 grid on
 plot(I,P0);
 axis([0 5 0 190]);
 xlabel('Current in amp');
 ylabel('Power in watt');
 title('I-P curves with different ambient tempereatures')
 legend('00^\circC',' 25^\circC',' 50^\circC',' 75^\circC','↙
 100^\circC','Location','NorthEast')
 legend BOXOFF
 hold on;
 end
```

A.4 Script for generating plots of characteristic curves with different values of series resistance

```
Tr=25+273;
T1=25+273; % Reference temperature in degree
S=1000 ; % Solar radiation in mW/sq.cm
Rs = [10 7 5 3 .07];
A=1.339;
ki=3.15e-5; % in A/K
Iscr=4.49; % SC Current at ref. temp. in A
Vocn = 43.2;
k=1.38065*10^(-23); % Boltzmann constant
q=1.6022*10^(-19); % charge of an electron
Eg = 1.79;
Ns=72;
V0=[0:1:45];
I = zeros(size(V0));
  Rp=693.7;
Vt= k * Tr/q;
for i=1:5
Iph=(Iscr+ki*(T1-Tr))*(S/1000);
Irr = Iscr / (exp (Vocn/A/Ns/Vt)-1);
Irs=Irr*((T1/Tr).^3)*exp(q*Eg/(k*A)*((1/Tr)-(1/T1)));
for j = 1: length(V0)
     U(j) = Iph - Irs .* (exp((V0(j) + I(j).*Rs(i))./ Vt/Ns/A)- 1) -
     ((V0(j) + I(j).*Rs(i)))./ Rp - I(j);
   while (abs(U(j))>.001)
     % Solves U = I - f(I,V) = 0 with Newton-Raphson
   U(j) = Iph - Irs * (exp((V0(j) + I(j).*Rs(i))/ Vt/Ns/A)- 1) - ((V0(j)
   + I(j).*Rs(i)))/ Rp - I(j); % function of current F(I(j))
   g_div(j) = -Irs.*Rs(i) ./Vt/Ns/A*exp((V0(j) + I(j).*Rs(i))./ Vt/Ns/A)
   - Rs(i)/Rp -1; % derevative of previouse equation
   I_(j) = I(j)-U(j)/g_div(j); % next value = Xn- F(I(j))/divv(F(I(j)))
   I(j)= I_(j); % PV current.
end
end
```

```
 P0 = V0.*I;
figure(1)
grid on
plot(V0,I);
axis([0 45 0 5]);
xlabel('Voltage in volt','FontSize',18);
ylabel('Current in amp','FontSize',18);
hold on;
figure(2)
grid on
plot(V0,P0);
axis([0 45 0 170]);
xlabel('Voltage in volt','FontSize',18);
ylabel('Power in watt','FontSize',18);
hold on;
figure(3)
grid on
plot(I,P0);
axis([0 5 0 170]);
xlabel('Current in amp','FontSize',18);
ylabel('Power in watt','FontSize',18);
legend('Rs = 10','Rs = 7','Rs = 5','Rs = 3','Rs = .07','Location','NorthWest')
set(legend,'FontSize',18);
legend BOXOFF
hold on;
end
```

A.5 Script for generating plots of characteristic curves with different values of shunt resistance

```
Tr=25+273;
T1=25+273; % Reference temperature in degree
S=1000 ; % Solar radiation in mW/sq.cm
Rp = [1 10 30 50 80 100 200 300 450 600 700 900 1000];
A=1.339;
ki=3.15e-5; % in A/K
Iscr=4.49; % SC Current at ref. temp. in A
Vocn = 43.2;
k=1.38065*10^(-23); % Boltzmann constant
q=1.6022*10^(-19); % charge of an electron
Eg = 1.79;
Ns=72;
V0=[0:1:80];
```

```
I = zeros(size(V0));
Rs= .07;
Vt= k * Tr/q;
for i=1:13
Iph=(Iscr+ki*(T1-Tr))*(S/1000);
Irr = Iscr / (exp (Vocn/A/Ns/Vt)-1);
Irs=Irr*((T1/Tr).^3)*exp(q*Eg/(k*A)*((1/Tr)-(1/T1)));
for j = 1: length(V0)
     U(j) = Iph - Irs * (exp((V0(j) + I(j)*Rs)/ Vt/Ns/A)- 1) - ((V0(j) + I(j)*Rs))/ Rp(i)↙
- I(j);
   while (abs(U(j))>.001)
      U(j) = Iph - Irs * (exp((V0(j) + I(j)*Rs)/ Vt/Ns/A)- 1) - ((V0(j) + I(j)*Rs))/ Rp↙
(i) - I(j); % function of current F(I(j))
      g_div(j) = -Irs*Rs /Vt/Ns/A*exp((V0(j) + I(j)*Rs)/ Vt/Ns/A)- Rs/Rp(i) -1; %↙
derevative of previouse equation
      I_(j) = I(j)-U(j)/g_div(j); % next value = Xn- F(I(j))/divv(F(I(j)))
      I(j)= I_(j); % PV current.
   end
   end P0 = V0.*I;
figure(1)
grid on
plot(V0,I);
axis([0 45 0 5]);
xlabel('Voltage in volt','FontSize',18);
ylabel('Current in amp','FontSize',18);
legend('Rp = 1.0','Rp = 10','Rp = 30','Rp = 50','Rp = 80','Rp = 100','Rp = 200','Rp =↙
300','Rp = 450','Rp = 600','Rp = 700','Rp = 900','Rp = 1000','Location','SouthWest')
set(legend,'FontSize',10);
legend BOXOFF
hold on;
figure(2)
grid on
plot(V0,P0);
axis([0 45 0 170]);
xlabel('Voltage in volt','FontSize',18);
ylabel('Power in watt','FontSize',18);
legend('Rp = 1.0','Rp = 10','Rp = 30','Rp = 50','Rp = 80','Rp = 100','Rp = 200','Rp =↙

300','Rp = 450','Rp = 600','Rp = 700','Rp = 900','Rp = 1000','Location','SouthWest')
set(legend,'FontSize',10);
legend BOXOFF
hold on;
figure(3)
grid on
plot(I,P0);
axis([0 5 0 170]);
xlabel('Current in amp','FontSize',18);
ylabel('Power in watt','FontSize',18);
hold on;
end
```

A.6 Script for generating plots of characteristic curves with different values of a diode ideality factor

```
T1=25+273; % Reference temperature in degree
S=1000 ; % Solar radiation in mW/sq.cm
A = [ 1 1.2 1.339 1.4 1.5];
ki=3.15e-5; % in A/K
Iscr=4.49; % SC Current at ref. temp. in A
Vocn = 43.2;
k=1.38065*10^(-23); % Boltzmann constant
q=1.6022*10^(-19); % charge of an electron
Eg = 1.79;
Np=1;
Ns=72;
V0=[0:1:80];
I = zeros(size(V0));
Rs= .07;
Rp=693.7;
Vt= k * Tr/q;
for i=1:5
Iph=(Iscr+ki*(T1-Tr))*(S/1000);
Irr = Iscr / (exp (Vocn/A(i)/Ns/Vt)-1);
Irs=Irr*((T1/Tr).^3)*exp(q*Eg/(k*A(i))*((1/Tr)-(1/T1)));
for j = 1: length(V0)
    U(j) = Iph - Irs * (exp((V0(j) + I(j)*Rs)/ Vt/Ns/A(i))- 1) - ((V0(j) + I(j)*Rs))/ Rp
- I(j);
  while (abs(U(j))>.001)
    % Solves U = I - f(I,V) = 0 with Newton-Raphson
     U(j) = Iph - Irs * (exp((V0(j) + I(j)*Rs)/ Vt/Ns/A(i))- 1) -
     ((V0(j) + I(j)*Rs))/ Rp - I(j); % function of current F(I(j))
     g_div(j) = -Irs*Rs /Vt/Ns/A(i)*exp((V0(j) + I(j)*Rs)/ Vt/Ns/A(i))- Rs/Rp -1;
     I_(j) = I(j)-U(j)/g_div(j); % next value = Xn- F(I(j))/divv(F(I(j)))
     I(j)= I_(j); % PV current.
  end
  end
 P0 = V0.*I;
figure(1)
grid on
plot(V0,I);
axis([0 45 0 5]);
xlabel('Voltage in volt','FontSize',18);
ylabel('Current in amp','FontSize',18);
legend('m = 1.0','m = 1.2','m = 1.339','m = 1.4','m = 1.5','Location','SouthWest')
set(legend,'FontSize',18);
legend BOXOFF
hold on;
```

```
figure(2)
grid on
plot(V0,P0);
axis([0 45 0 170]);
xlabel('Voltage in volt','FontSize',18);
ylabel('Power in watt','FontSize',18);
hold on;
figure(3)
grid on
plot(I,P0);
axis([0 5 0 170]);
xlabel('Current in amp','FontSize',18);
ylabel('Power in watt','FontSize',18);
legend('m = 1.0','m = 1.2','m = 1.339','m = 1.4','m = 1.5','Location','NorthWest')
set(legend,'FontSize',18);
legend BOXOFF
hold on;
end
```

References

[1] "A Conventional Crystalline Silicon Solar -Solar Cell" [Online]. Available: Wikipedia https://en.wikipedia.org/wiki/Solar_cell.

[2] Amardeep Chaudhary, Shriya Gupta, Dhriti Pande, Fazal Mahfooz, Gunjan Varshney, "Effect of Partial Shading on Characteristics of PV Panel using Simscape," Journal of Engineering Research and Applications, ISSN: 2248-9622, Vol. 5, Issue 10, (Part - 2), pp.85-89, October, 2015.

[3] C Ko,Jae-Sub, Chung, and Dong-Hwa, "Reconfiguration of PV Module Considering the Shadow Influence of Photovoltaic System," The Korean Institute of Electrical Installation Engineers, Volume 27, Issue 2, pp.36-44, 2013.

[4] "Bypass Diodes in Solar Panels" [Online]. Available: http://www.electronicshub.org/bypass-diodes-in-solar-panels.

[5] S. Silvestre and A. Chouder, "Effects of Shading on Photovoltaic Module Performance," Progress in Photovoltaics: Research and Applications, no. 16, p. 141–149, 2008.

[6] Tomas Markvart, "Solar Electricity," 2nd Edition, Wiley, 2000.

[7] Luis Castaner and Santiago Silvestre, "Modelling Photovoltaic Systems using Pspice," University of New South Wales, Sydney April, 2002.

[8] S. MacAlpine, "Beyond the Module Model and into the Array: Mismatch in Series Strings," IEEE, pp. 3392–3396, 2012.

[9] Ramabadran, Ramaprabha and Mathur, Badrilal, "MATLAB Based Modelling and Performance Study of Series Connected SPVA under Partial Shaded Conditions," journal of sustainable development /vol.2.no.3/November, 2009.

[10] Peter Bulanyi, and Rodd Zhang, “Shading Analysis & Improvement for Distributed Residential Grid Connected Photovoltaics Systems,” The 52nd Annual Conference of the Australian Solar Council, 2014.

[11] C. Deline, “Partially Shaded Operation of a Grid Tied PV System,” Photovoltaic Specialists Conference, PVSC, pp. 001268–001273, June, 2009.

[12] J. So, B. Yu, and Choy, “Performance Monitoring and Analysis of Middle Scale Grid Connected PV System,” The 7th International Conference on Power Electronics / EXCO, Daegu, Korea, October 22-26, 2007.

[13] Ryan M. Smith, Dirk C. Jordan, and Sarah R. Kurtz, “Outdoor PV Module Degradation of Current-Voltage Parameters," World Renewable Energy Forum Denver, Colorado May, 2012.

[14] Dunlop, E.D. and Halton, D., "The Performance of Crystalline Silicon Photovoltaic Solar Modules after 22 Years of Continuous Outdoor Exposure," Progress in Photovoltaics: Research and Applications, vol. 14, pp. 53-64, 2006.

[15] M.C. Alonso, J.M. Ruizb and W. Herrmannc, “Computer Simulation of Shading Effects in Photovoltaic Arrays," Cologne, Germany, September, 2005.

[16] Martinez-Moreno, F., Muñoz, J. and Lorenzo, E., "A Model to Estimate Shadows Impact on PV Generators Power," In 22nd European Photovoltaic Solar Energy Conference, pp. 2716-8, Milan, Italy, 2007.

[17] N. Martin, M.C. Alsonso-Garcia, F. Chenlo, and P. Sánchez-Friera, “Electrical and Thermal Characterization of PV Modules under Partial Shadowing,” In the proceedings of the 23rd EU PVSEC, Valencia, Spain, 1-5 September, 2008.

[18] Mermoud, A., "Partial Shading on PV Arrays: Bypass Diode Benefits Analysis, "European Photovoltaic Solar Energy Conference – Valencia, Spain, 6-10 September, 2010.

[19] "Stand alone solar PV systems," [Online] Available http://www.powerfromthesun.net

[20] Deutsche Gesellshaft and Für Sonnenenergie, "Planning and Installing Photovoltaic Systems: A Guide for Installers, Architects and Engineers," second edition, London, UK, 2008.

[21] P.Sudeepika, and G.Md. Gayaz Khan, "Analysis of Mathematical Model of PV Cell Module in Matlab/Simulink Environment," International Journal of Advanced Research in Electrical, Electronics and Instrumentation Engineering, March, 2014.

[22] Castañer, L., and Silvestre, "Modeling of Photovoltaic Cell using Free Software Application for Training and Design Circuit in Photovoltaic Solar Energy," John Wiley and sons LTD, 2002.

[23] Nofuentes, G., and Hernández, "Analysis of the Possibilities to Omit Blocking and Bypass Diodes using a Standard Circuit Simulator," In 14th European Photovoltaic Solar Energy Conference, pp. 1094-6, Barcelona, Spain, 1997.

[24] Alonso, R. and Román, E., "Simulation of Heterogeneous PV Systems," In 20th European Photovoltaic Solar Energy Conference, pp. 2071-3, Barcelona, Spain, 2005.

[25] Le-Pivert, X. and Poggi, P., "Experimental Analysis and Simulation of Shading Effects on I-V Curve and MPPT Behaviour," In 22nd European Photovoltaic Solar Energy Conference, pp. 3174-5, Milan, Italy, 2007.

[26] Alessandro Virtuani1 and Davide Strepparava1, “Modeling the Performance of Amorphous and Crystalline Silicon Photovoltaic Modules for Different Types of Building Integration Conditions," University of Applied Sciences and Arts of Southern Switzerland, Switzerland, 2015.

[27] Merten, J., Asensi, J.M., et al, "Improved Equivalent Circuit and Analytical Model for Amorphous Silicon Solar Cells and Modules,” IEEE Transactions on Electron Devices, vol. 45, pp. 423-9, 1998.

[28] Walker, G., "Evaluating MPPT Converter Topologies Using a MATLAB PV Model,” Journal of Electrical and Electronics Engineering, Australia, vol. 21, pp. 49-55, 2001.

[29] Xiao, W., Dunford, W.G. and Capel, A., "A novel modeling method for photovoltaic cells," In IEEE 35th Annual Power Electronics Specialists Conference, 20th-25th June, pp. 1950-6, Aachen, Germany, 2004.

[30] Ahmed Bouraiou, Messaoud Hamoudaa ,Abdelkader Chakerb ,Mohammed Sadoka ,Mohammed Mostefaouia , and Salah Lachtar, "Modeling and Simulation of Photovoltaic Module and Array based on One and Two Diode Model Using Matlab/Simulink,” The International Conference on Technologies and Materials for Renewable Energy, Environment and Sustainability –TMREES, 2015.

[31] Jangwoo Park, Hong-geun Kim, Yongyun Cho, and Changsun Shin, “Simple Modeling and Simulation of Photovoltaic Panels Using Matlab/Simulink,” Advanced Science and Technology Letters Vol.73, pp.147-155, 2014.

[32] Greenspan, D., “Discrete Numerical Methods in Physics and Engineering,” Section .5 the generalized newton's method, pp. 12-22, Academic Press Inc., 1974.

[33] W. De Soto, S. A. Klein, and W. A. Beckman, “Improvement and Validation of a Model for Photovoltaic Array Performance,” Solar Energy, 80(1):78–88, January, 2006.

[34] Q. Kou, S. A. Klein, and W. A. Beckman, “A Method for Estimating the Long Term Performance of Direct Coupled PV Pumping Systems,” Solar Energy, 64(1-3):33–40, September, 1998.

[35] R. A. Messenger and J. Ventre, “Photovoltaic Systems Engineering”. Textbook - 528 Pages - February 26, 2010.

[36] K.H. Hussein, I. Muta, T. Hoshino, and M. Osakada, “Maximum Photovoltaic Power Tracking: an Algorithm for Rapidly Changing Atmospheric Conditions,” In Generation, Transmission and Distribution, IEE Proceedings, January, 1995.

[37] Geoff Walker, “Evaluating MPPT Converter Topologies using a Matlab PV Model,” Journal of Electrical & Electronics Engineering, Australia, 2001.

[38] M. A. Vitorino, L. V. Hartmann, A. M. N. Lima, and M. B. R. Correa, “Using the Model of the Solar Cell for Determining the Maximum Power Point of Photovoltaic Systems”. In Proc. European Conference on Power Electronics and Applications, p. 1–10, 2007.

[39] Xuan Hieu Nguyen and Minh Phuong Nguyen, “Mathematical Modeling of Photovoltaic Cell/Module/Arrays with Tags in Matlab/Simulink,” Environmental Systems Research Dec., 2015.

[40] Abdulkadir M, Samosir AS, and Yatim, “Modeling and Simulation Based Approach of Photovoltaic System in Simulink Model,” 2012.

[41] “Theory of I-V characterization, Short circuit current, open circuit voltage, Maximum Power, Fill factor, Efficiency, Shunt and series resistance” [Online]. Available: http://zone.ni.com/devzone/cda/tut/p/id/7230.

[42] Nader Anani, M. Shahid, Omar Al-kharji and Joao Ponciano, “A CAD Package for Modeling and Simulation of PV Arrays under Partial Shading Conditions,” Mediterranean Green Energy Forum, 2013.

[43] “Nominal Operating Cell Temperature” [Online]. Available: http://www.pveducation.org/pvcdrom/modules/nominal-operating-cell temperature.

[44] F. Reil, A. Sepanski, W. Vaasen, B. V. Heeckeren, S. Raubach, M. Vosen, M. Thiele, G. Volberg, A. Schulz, H. Schmidt, H. Laukamp, M. Halfmann, B. Bansemer, and A. Loebbert, “Determination of Arcing Risks in PV Modules with Derivation of Risk Minimization Measures" , IEEE Photovoltaic Specialists Conf., June, 2013.

[45] S. Ben-Menahem and S. C. Yang, “Online Photovoltaic Array Hot Spot Bayesian Diagnostics from Streaming String Level Electric Data," Proc. IEEE Photovoltaic Specialists Conf., June, 2012.

[46] S. A. Spanoche, J. D. Stewart, S. L. Hawley, and I. E. Opris, and Modelbased, “Method for Partially Shaded PV modules Hot Spot Suppression," IEEE Photovoltaic Specialists Conf., pp. 1-7, June, 2012.

[47] Otwin Breitenstein, Jan Bauer, Karsten Bothe, Wolfram Kwapil, Dominik Lausch, Uwe Rau, Jan Schmidt, and Matthias Schneemann, “ Understanding Junction Breakdown in Multicrystalline Solar Cells”, April, 2013.

[48] A. Amerasekera, M.-C. Chang, J. Seitchik, A. Chatterjee, K. Mayaram, and J.-H. Chern, “Self-heating Effects in Basic Semiconductor Structures”, IEEE Trans. Electron Devices, vol. 40, no. 10, pp. 1836-1844, 2000.

[49] D. L. King, J. A. Kratochvil, and M. A. Quintana, “Applications for Infrared Imaging Equipment in Photovoltaic Cell, Modules and System Testing”, Sandia National Laboratories, Albuquerque, August, 2012.

[50] Stefan Wendlandt, Alexander Drobisch, Torfinn Buseth, Stefan Krauter and Paul Grunow, “Hot Spot Risk Analysis on Silicon Cells Modules”. Photovoltaic Institute Berlin AG, Wrangelstr. Berlin, Germany, September, 2010.

[51] John H. Wohlgemuth and Sarah R. Kurtz, “How Can We Make PV Modules Safer,” Photovoltaic Specialists Conference Austin, Texas June 3–8, 2012.

[52] N. Tyutyundzhiev, F. Martínez-Moreno, J. Leloux, and L. Narvarte, “Experimental Investigation of Hotspot Detection and Isolation in Shaded Photovoltaic Cells”, International Journal of Science and Research (IJSR) ISSN, 2013.

[53] Tyutyundzhiev, N, Martinez-Moreno, F, Leloux, J, and Navarte, “Equipment and Procedures for On-Site Testing of PV Panels and BIPV,” 29th European Photovoltaic Solar Energy Conference (PVSEC), Sep., 2014.

[54] Kazutaka, ITAKO and Hossam, BAKHSH, “Primary Investigation for Real Time Hot Spot Detection of PV Generation System”, May, 2015.

[55] S. Vergura, O. Falcone. , “Filtering and Processing IR Images of PV Modules” Las Palmas de Gran Canaria (Spain), 13th to 15th April, 2011.

[56] H. Benis1, H. Ben cheikh el hocine 1, A. Bouden, “The Hot Spot Phenomena in Shadowed ENR System”, International Conference on Renewable Energies and Power Quality, March, 2012.

[57] Daniele Rossi, Martin Omaña, Daniele Giaffreda, and Cecilia Metra, “Modeling and Detection of Hot Spot in Shaded Photovoltaic Cells,” June, 2015.

[58] Rodrigo Moretón, Eduardo Lorenzo, Jonathan Leloux, and José Manuel Carrillo, “Dealing in Practice With Hot Spots,” European Photovoltaic Solar Energy Conference and Exhibition, Amsterdam, 2014.

[59] Dhass. A.D., Natarajan E., and Lakshmi Ponnusamy, “Influence of Shunt Resistance on the Performance of Solar Photovoltaic Cell,” International Conference on Emerging Trends in Electrical Engineering and Energy Management, IEEE, 2012.

[60] Molen Broek, D.w Waddington, and K.A. Emery, “Hot Spot Susceptibility and Testing Of PV Modules,” CH2953-8/91/0000-0547, 1991.

[61] “Hot Spot heating” [Online] Available: http://pvcdrom.pveducation.html.

[62] W. Herrmann, W. Wiesner, W. Vaanen, “Hot Spot Investigations on PV Modules: New Concepts for a Test Standard and Consequences for Module Design with Respect to Bypass Diodes,” 26th PVSC; Sept. 30-0ct. 3, 1997.

[63] K Al Abdullah , Faisal Al Alloush , Ali Jaafar , and C. Salame , “Study of the Effects Related to the Electric Reverse Stress Currents on the Mono-Si Solar Cell Electrical Parameters,” TerraGreen 13 International Conference, 2013.

[64] J. W. Bishop, "Microplasma Breakdown and Hot Spots in Silicon Solar Cells," Solar Cells, vol.26, no.4, pp.335-349, 1989.

[65] J. W. Bishop, "Computer Simulation of the Effects of Electrical Mismatches in Photovoltaic Cell Interconnection Circuits," Solar Cells, vol.25, pp.73-89, 1988.

[66] G. Bhattacharya and C. Neogy, "Removal of the Hot Spot Problem in Photovoltaic Modules and Arrays," Solar cells, vol.31, no.1, pp.1-12, 1991.

[67] Ali M. Humada, Mohd Bin Sulaiman, Mojgan Hojabr, Hussein M. Hamada and Mushtaq N., "A Review on Photovoltaic Array Behavior, Configuration Strategies and Models under Mismatch Conditions," ARPN Journal of Engineering and Applied Sciences, April, 2016.

[68] Govindasamy Mani, Tamizh Mani and Samir Sharma, "Hot Spot Evaluation of Photovoltaic Modules, Photovoltaic Testing Laboratory," Arizona State University, Mesa, AZ, USA, 2008.

[69] M. Danner and K. Bucher, "Reverse Characteristics of Commercial Silicon Solar Cells Impact on Hot Spot Temperatures and Module Integrity," in Proc. IEEE Photovoltaic Specialists Conf., pp. 1137-1140, 1997.

[70] H. Yang, W. Xu, H. Wang, and M. Narayanan, "Investigation of Reverse Current for Crystalline Silicon Solar Cells New Concept for a Test Standard about the Reverse Current," in Proc. IEEE Photovoltaic Specialists Conf., pp. 2806{2810},2010.

[71] O. Breitenstein, J.P. Rakotoniaina, T. Pernau, W. Warta, and J. Isenberg, "Lock-In Thermography -A Universal Tool for Local Analysis of Solar Cells," 20th European Photovoltaic Solar Energy Conference, Barcelona, Spain, 6-10 June, 2005.

[72] "Solar Cells" [Online]. Available: http://www.energy-fundamentals.eu/16.htm.

[73] “Photovoltaic blog- solar energy blog: Solar News- photovoltaic frauds” [Online]. Available: http://myphotovoltaicsolar.blogspot.com/2012/05/noct-is-important-in-solar-panels.html_sm_au_=iVVr47FpvNS61FQM

Vitae

Name :Ibrahim Hassan Ali Banat

Nationality :Palestinian

Date of Birth :12/19/1988

Email :g201406700@kfupm.edu.sa

Address :Dhahran, Kingdom of Saudi Arabia

Academic Background

1. Islamic University of Gaza, IUG Gaza, Palestine, Sep. 2006 - Feb. 2011. Bachelor Degree in Electrical Engineering.
2. Higher Secondary School, Science Stream Gaza, Palestine, July - 2006. Gifted Secondary School.

Work Experience

1. Engineering Consulting Office, Dec.2013 to July 2014, Electrical Engineer of Sheikh Hamad Hospital for Rehabilitation and Prosthetic Limbs Project.
2. Ministry of Labor, Jan-July 2013, General Directorate of Vocational Training Trainer for vocational training courses.
3. Ministry of Social Affairs, July 2012 to Jan. 2013, Electrical Engineer of the Information Systems Unit.

Publications:

1. Ibrahim Banat, Ahmed Selim and Mohammed Almuhini, “Reliability Assessment of a Stand-Alone Hybrid System Using Monte Carlo Simulation”, 2016 13th International Multi-Conference on Systems, Signals & Devices (SSD). Leipzig, Germany.
2. I.H. Banat, C. A. Belhadj and M. Deriche, “A Detailed Analysis of Photovoltaic Panel Hot Spot Phenomena based on the Bishop Model” (submitted).
3. I.H. Banat, C. A. Belhadj and M. Deriche, “Photovoltaic Panel Hot Spot Phenomenon Formation Mechanism and Tracking” (under preparation).